

SPECTROSCOPIC EVIDENCE FOR THE OCCURRENCE OF NITRATES IN LIGNITES

Clarence Karr, Jr., Patricia A. Estep, and John J. Kovach

Morgantown Coal Research Center, Bureau of Mines,
U. S. Department of the Interior, Morgantown, W. Va. 26505

INTRODUCTION

As part of a broad program of coal research at the Morgantown Coal Research Center, U. S. Bureau of Mines, extensive studies are being conducted on minerals in coal using a variety of analytical techniques. A method was successfully applied for obtaining unaltered mineral matter from coal by means of an electronic low-temperature asher (1). Significant amounts of sodium and alkaline earth nitrates were identified in lignite ashes obtained by this technique. Nitrates have not been found, however, in the ashes from any of the bituminous or anthracite coals examined to date; nitrates appear to predominate only in the ashes of lignites from the Fort Union Formation of the Great Plains coal area. These findings raised the question as to whether nitrates are formed by chemical reaction in the oxygen plasma of the asher, or are original mineral constituents of the coals. It was therefore desirable to determine, through independent methods, if nitrates are present in lignite.

This paper describes the water extraction of inorganic nitrates and their identification in the extracts by infrared spectroscopy. The presence of nitrates as original mineral constituents was confirmed, but the amount of nitrate that may have been chemically produced in the asher was not determined. The amounts of nitrates in these lignites were estimated from x-ray powder patterns of the untreated whole coals. Oxalates and sulfates were also identified by infrared spectroscopy in the water-soluble material.

EXPERIMENTAL

Coal samples were preground for 30 min. in a tungsten carbide ball mill (Spex)* and dried at 105° C for 4 hr. under a 300 ml/min. stream of nitrogen. When the moisture content is high (over about 20 pct), the coal must be predried for efficient grinding.

Infrared Spectroscopy

Pellets were prepared for infrared analysis by blending 1 mg of the sample with 500 mg of cesium iodide powder and preparing the pellet by triple pressing. The resulting pellet, 0.80 mm by 13 mm, was then scanned immediately on a Perkin-Elmer 621 infrared grating spectrophotometer purged with dry air.

* Reference to specific brands is made for identification only and does not imply endorsement by the Bureau of Mines.

Low-Temperature Oxidation

A one-gram sample of preground coal was ashed in Tracerlab's Model LTA-600L low-temperature asher at 145° C. A stream of excited oxygen produced by a radio frequency electromagnetic field of 13.56 MHz, passed over the coal at 1 mm Hg pressure, and completely removed the organic matter in 70 to 90 hr. Temperature measurements were made with a Huggins Laboratories Mark I Infrascop.

Water Extraction

Stepwise water extractions were conducted on three lignites. The available analytical data on the original coals are shown in Table 1. The procedure is described as follows: A preground sample of coal of known moisture content was placed in a Whatman paper Soxhlet extraction thimble between two layers of glass wool inert filler. All equipment was prewashed with distilled-deionized water. Sufficient distilled-deionized water (200 ml) was added to completely cover the sample when the thimble was placed in a 1,000 ml beaker. The sample was covered with water at all times and the water temperature was held at 90° C for 2 hr. The water solution was then removed, filtered, and carefully evaporated to dryness on a hot plate. An infrared spectrum was then obtained on this water soluble residue. The extraction was continued in this manner for a minimum of 5 to 10 separate extractions, each with a fresh volume of water as extractant. The extractions were not exhaustive or quantitative, but rather were conducted until a relatively invariant infrared spectrum was obtained.

X-ray Diffraction

Samples were mounted in 0.5 mm glass capillaries and were analyzed with iron-filtered $\text{CoK}\alpha$ radiation, using a two radian Debye-Scherrer camera for optimum resolution. The average exposure time for coal samples was 12 hr., and the use of cobalt radiation minimized the background intensity. Both low-temperature ash samples and water extraction residues provided good patterns with exposure times of 7 to 8 hr.

RESULTS AND DISCUSSION

Water Extractions

Nitrates can be water extracted from lignite only under certain conditions, and there are apparently several factors involved in a successful extraction. Several initial extraction attempts failed. For example, an extraction was attempted on the Beulah, N. D., lignite as received, with no pregrinding, and very little nitrate was extracted. Another sample of the same coal was then preground in a tungsten carbide ball mill and the identical extraction procedure repeated. Successful extraction of nitrates was then achieved and, in addition, the total material extracted was increased. Thus it became apparent that the particle size of the coal plays an important role in the nitrate extraction. For a variation in extraction technique, a 90-hr. 90° C extraction of lignite from Minot, N. D., was subsequently made in an ordinary Soxhlet apparatus, using 3.7 grams of coal and 150 ml of water. The infrared spectrum of the extract (curve a, Figure 1) showed that it

was predominantly sodium sulfate, with only a small amount of nitrates, and qualitatively very similar to the first extract from Dawson County, Mont., lignite obtained by the described extraction in a beaker after only 2 hr. (extract 1, Figure 2). It is apparent that the extraction process is not a simple function of relative solubilities, but must be a complex interplay of the ion exchange properties of the various ions present, their concentrations, and the adsorption properties of the coal substance. The salts extracted thus represent the equilibrium conditions achieved. The complexity of the system is further emphasized by the fact that sodium sulfate was not detected in the low-temperature ash from the Minot, N. D., coal, and that nitrates are generally much more soluble in water than sulfates. Sodium sulfate could not have decomposed in the low-temperature ash, as demonstrated by the fact that it is found in boiler deposits that are formed at much higher temperatures. The phenomenon responsible for the selective tenacity that the coal has for nitrates remains unexplained. One possibility is that nitrates are encapsulated in the plant structure retained by this low-rank coal. Another possibility is that nitrates are preferentially adsorbed on clays in the coal or at active sites in the coal structure. It is not known if the discrepancy between the amounts of nitrate extracted (less than 2 wt pct of the coal) and the amounts found in the low-temperature ashes is due to the production of additional nitrate during ashing.

Infrared Analysis

It was not possible to verify the presence of nitrates from infrared spectra of the coal itself because of the high background absorption of organic material. The infrared spectra of the material from five successive extraction steps for the Montana coal are shown in Figure 2. The overall spectral characteristics show that the residues are predominantly inorganic. The weak CH stretching vibrations appearing at 2850 and 2930 cm^{-1} in all extracts are assigned to fine residual coal particles which could not be filtered. Extract I is predominantly sodium sulfate, as evidenced by the strong fundamental vibration at 1128 cm^{-1} , characteristic for the sulfate ion, and the weaker bands at 990, 628, 612, and 225 cm^{-1} , specific for sodium sulfate. The minor bands are unique and make possible a clear distinction between sodium sulfate and other probable sulfates such as calcium and magnesium sulfates. Sodium sulfate bands can be followed through successive extracts and are seen to gradually decrease. Also in the first extract there appears a weak but definite absorption band at 1360 cm^{-1} . The intensity of this band increases in each successive extract, as seen in Figure 2, until it becomes a major band in extract 5.

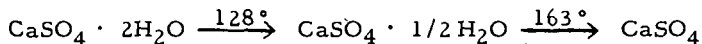
A careful study of many infrared spectral-structure correlations (2, 3, 4, 5, 6, 7) shows that there are few inorganic ions absorbing in this spectral region. Table 2 is a compilation of data from these references, showing the only possible assignments if one makes the regular assumption that the band at 1360 cm^{-1} is a characteristic group frequency, representing a class of ions. This assumption is well justified on the basis of the intensity of the band. From the data in this table and the infrared spectra of the extracts in Figure 2, a systematic elimination of all ions can be made with the exception of nitrates. For example, the nitrite ion can be readily eliminated on the basis that a strong asymmetric stretch (ν_3) for the N-O bond is required near 1260 cm^{-1} (7), and this cannot be observed in the

spectra of any of the extracts. Tetraborates, $(B_4O_7)^{2-}$, exhibiting very complex infrared spectra, require a strong absorption near 1000 cm^{-1} and metaborates, $(BO_2)^-$, require one near 950 cm^{-1} . Neither are observed in any of the spectra of the extracts.

With nitrate as the remaining possibility, the infrared spectra of a large number of inorganic nitrates were examined, both from the literature (8, 9, 10, 11, 12, 13) and from this laboratory. The absorption band observed in nearly all inorganic nitrates near 1360 cm^{-1} has been assigned to the asymmetric N-O stretching vibration (ν_3) of the nitrate ion. Its very narrow range for the inorganic class of nitrates (30 cm^{-1}) increases its specificity and usefulness. The nitrate interpretation is given additional strong support by the observation of a weak band at 825 cm^{-1} , the out-of-plane bending vibration (ν_2) for the nitrate ion, appearing well resolved in the fourth and fifth extracts, where the 1360 cm^{-1} band has become very intense. It is not possible, from the infrared spectra of these extracts alone, to establish with certainty the identity of the specific cation or cations accompanying the nitrate ion. Within nitrates as a class, the ν_2 vibration varies in position and can be used along with additional bands for a specific identification of the cation. Figure 3 presents the infrared spectra of sodium nitrate and calcium nitrate, demonstrating the relative simplicity of the infrared spectra for inorganic nitrates in general and shows the reduced intensities of additional bands. These weaker bands could not be observed in the water extracts, but in the low-temperature ashes, where nitrates appear more concentrated, all of these weaker bands have been observed.

The shoulder appearing at 1400 cm^{-1} , along with the 1360 cm^{-1} band in the water extracts, suggests the presence of alkaline earth nitrates. The splitting of the N-O stretching vibration (ν_3) into two bands for polyvalent metal nitrates and specifically for alkaline earth nitrates has been discussed by Vratny (9), Ferraro (11), and Buijs (12). This split, demonstrated in the spectrum of calcium nitrate in Figure 3, has been assigned to a reduction in symmetry and also to increasing covalent character of the nitrate ion. Infrared spectra of the low-temperature ashes give even stronger evidence for the presence of alkaline earth nitrates: The ν_3 split is observed, the ν_2 for calcium and magnesium nitrates is observed, and the bands due to water of hydration are more intense, as required for these nitrates. Carbonates in the water extracts are a possible assignment for the 1400 cm^{-1} band. However, the carbonate ν_2 out-of-plane bending in the 860 to 880 cm^{-1} region, comparable in intensity to the ν_2 for nitrates, was not observed in spectra of the extracts or in the low-temperature ashes.

As the extraction continues, the hemihydrate of calcium sulfate ($CaSO_4 \cdot 1/2H_2O$) gradually appears and can be positively identified in extract 5 by its characteristic bands at 650 and 592 cm^{-1} , as well as by the strong sulfate group vibration at 1147 cm^{-1} . The distinction between $CaSO_4$, $CaSO_4 \cdot 1/2H_2O$, and $CaSO_4 \cdot 2H_2O$ can be readily made in the infrared (1). The presence of calcium sulfate in the form of the hemihydrate indicates that the maximum temperature during evaporation of water from the extract lies between 128° and 163° C because of the following known conversions:



This indicates that the extract was not subjected to high temperatures and precludes oxidation. The position of calcium sulfate in the extraction after sodium sulfate is in line with the relative cation exchange power of calcium and sodium. Kaolinite, a clay mineral, appears in significant amounts in extracts 3 and 4 and is identified by its bands at 3695, 3620, 1100, 1030, 1010, 930, 910, 790, 750, 690, 530, 462, 425, 340, and 268 cm^{-1} . Its presence in these water extracts indicates a particle size too fine to be filtered. The strong, broad absorption bands at 3440 and 1613 cm^{-1} are vibrations assigned to water of crystallization.

The bands at 1330 and 777 cm^{-1} in this extraction were observed in the same relative intensities in all water extractions attempted, and were suspected of belonging to oxalates. Support for this interpretation was obtained from a methanol separation made on the water extract of the Minot, N. D., coal. The water extract (curve a, Figure 1) shows the suspected oxalate bands at 1330 and 777 cm^{-1} , with medium intensities. Curves (b) and (c) are the infrared spectra of the methanol soluble and methanol insoluble material, respectively. Consistent with the known insolubility of oxalates in alcohols, these bands are enhanced in the methanol insoluble material. The position and relative intensities of these two bands, along with newly resolved bands at 1640 and 507 cm^{-1} seen in curve (c) of Figure 1, are in good agreement with the infrared spectra of sodium and calcium oxalates. The observed frequencies of 1640, 1330, and 777 can be assigned to the carboxylate (O-C-O) vibrations of the asymmetric stretch (ν_9), the symmetric stretch (ν_{11}), and a deformation (ν_{12}), respectively (14). The higher solubilities of alkali oxalates compared to those of alkaline earth oxalates would support the presence of sodium oxalate in the water extracts, although increased solubilities are known when soluble oxalates combine with insoluble oxalates to form double salts. Also, calcium oxalate requires two additional medium bands at 660 and 305 cm^{-1} , which do not appear. If calcium oxalates were present in small amounts, it could be in the form of a fine particle suspension, similar to the occurrence of kaolinite in these water extracts. In view of the widespread occurrence of oxalates in plant matter, their identification in lignites is not at all unlikely.

The methanol separation shown in Figure 1 provides additional support for the presence of nitrates in lignite water extracts. As previously described, this 90-hr. Soxhlet extraction yielded only minor amounts of nitrate, as indicated by the weak absorption at 1360 cm^{-1} in curve (a). The enhancement of this band, seen in curve (b), shows that methanol has selectively dissolved nitrate, while the sodium sulfate at 1128, 990, 628, 612, and 225 cm^{-1} in curve (c) remains predominantly in the insoluble portion. This separation is in good accord with the known relative solubilities in methanol, and with methanol solubility studies on mixtures of sodium nitrate and sodium sulfate.

The stepwise extractions on the two North Dakota coals proceeded in a qualitatively similar fashion to that shown in Figure 2 for the Montana coal, achieving the same concentration of nitrate but with considerably higher amounts of oxalates. Atomic absorption analyses on the Minot, N. D., coal, both prior to and following the extraction, show that essentially all sodium was removable with distilled, demineralized water.

X-ray Analysis

X-ray powder patterns were obtained on water extracts and on the original coal samples in order to verify the presence of nitrates. Good peak-to-background ratios were obtained from the coal samples by using $\text{CoK}\alpha$ radiation (1.79 Å), although long exposure times (12 hr.) were required. The use of radiation with shorter wavelengths (e. g. . $\text{CuK}\alpha$. 1.54 Å) resulted in a high background, presumably because of increased Compton scattering by the organic matrix.

The interplanar spacings obtained for the Montana coal, and the ASTM data (15) for the minerals identified, are listed in Table 3. X-ray analysis of the coal samples indicated the presence of quartz, kaolinite, gypsum ($\text{CaSO}_4 \cdot 2\text{H}_2\text{O}$), and the nitrates of calcium and sodium. Several low-intensity lines from the ASTM data are not listed. Some kaolinite lines are absent presumably due to preferred orientation effects. The form of calcium sulfate generally occurring in coal is gypsum (1), and this is an important factor in the x-ray interpretation. Upon being subjected to low-temperature ashing or evaporation after water extraction, gypsum dehydrates to the hemihydrate. The x-ray spectral lines for the hemihydrate overlap the lines of sodium nitrate, precluding the positive identification of sodium nitrate in either the low-temperature ash or the water extract. Gypsum, however, with a completely different crystal structure, has a set of lines that do not seriously overlap those of sodium nitrate. In addition, both CaSO_4 and $\text{CaSO}_4 \cdot 1/2\text{H}_2\text{O}$ have specific lines that were used in determining that they were not present in the coal. As a result, the presence of sodium nitrate can be verified in the original coals, using the strong line at 3.03 Å and the weaker line at 1.463 Å. On the basis of the observed intensities of the sodium nitrate lines, its amount was estimated to be about 5 wt pct. The intensities of the x-ray lines were considerably greater than those for the minimum detectable amount, about 1 wt pct.

Several lines for calcium nitrate were present in the powder pattern of the Beulah, N. D., lignite and this supported the infrared evidence of alkaline earth nitrates in the water extract of this lignite. The presence of sodium oxalate could not be verified by x-ray of the lignites because all the strong lines of this compound were overlapped by those of other substances present. However, the absence of the unique lines for potassium and calcium oxalates and hydrates indicated that these particular oxalates were not present.

ACKNOWLEDGMENTS

Special thanks are due Edward E. Childers, Morgantown Coal Research Center, for obtaining infrared spectra and conducting the low-temperature oxidations on the coals. We also thank John J. Renton, Geology Department, West Virginia University, for x-ray data, and Edward L. Obermiller, Consolidation Coal Company, Library, Pa., for analytical data.

REFERENCES

1. Estep, Patricia A., Kovach, John J., and Karr, Clarence, Jr. Quantitative Infrared Multicomponent Determination of Minerals Occurring in Coal. *Anal. Chem.*, 1968 (Feb.), 40, 358 to 363.
2. Ferraro, John R. *Inorganic Infrared Spectroscopy*. J. Chem. Ed., 1961 (April), 38, 201 to 208.
3. Yoganarasimhan, S. R., and Rao, C. N. R. Correlation Chart for Group -1 Frequencies in Inorganic Substances for the Infrared Region $4000 - 300 \text{ cm}^{-1}$. *Chemist-Analyst*, 1962; 51, 21 to 23.
4. Miller, Foil A., and Wilkins, Charles H. Infrared Spectra and Characteristic Frequencies of Inorganic Ions. *Anal. Chem.*, 1952 (Aug.), 24, 1253 to 1294.
5. Colthup, N. B., Daly, L. H., and Wiberley, S. E. *Introduction to Infrared and Raman Spectroscopy*. Academic Press, Inc., New York, 1964, 511 pp.
6. Nakamoto, Kazuo. *Infrared Spectra of Inorganic and Coordination Compounds*. John Wiley & Sons, Inc., New York, 1963, 328 pp.
7. Bellamy, L. J. *The Infra-red Spectra of Complex Molecules*. John Wiley & Sons, Inc., New York, 1958, 425 pp.
8. Kalbus, Gene Edgar. *The Infrared Examination of Inorganic Materials*. University Microfilms, Inc., Ann Arbor, Michigan, 1957, 207 pp.
9. Vratny, Frederick. Infrared Spectra of Metal Nitrates. *Appl. Spectroscopy*, 1959, 13, 59 to 70.
10. Sadtler Research Laboratories, Philadelphia, Pa. *High Resolution Spectra of Inorganics and Related Compounds*. Vols. 1 and 2, 1965; vols. 3 and 4, 1967.
11. Ferraro, John R. The Nitrate Symmetry in Metallic Nitrates. *J. Molecular Spectroscopy*, 1960, 4, 99 to 105.
12. Buijs, K., and Schutte, C. J. H. The Infra-red Spectra of the Anhydrous Nitrates of Some Alkali and Alkaline Earth Metals. *Spectrochim. Acta*, 1962, 18, 307 to 313.
13. Miller, Foil A., and Carlson, Gerald L. Infrared Spectra of Inorganic Ions in the Cesium Bromide Region ($700-300 \text{ cm}^{-1}$). *Spectrochim. Acta*, 1960, 16, 135 to 235.
14. Schmelz, M. Judith, Miyazawa, Tatsuo, Mizushima, San-ichiro, Lane, T. J., and Quagliano, J. V. Infra-red Absorption Spectra of Inorganic Coordination Complexes--IX. Infra-red Spectra of Oxalato Complexes. *Spectrochim. Acta*, 1957, 9, 51 to 58.

15. American Society for Testing and Materials, 1916 Race Street, Philadelphia, Pa. X-Ray Powder Data File, 1966, 1 to 683.

TABLE 1. Lignite analyses, percent

	R. A. Newton mine, Dawson County, Mont.	Beulah, Mercer County, N. D.	Minot, Ward County, N. D.
Nitrogen	0.61	0.56	1.13
Moisture	26.2	37.6	38.4
Low-temperature ash	24.0	12.0	9.6
High-temperature ash	19.3	6.56	5.19
High-temperature ash composition:			
Na ₂ O	6.6	8.9	13.2
CaO	11.7	20.4	34.2
MgO	3.8	7.2	7.1
K ₂ O	0.8	0.4	0.75

TABLE 2. Possible polyatomic ions absorbing at 1360 cm⁻¹*

Ion	Absorption in spectral** region of 1360 cm ⁻¹		Additional absorption bands required
	Average of range cm ⁻¹	Range cm ⁻¹	Average of range cm ⁻¹
<u>N-O Stretching Vibration</u>			
1. Nitrate, (NO ₃) ⁻	1360 (s)	30	820 (m, sharp)
2. Nitrite, (NO ₂) ⁻	1350 (w)	50	1260 (s) 800 (w)
<u>B-O Stretching Vibration</u>			
3. Tetraborate, (B ₄ O ₇) ²⁻	1400 (m-s)	110	1000 (s) 1080 (w-s)
4. Metaborate, (BO ₂) ⁻	1340 (m-s)	70	950 (s)

* Composite data from references 2 through 13.

**Intensity designations in parentheses are: s = strong, m = medium, w = weak.

TABLE 3. X-ray analysis of Dawson County, Mont., lignite

dÅ	Relative intensity*	Identification	NaNO ₃	Gypsum	Kaolinite	Quartz
7.65	M	Gypsum		7.58 ¹⁰⁰		
7.07	M	Kaolinite			7.15 ¹⁰⁰	
4.41	W	Kaolinite			4.45 ⁵⁰	
4.28	S	Gypsum, kaolinite, quartz		4.27 ⁵¹	4.35 ⁶⁰	4.26 ³⁵
4.13	W	Kaolinite			4.17 ⁶⁰ or 4.12 ³⁰	
3.83	W	NaNO ₃ , gypsum, kaolinite	3.89 ⁶	3.79 ²¹	3.84 ⁴⁰	
3.55	M	Kaolinite			3.57 ¹⁰⁰	
3.36	W	Kaolinite			3.37 ⁴⁰	
3.32	W	Quartz				3.343 ¹⁰⁰
3.26	W					
3.20	W					
3.18	W	Gypsum, kaolinite		3.163 ³	3.14 ²⁰	
3.08	M	Gypsum, kaolinite		3.059 ⁵⁷	3.09 ²⁰	
3.03	M	NaNO ₃	3.03 ¹⁰⁰			
2.97	VW					
2.85	M	NaNO ₃ , gypsum	2.81 ¹⁵	2.867 ²⁷		
2.67	M	Gypsum, kaolinite		2.679 ²⁸	2.75 ²⁰	
2.55	W	NaNO ₃ , gypsum, kaolinite	2.53 ⁹	2.591 ⁴	2.55 ⁷⁰	
2.50	W	Gypsum, kaolinite, quartz		2.495 ⁶	2.52 ⁴⁰ or 2.486 ⁸⁰	2.458 ¹²
2.32	MW	NaNO ₃ , kaolinite	2.311 ²⁴		2.374 ⁷⁰ or 2.331 ⁹⁰	

Continued

TABLE 3. X-ray analysis of Dawson County, Mont., lignite (continued)

dÅ	Relative intensity*	Identification	NaNO ₃	Gypsum	Kaolinite	Quartz
2.27	W	Kaolinite, quartz			2.284 ⁸⁰	2.282 ¹²
2.20	VW	Kaolinite, quartz			2.182 ³⁰	2.237 ⁶
2.11	W	NaNO ₃ , kaolinite, quartz	2.125 ⁹		2.127 ²⁰	2.128 ⁹
2.08	W	Gypsum		2.080 ¹⁰		
2.04	W	Gypsum, kaolinite		2.073 ⁸	2.057 ⁵	
1.98	W	NaNO ₃ , kaolinite, quartz	1.947 ⁴		1.985 ⁷⁰	1.98 ⁶
1.89	W	NaNO ₃ , gypsum, kaolinite	1.898 ¹⁶	1.898 ¹⁶	1.892 ²⁰	
1.88	W	NaNO ₃ , gypsum, kaolinite	1.880 ⁷	1.879 ¹⁰	1.865 ⁵	
1.81	W	Gypsum, kaolinite, quartz		1.812 ¹⁰	1.835 ⁴⁰	1.817 ¹⁷
1.77	W	Gypsum, kaolinite		1.778 ¹⁰	1.778 ⁶⁰	
1.66	W	NaNO ₃ , gypsum, kaolinite, quartz	1.652 ⁴	1.664 ⁴	1.682 ¹⁰	1.672 ⁷
1.61	W	NaNO ₃ , gypsum, kaolinite	1.629 ⁴	1.621 ⁶	1.616 ⁷⁰	
1.54	W	NaNO ₃ , quartz	1.544 ²			1.541 ¹⁵
1.48	W	NaNO ₃	1.463 ⁴			

* S = strong, M = medium, W = weak, V = very.

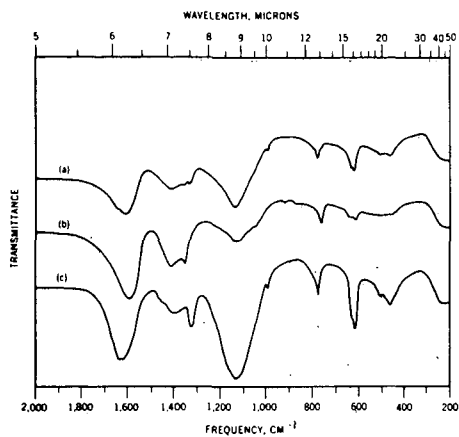


FIGURE 1. - Infrared spectra of (a) Soxhlet water extract of a North Dakota lignite; (b) methanol soluble material from (a); (c) methanol insoluble material from (a).

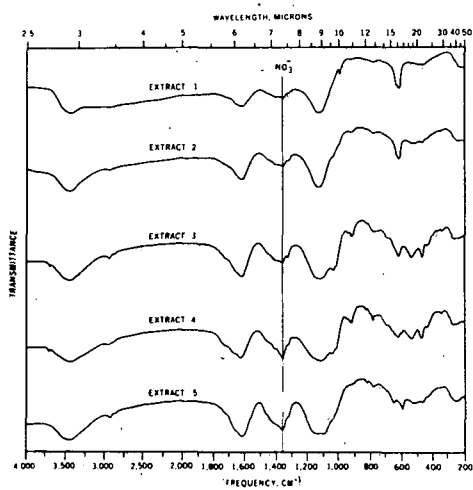


FIGURE 2. - Infrared spectra of successive water extracts from a Montana lignite.

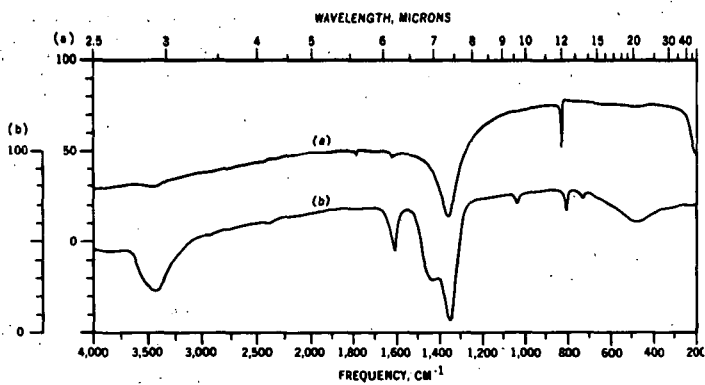


FIGURE 3. - Infrared spectra of (a) sodium nitrate, NaNO_3 ; (b) calcium nitrate, $\text{Ca}(\text{NO}_3)_2 \cdot 4\text{H}_2\text{O}$.

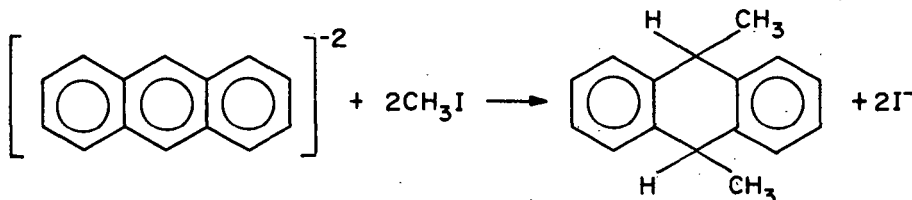
SOLVATION AND REDUCTIVE ALKYLATION OF COAL VIA A
"COAL ANION" INTERMEDIATE

Heinz W. Sternberg and Charles L. Delle Donne

Pittsburgh Coal Research Center, Bureau of Mines,
U. S. Department of the Interior,
4800 Forbes Avenue, Pittsburgh, Pennsylvania 15213

INTRODUCTION

During the last decade a large amount of work has been published on the formation, structure, and reactions of aromatic hydrocarbon anions.^{1,2} These anions are readily formed when aromatic hydrocarbons, dissolved in a suitable solvent, are treated with alkali metals. For example, naphthalene³ dissolved in tetrahydrofuran or hexamethylphosphoramide, $[(CH_3)_2N]_3PO$, reacts with one or two moles of lithium to form the green naphthalene mono-anion, $[C_{10}H_8]^-$ or the red naphthalene di-anion $[C_{10}H_8]^{2-}$ depending on the amount of lithium used. Aromatic hydrocarbon anions react with a wide variety of reagents such as alkyl halides,² carbon dioxide,⁴ acetyl chloride,⁵ aldehydes,⁶ ketones⁶ and compounds containing active hydrogen atoms such as alcohols and water.⁷ For example, anthracene di-anion reacts⁸ with methyl iodide to give among other products 9,10-dimethyl-9,10-dihydroanthracene:



Since coal is believed to contain clusters of condensed aromatic rings, we thought that it might be possible to introduce alkyl groups into the coal molecule by forming aromatic hydrocarbon anions in the coal molecule and then allowing these anions to react with alkyl halides.

EXPERIMENTAL DATA AND RESULTS

Reagents. - Metallic lithium, naphthalene, and hexamethylphosphoramide, (HMPA), were of the highest purity available commercially. Lithium and naphthalene were used as received. HMPA was purified by vacuum distillation and the fraction boiling between 89° and 92° at 4 to 5 mm were used.

Coal. - In all experiments, a hand-picked Pocahontas (lvb) vitrain sample (ground to pass 325 mesh) was used.

Solvation of Coal by Treatment with Lithium in HMPA. - Under a protective cover of nitrogen, 0.1247 gram of vitrain, 0.22 millimole (0.0152 gram) of lithium, and 15 ml of HMPA were placed in a test tube provided with a screw cap. The sealed test tube was gently tumbled (about 40 revolutions per minute) for 8 hours to provide adequate agitation. The contents of the test tube were then centrifuged. The supernatant dark-red solution was pipetted off and the residue treated with 15 ml of HMPA; the resulting suspension was centrifuged and the supernatant solution pipetted off as before. The residue was washed with water until the washings were neutral and the residue was collected on a weighed glass filter. After

drying in vacuo at 100°C, the residue weighed 0.0135 gram, corresponding to 10.8 percent of the original sample. This showed that 89.2 percent of the vitrain was solvated by treatment with lithium in HMPA. By itself, HMPA is only capable of solvating 3 percent of the vitrain.

Alkylation of Naphthalene. - A 1.005 gram sample of naphthalene (7.85 millimoles) and 150 ml of HMPA were placed in a 500 ml Erlenmeyer flask under a protective cover of nitrogen and 0.1328 gram (19.1 millimoles) of lithium wire cut into small pieces was added to the flask. The contents of the flask were stirred by means of a glass enclosed magnetic stirring bar for 8 hours, during which time the color of the solution turned first to a dark green (color of the mono-anion) and then to a dark red (color of the di-anion of naphthalene). The solution was cooled to 5°C and 2.4 ml (30 millimoles) of ethyl iodide was slowly added to the solution with stirring. The reaction mixture was poured into ice water and the aqueous mixture was extracted with pentane. The pentane extract was in turn treated with dilute acid, sodium bicarbonate solution and water to remove any HMPA, and the pentane extract was then freed of pentane. Mass spectrometric and glc analyses of the reaction product indicated that about 30 percent of the naphthalene had been converted to a mixture consisting of di- and tetra-hydro derivatives of mono- and di-methyl and ethyl naphthalene. The main product, on the basis of relative mass peak heights, consisted of equal amounts of ethyl- and diethyldihydro-naphthalene. The reaction product was again alkylated as described above. Analysis of the reaction product from this second alkylation indicated that the overall amount of naphthalene converted was 70 percent, the main product again being ethyl- and diethyldihydronaphthalene.

Alkylation of Coal. - A 1.5290-gram sample of the vitrain (ground to pass 325 mesh) and 150 ml of HMPA were placed in a 500 ml Erlenmeyer flask under a protective cover of nitrogen and 0.2073 gram (29.9 millimoles) of lithium wire was added to the contents of the flask. After the contents of the flask had been stirred for 8 hours, 3 ml (37.5 millimoles) of ethyl iodide was added as described above for the alkylation of naphthalene. The reaction mixture was poured into oxygen-free ice water. The precipitate was washed repeatedly first with water until the washings were neutral and then with ethanol to remove any trace of HMPA. The recovered material, dried in vacuo at 100°, weighed 1.6962 grams and was 35 percent soluble in benzene at room temperature. A 0.4790-gram sample of the recovered coal was again subjected to alkylation with proportional amounts of HMPA and lithium (60 ml and 0.0754 gram, respectively) as described above. The weight of the recovered material was 0.6263 gram and the benzene solubility 86 percent. Table 1 shows the ultimate analysis for the original vitrain, and for the vitrains after the first and second alkylation. Table 2 gives the benzene solubilities of the original and alkylated vitrains at room temperature. Figure 1 shows the infrared spectrum (KBr-pellet) of the original vitrain, that of the vitrain subjected to one and that of the vitrain subjected to two alkylations.

TABLE 1. - Ultimate analysis¹ of alkylated Pocahontas #3 vitrain

	C	H	N	S	O ²	P	I	Ash
Original vitrain	84.85	4.35	1.14	0.63	3.40	0.00	0.00	5.63
First alkylation	82.99	5.92	1.43	.53	4.22	.01	.84	4.06
Second alkylation	81.94	6.69	1.64	.47	3.06	.26	.00	5.94

¹ Dry basis.

² By difference.

TABLE 2. Benzene solubility of original and alkylated Pocahontas vitrain

<u>Vitrains</u>	<u>Percent soluble</u>
Original vitrain	0.5
First alkylation	35.2
Second alkylation	85.8

DISCUSSION

Solvation of Coal, Formation of "Coal Anion"

Although only 3 percent soluble in HMPA, coal becomes almost 90 percent soluble on addition of lithium to a suspension of coal in HMPA. This tremendous increase in solubility on addition of lithium is almost certainly due to the formation of aromatic anions of large volume produced by the transfer of electrons to the coal molecule according to



These negatively charged aromatic clusters probably repel each other and are readily solvated because their charges are distributed over a large volume. The lithium cation on the other hand is effectively solvated by HMPA. Whatever the explanation, the high solubility of the "coal anion" offers an opportunity to introduce alkyl groups into the coal molecule.

Alkylation of Naphthalene

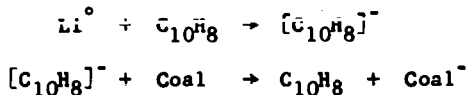
Before attempting to alkylate coal via the "coal anion" in HMPA we explored the feasibility of alkylating a model compound, i.e., naphthalene in this solvent. Treatment of naphthalene with lithium in HMPA produced the dianion $[\text{C}_{10}\text{H}_8]^{-2}$, but alkylation of the di-anion with ethyl iodide yielded in addition to the expected ethyl derivatives also small amounts of methyl derivatives of naphthalene, di- and tetrahydronaphthalene. Apparently, HMPA acted to some extent as a methylating agent under the conditions of our experiment.

Alkylation of Coal

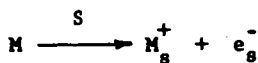
Alkylation of coal with ethyl iodide, carried out by the same procedure as the alkylation of naphthalene, yielded an ethylated coal, which was 35 percent soluble in benzene at room temperature and whose infrared spectrum (KBr-pellet) showed distinct bands (Figure 1) attributable to a methyl group (7.25 μ) and its associated stretching vibration (3.4 μ). A second alkylation of the recovered coal yielded a product which was now 85 percent soluble in benzene and whose IR spectrum (Figure 1) shows bands of increased intensity at 3.4 μ and 7.25 μ . A rough estimate of the amount of ethyl groups introduced into the coal may be obtained by assuming that the increase in weight of the recovered material over the starting coal after alkylation is due to the addition of ethyl groups. On the basis of this assumption the amount of ethyl groups introduced into the coal molecule after two alkylations corresponds to about one methyl group per 5 carbon atoms. Some methylation in addition to ethylation of the coal may have taken place in analogy to the reductive ethylation of naphthalene in HMPA described in the experimental part.

Alkylation of Coal in Tetrahydrofuran

Alkylation of coal is not restricted to the use of HMPA. For example, exploratory experiments have shown that coal can be readily alkylated in tetrahydrofuran provided a small amount of naphthalene is added which functions as an electron transfer agent



in the formation of the coal anion. In the case of HMPA, an electron transfer agent is not required since alkali metals readily dissolve in HMPA with formation of solvated cations and solvated electrons according to



where S stands for the solvent, HMPA.^{9,10}

Structure of Coal and of Petroleum Asphaltenes

The fact that introduction of alkyl groups into the coal structure produces a benzene soluble material points to a relationship between alkylated coal and petroleum asphaltenes. The latter are soluble in benzene in spite of the fact that they contain a larger number of rings^{11,12} (8 to 9) per cluster than coal¹² (3 to 4 rings per cluster). However, petroleum asphaltenes, in contrast to coal, contain a considerable number of alkyl groups attached to the aromatic clusters.¹¹ The fact that the introduction of alkyl groups into coal converts coal into a benzene soluble product indicates that the difference between coal and petroleum asphaltenes is not one of molecular size but one of molecular structure.

SUMMARY

Pocahontas (lvb) coal which is only sparingly (3 percent) soluble in hexamethylphosphoramide (HMPA) becomes 90 percent soluble when treated with a solution of lithium in HMPA. This high solubility is probably due to the formation of readily solvated aromatic anions of large volume; these anions are produced by the transfer of electrons from lithium to the aromatic nuclei in coal and readily react with alkylating agents such as ethyl iodide with addition of alkyl groups. The alkylated coal containing approximately one alkyl group per 5 carbon atoms is 86 percent soluble in benzene at room temperature. This method of alkylating coal is a new method for introducing functional groups into the coal molecule, it is not restricted to the use of HMPA as a solvent and should prove useful for modifying the physical and chemical properties of coal. The fact that introduction of alkyl groups into coal converts coal into a benzene soluble material points to a relationship between coal and petroleum asphaltenes and indicates that the difference between coal and petroleum asphaltenes is not one of molecular size but of molecular structure.

ACKNOWLEDGEMENTS

The authors wish to thank Janet L. Shultz for mass spectrometric and John Queiser for infrared analyses.

REFERENCES

1. De Boer, E. "Electronic Structure of Alkali Metal Adducts of Aromatic Hydrocarbons" in *Advances in Organometallic Chemistry*, F. G. A. Stone and R. West, Ed., Academic Press, New York, 1964.
2. Symposium on Electron Affinities of Aromatic Hydrocarbons and Chemistry of Radical Ions, Am. Chem. Soc., Div. Petroleum Chemistry, Preprints, April 1968, vol. 13, No. 2.
3. Normant, H. *Angew. Chem. Internat. Edit.*, 6, 1046 (1967).
4. Wawzonek, S. and Wearing, D. *J. Am. Chem. Soc.*, 81, 2067 (1959).
5. Cantrell, T. S. and Schechter, H. *J. Am. Chem. Soc.*, 89, 5868 (1967).
6. Cantrell, T. S. and Schechter, H. *J. Am. Chem. Soc.*, 89, 5877 (1967).
7. Scott, N. D., Walker, J. F., and Hansley, V. L. *J. Am. Chem. Soc.*, 58, 2442 (1936).
8. Gerdil, R. and Lucken, E. A. C. *Helv. Chim. Acta*, 44 1966 (1961).
9. Fraenkel, G., Ellis, S. H., and Dix, D. T. *J. Am. Chem. Soc.*, 87, 1406 (1965).
10. Sternberg, H. W., Markby, R. E., Wender, I., and Mohilner, D. M. *J. Am. Chem. Soc.*, 89, 186 (1967).
11. Winniford, R. S. and Bersohn, M. *Am. Chem. Soc., Div. Fuel Chem., Preprints*, Sept. 1962, 21-32; *C.A.*, 61, 509 (1964).
12. Friedel, R. A. and Retcofsky, H. "Proceedings of the Fifth Carbon Conference" Volume II, p. 149-165, Pergamon Press, New York, 1963.

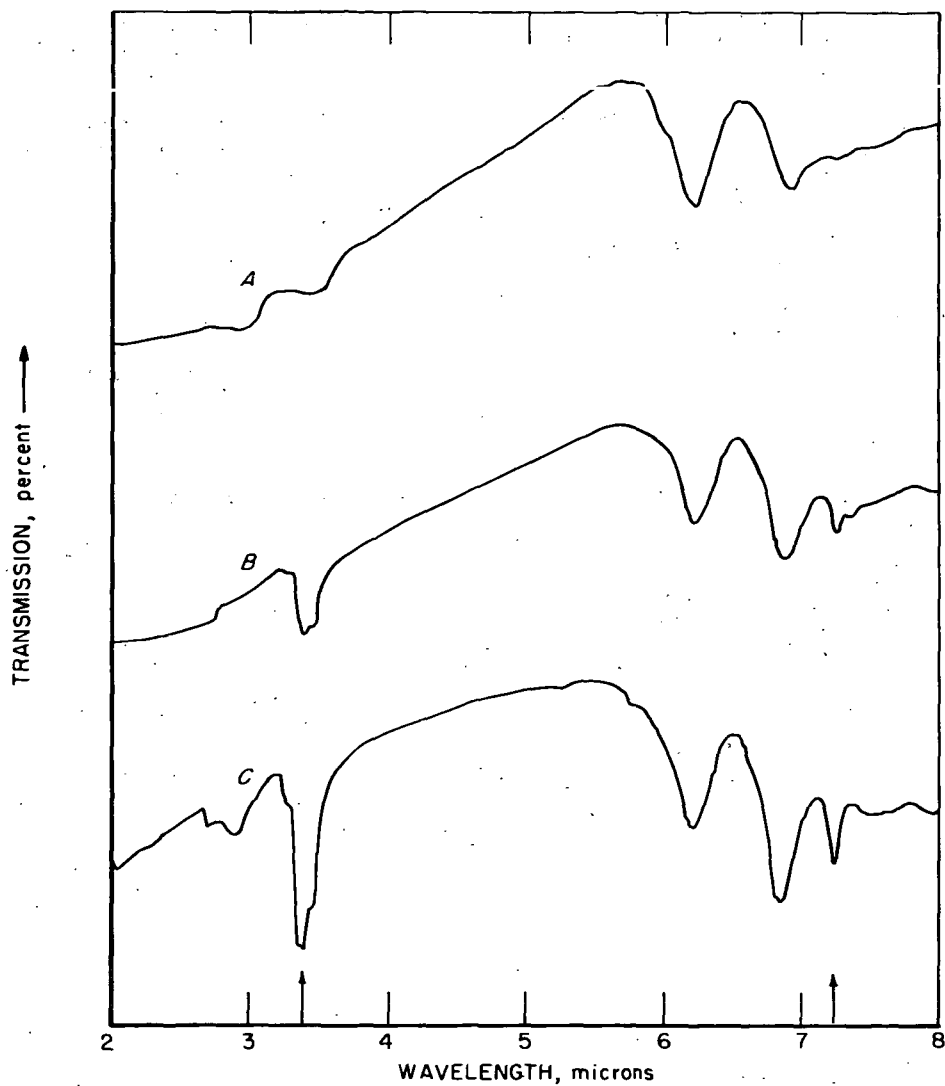


Figure 1.—Spectra of original and alkylated Pocahontas vitrains (*A*) original, (*B*) after one alkylation, (*C*) after two alkylations. Arrows indicate bands attributable to methyl group (7.25μ) and associated C-H stretching vibration (3.4μ).

L-10519

DESULPHURISATION OF COAL-OIL MIXTURES BY ATTRITION GRINDING
WITH ACTIVATED IRON POWDER*

Joseph Winkler

General Foam Division
Tenneco Chemicals, Inc.
Valmont Industrial Park
Hazleton, Pennsylvania 18201INTRODUCTION:

Industrial progress and life itself inseparably depend on the quality of resources of water, land, and in particular, the air which we breathe. Air pollution, therefore, is of primary public concern and in all industrialized nations various steps are being undertaken to keep the air clean.

One of the main culprits of air pollution are fumes and gases from the combustion of fossile fuels. The principal toxic constituents of combustion gases are Sulphur Oxides from the Sulphur contained in Coal and in Fuel-Oils, derived from high-sulphurous crude oils. Excessive pollution of Air with combustion gases containing these sulphur oxides is understandably increasing with population growth, urbanisation and industrial expansion. No wonder, therefore, that in the United States, the 90th Congress passed the Air Pollution Bill No. 780 late in 1967 and has authorized close to a half billion dollars for a three-year program to combat Air Pollution. One of the points of this bill is for the U. S. Department of Health, Education, and Welfare to conduct Research on fuel beneficiation, leading to the elimination of Sulphur Oxides emission into the atmosphere.

To control air pollution caused by fumes and gases from combustion of high-sulphur fossile fuels, two basic approaches can be made:

1. To clean the combustion fumes and gases from Sulphur Oxides at their generation source prior to the release into the atmosphere;
2. To reduce the sulphur content of the fossile fuels BEFORE their combustion.

This short presentation is in the scope of the second approach, and I am attempting to show an economical, new way to remove Sulphur from Coal-Oil Mixtures.

I am fully aware that the experimental data presented herein is not conclusive and many questions remain to be answered by conducting of more detailed Research and Development work. This future work, however, should follow-up the present feasibility study in which, as it is given in the title of this lecture, organically bonded sulphur

• United States Patent 3,282,826 by Joseph Winkler

is being substantially removed from a Coal-Oil mixture by attrition grinding with activated powdery Iron.

Metals such as Iron, Nickel, Copper, Tin, Bronze, Lager Metal, etc. are capable to scavenge organically bonded sulphur from hydrocarbon type lube-oils under condition of friction. This has been well known for many decades.

For example, a lubricating oil which still contains some organically bonded sulphur because of insufficient refining, in use, very soon starts to show sludge formation. This sludge always analyzes for metallic sulphides.

It appears, therefore, that under high frictional forces occurring during the lubricating process in spite that the reactive surfaces of the contacting metallic surfaces are rather small and separated by a lubricating film, nevertheless, in time the organically bonded sulphur in the lubricating oil becomes slowly scavenged by the abraded minute metallic particles. In general, this phenomenon can be explained by the energetic preference of sulphur atoms to be bonded to metallic atoms rather than to carbon atoms.

As Metal Sulphides are insoluble in the lube-oil, this reaction proceeds further as the equilibrically preferred reaction.

When more favorable conditions are created, in which the used metal is in the form of a high surfaced fine powder, and its mixture with a sulphur containing oil-coal is most frequently and intimately attritionally mixed in a ball mill, it is obvious that in a shorter time a larger part of the organically bonded sulphur in the coal-oil mixture shall be scavenged by the metallic powder. The coal-oil mixture, from which molecules the sulphur atoms were abstracted, will under the reaction conditions partly depolymerise and partly polymerise, but in general a fluid fuel will result with a low sulphur content.

When this pasty reaction mixture is now diluted with a high boiling, good solvent, such as Tetralin* and centrifuged, the unreacted Metal and the Metal Sulphide having a relatively high specific gravity are easily separated from the reaction fluid, which now consists of an intimate dispersion of unreacted coal in an oily phase. After removal of the solvent, a low-sulphur, low-ash fuel results.

For the herein presented few exploratory experiments, the least expensive metal Iron Powder was used, although it might have been expected that Zinc, Tin, and Aluminum powders would perform better because of their higher atomic bond energy with Sulphur than Carbon.

However, the surface of Iron Powder easily becomes contaminated with reaction products with moist air, therefore, all commercial Iron Powders, even those which were made by hydrogen reduction have a partly oxidized surface. For that reason it was decided to prepare as much as possible a surface clean Iron Powder by the

* Tetralin - 1,2,3,4-Tetrahydronaphtalene - sp.gr. 60/60°F. = 0.971
m.p. = -30°C.; b.p. = 207°C.

following preactivation procedure:

A 0.1% benzene-absolute alcohol solution-dispersion of a mixture of three chemicals was percolated through the Iron powder.

This mixture consisted of a Cationic reducing wetting agent with an Organo-Tin compound doped with an Organo-Lead compound. (For patent reasons I do not feel free at this time to exactly identify these compounds.) After drying of the Iron powder in Nitrogen, it retained on the surface a plated-out, extra thin, metallic Tin film, whose weight was less than 0.05% of the weight of the Iron powder. Thus, what we really did was to deposit on the commercial Iron powder of a thin Tin-plate which, as we could observe under the microscope, was tenaciously adhering to the Iron powder surface even after the Iron powder was mixed into the coal-oil paste. This composition was applied with the expectation that the Tin plated Iron surface will initiate a Sulphur scavenging reaction, reminiscent of Melamid's Oil-Molten Tin cracking experience. The Tin plating of the Iron powder also appeared to prevent conglomeration of the Iron powder in the course of the grinding process.

Certainly, further considerable work should be done to explore how this really works and whether better wetting agents and activators can be found for that purpose. The use of radioactive tagging elements such as tritium and Fe_{59} incorporated into the wetting-activating compounds may elucidate their action.

EXPERIMENTAL:

I wish here to emphasize that the following presented herein few experiments should not give the impression that there is already on hand a developed method for Desulphurisation of Coal-Oil Mixtures. This is only a Feasibility Study in which I am only tentatively showing that by Attritional Grinding of a high-Sulphur containing paste made by solublizing Coal in Mineral Oil with a Sulphur Scavenging Metal such as inexpensive Iron powder, a quasi-metathetic reaction substantially appears to occur; this leading to a low-in-sulphur fuel, while producing Iron Sulphide as a commercially desirable by-product.

In order that this new method becomes inexpensive and practical, it should perform already at temperatures not much higher than 275°C.

Also the mixing-grinding reactor residence time should not be longer than 5 - 10 minutes. The reaction should also proceed preferably without the use of hydrogen because this requires high pressure working conditions. Hydrodesulphurisation is a too costly process for making a fuel only.

Finally, this new process should not produce appreciable amounts of low boiling volatiles resulting from high temperature decomposition of the oil and coal; this necessarily requiring a costly post-distillation step.

Only then, we may expect that the total production costs of a BTU shall be low enough to make it a practical desulphurisation method, competitive with the presently suggested H-oil process, which is using catalytic, high pressure hydrogenation of mineral oils.

Keeping all these considerations in view, for this limited feasibility study I have arbitrarily selected a conservative set of reaction constants, leaving for future much more extensive R & D work to find more efficiently working conditions:

The grinding time was five minutes at the grinding temperature of 250°C.

The grinder, equipped with a venting valve, was the well-known Union Process Company's Research Model Attritor No. 01.

This model has a grinding tank with a capacity of 750 cc. and delivered capacity of 200 - 400 cc.

To work at the intended high temperatures of 250 - 275°C., it was specially equipped with electrical wire heating and proper Teflon gasketing.

As grinding aids, steel balls of 15 mm. diameter were used.

The obtained from a supplier coal was predried and preground to an average 100 mesh. It was prepared from a high volatile coal grit, mined in the Mathies Mine in Washington county, near Pittsburgh, Pennsylvania. Its analysis after drying and grinding was:

Total Sulphur Content	1.70%	(of this, pyrite sulphur analyzed at 0.2%)
1. Moisture	0.10%	
2. Volatiles	39.00%	
3. Fixed Carbon	55.00%	
4. Ash	5.90%	
	<u>100.00%</u>	

The Iron Powder was a Niagara 100 mesh grade from the Pyron Company, a subsidiary of AMAX. It was an almost 100% pure hydrogen reduced Iron.

A constant weight ratio of 1:1 of coal powder to the solubilizing-grinding oil was kept in all experiments. At room temperature, depending on the physical and chemical properties of the used oil, the resulting mixture was a soft to firm paste. At the reaction temperature of 250°C. all these pastes were still thixotropic fluids evolving some volatile fumes; this again depending primarily upon its IBP and the composition and volatility of the used oil. The Fuel Oil No. 6 fumed the most because of its lowest IBP of only 489°F.

For our experiments we have selected four grades of grinding oils:

1. A high naphthenic, low in aromatics oil: Tufflo 6094 from Sinclair Oil Company. This oil analyzed: Aromatics - 8% and total sulphur - Less than 0.001%

2. A high aromatic oil: Mobilsol 66 from Mobil Oil Company. This oil analyzed: Aromatics - 95% and total sulphur - only 0.4%

3. A high aromatic oil: Aromatic RFC Extract and Concentrate from Enjay Chemical Company. This oil analyzed: Aromatics - 88% and total sulphur - 1.30%

4. A typical Fuel Oil No. 6 from Humble Oil and Refining Company. This oil analyzed: Aromatics - 65% and total sulphur - 2.60%

It is evident from the above and Table I, which gives a more complete analysis of these four grinding oils, that two highly aromatic oils were used, but one with a low and the other with a relatively high Sulphur content.

A third oil, Tufflo 6094, which is very low in aromatics and sulphur-free, was tested. It was interesting to test such an oil for its solubilizing power for the coal powder and consequently to find out what relatively the percentage of sulphur removal from the coal will result when dispersed and solubilized in such a poorly solvating oil.

Finally, for practical reasons a typical Fuel Oil No. 6 (Bunker Oil C) was included. This, first to establish its solubilizing power for a coal, and at the same time to tentatively find out whether our new process can substantially reduce the Sulphur content in such a coal-oil mixture to the desired below one percent.

Thus, with one type of a high volatile coal and four grades of grinding oil, four double basic experiments were run as follows:

Each grinding oil and the Coal-Iron powder were mixed: One batch while only using the agitator without the steel balls in the Attritor No. 01; the pairing batch was made with the steel balls. For this twin experiment all other conditions of time, temperature, and amount of ingredients, etc. were identical.

The results of these eight typical experiments are presented in Table II.

PROCEDURE:

Before their discussion I wish to detail the experimental procedure applied for any single run:

In a separate stainless steel one liter beaker, equal weight parts of the before described dried coal powder and the oil at a temperature of 100°C. were spatula mixed until a uniform paste resulted. To this paste a calculated amount of freshly activated Iron powder was admixed.

For each experiment the Iron powder was calculated on the basis of the average Sulphur content in the 1:1 oil-coal mix, sufficient to fully scavenge the Sulphur giving FeS. From this mixture a small known sample was removed and held back for analysis. When Steel Balls were used, these balls put into Attritor 01 up to about 25% of its volume; this while moving around the steel balls in the tank of the Attritor which was preheated to about 250°C. The also preheated to about 250°C. Coal-Oil-Iron Powder paste was added slowly--all while agitating the balls, thus filling-up all the free space between the balls until the total filled volume was about 75% and the average charge was 250 grams. When no steel balls were used, a steel double scraper with a tank wall tolerance of one millimeter was attached to the agitator and again the Attritor's tank was filled up to its 75% volume with the same Coal-Oil-Iron Powder mixture.

In all experiments, as indicated before, the volume of the scraper equaled the used volume of the steel balls.

The mixing time was, as before, 5 minutes while the reaction temperature was kept at 250°C. which, occasionally when steel balls were used climbed up to 275°C.--this mainly due to frictional heat.

After the reaction, the mixing and heating was discontinued and while hot the mixture was strained from the grinding balls (whenever they were used) and cooled to a temperature of about 150°C.

Four graduated 100 ml. centrifuge tubes were in the meantime filled to a half mark with Tetralin heated to 160°C. Into these tubes, while well mixing up to the 100 ml. mark the 150°C. hot, Coal-Oil-Iron powder reaction product was filled and all of the four tubes were centrifuged.

The centrifuge tubes were of the 3011-F45 type as depicted in Thomas Catalogue on page 221 with constricted neck and tampered bottom graduated from 0 to 1 in 0.05 ml., from 1 to 3 ml. in 0.2 ml., from 6 to 10 ml. in 0.5 ml., and 10 to 100 ml. in 1 ml. divisions.

The used centrifuge was the Explosion-Proof, International Model 2-EXD, as depicted in Thomas Catalogue on page 185. The centrifuging head for the tubes was the 2943-A15 type--each holding simultaneously four 100 ml. tubes, described above. The centrifuging speed was about 2100 rpm.

The centrifuge was not heated and centrifuging time was kept in all experiments at 5 minutes, while the centrifuging temperature fluctuated from the initial 150°C. to about 120°C. at the end due to intermittent cooling-off.

After centrifuging we could notice in the tubes four poorly visible layers:

1. In the bottom tip the unreacted blackish hard residue, which could be identified as Iron Powder, partly contaminated with Iron Sulphide.
2. On top of it, a black soft layer, identified as Iron Sulphide, partly contaminated with Coal particles.
3. On top of it an Oil-Tetralin-Coal deep brown viscous layer.
4. The upper top was a rather clear brown Oil-Tetralin solution.

Our main interest was to analyze the two upper liquid layers on its sulphur content, which was done in the following way:

When still hot the two upper layers were carefully decanted. Tetralin was added to the tube, well shaken, and again centrifuged. Afterwards, the upper liquid was again carefully decanted from the tube and this procedure was repeated once more. Thus, finally on the bottom of the centrifuge tube we had a Tetralin wet mixture of unreacted Iron Powder mixed with Iron Sulphide and sulphur-rich insoluble in Tetralin polymerisates. This Residue was carefully collected into a beaker, twice washed with Hexane and dried. From

this black powder the Iron particles as much as possible were magnetically removed and the remaining powder analyzed for Sulphur in a Parr Bomb by the usual BaSO_4 gravimetric method.

In all eight experiments we found a Sulphur content almost matching the Sulphur loss in the analyzed desulphurised oil-coal mixture.

The upper two layers from the centrifuges were mixed together with the Tetralin washings of the two lower layers, and Tetralin was distilled off from a small flask at about 200 - 210°C.

Finally we got a highly viscous, almost pasty, brown-black residue containing more or less suspended fine particulate coal; this depending upon the used grinding oil.

This residue was analyzed in a Parr Bomb for total sulphur. The results are presented on Table II.

In addition to these eight experiments a ninth experiment was made, in which the not activated Iron powder was used with the Coal-Fuel Oil No. 6 mixture. The comparative results are shown on Table III.

DISCUSSION AND CONCLUSIONS:

From the results shown on Tables II and III, we can tentatively make the following deductions:

1. Attritional grinding of a powdery high bituminous coal dispersed in a heavy mineral oil with Iron powder effected in five minutes at a temperature as low as 250°C. gives a higher degree of total sulphur removal than by conventional mixing. While for a straight mixing operation the Sulphur removal from three Coal-Oil mixtures averaged only 22%, attritional grinding with the same activated Iron Powder gave under otherwise identical working conditions a Total Sulphur removal as high as 53%.
2. Attritional grinding of a 1:1 dispersion of a high bituminous coal in Fuel Oil No. 6 with a non-activated Iron Powder and a specially activated Iron Powder gave a comparatively higher degree of Sulphur removal for the activated Iron Powder of 56% against 44% for the former.
3. For best Sulphur removal from Coal, the dispersing oil should contain predominantly aromatic compounds. This is shown clearly in Table II where two dispersing oils, one with an 8% aromatic content (Tufflo 6094), the other with 95% aromatic content (Mobilsol 66), were used for the same Coal. The first gave only an 11% Sulphur removal; the second gave 57% Sulphur removal.
4. The Sulphur removal from two Coal-Oil mixtures--the first being Mobilsol 66 which has a low Sulphur content of 0.4%, the second RFC Extract containing a triple percentage of Sulphur of 1.30%, give a similar percentage of removal of about 50%. This appears to imply that the Sulphur can be substantially removed not only from the Oil but also from the Coal, again provided that the Oil is of a highly aromatic type.

5. Mixtures of a Coal Powder, analyzing it at over one percent of total sulphur with a commercial Fuel Oil, which contains as high as 2.6% of organically bonded sulphur, can be desulphurised by the herein presented Attritional Grinding Method, while using a specially activated Iron Powder giving a down to less than one percent of Total Sulphur Fuel mixture.

FUTURE WORK:

The author believes that in R & D Work this process can be improved. This can be done by finding more favorable processing conditions. In particular, it is expected that by applying a higher reaction temperature and possibly increasing processing time over 5 minutes a higher degree of Sulphur removal can be attained.

It is also hoped that better Iron activators can be found--this may help in arriving at a lower in Sulphur Coal-Oil Fuel.

Further exploration of this new approach to Coal-Oil Desulphurisation appears worthwhile also for economical reasons. This because the expected processing conditions are rather mild, and the equipment for Grinding, Centrifuging, and Solvent Stripping are well developed and already available on an industrial scale. The high price of Sulphur, which by the presented method is produced as a by-product, should also contribute considerably to the lowering of processing costs.

TABLE I - PROPERTIES OF GRINDING OILS

Type of Grinding Oil	Tufflo 6094	Mobilsol 66	RFC Extract	Fuel Oil No. 6
Producer	Sinclair	Mobil	Enjay	Humble
Sulphur Content	None	0.4	1.3	2.6
Spec. Gr. 60/60°F.	0.9177	1.1050	1.054	0.969
Viscosity SSU at 100°F.	880	160	320	170
Viscosity SSU at 210°F.	190	38	62	35
Flash Point COC - °F.	425	385	405	180
ASTM Vac. Dist. (Cor. to Atm.)				
IBP	610	638	556	489
10%	780	697	644 (5%)	596
50%	821	724	776	927
90%	870 (95%)	793	1097	Cracked 971°F.
FBP	882	819	1126	Yield 62%
Clay/Gel Analysis				
Aromatics	8.0	95.0	88.0	65.0
Naphthenes + (Paraffin)	52 + (40)	1.0	10.0	12 + (8)
Polar Material	None	4.0	0.5	3.0
Asphaltenes	None	None	1.5	12.0
Carbon Type Analysis				
Aromatics Carbons	None			
Paraffinic Carbon	43			
Naphtenic Carbons	57			

TABLE II

Used Grinding Oil	Tufflo 6094	Mobilisol 66	RFC Extract	Fuel Oil No. 6
Analyzed total Sulphur content in the oil-coal mixture <u>prior</u> to the addition of the Iron Powder and before processing	0.85	1.05	1.50	2.15
Analyzed total Sulphur content in the oil-coal mixture after <u>only</u> mixing in the Attritor <u>01</u> without the steel balls	0.80 (or a re- duction in "S" content of 6%)	0.80 (or a re- duction in "S" content of 24%)	1.20 (or a re- duction in "S" content of 20%)	1.70 (or a re- duction in "S" content of 21%)
Analyzed total Sulphur content in the oil-coal mixture after attritional grinding with the steel balls	0.75 (or a re- duction in "S" content of 11%)	0.45 (or a re- duction in "S" content of 57%)	0.80 (or a re- duction in "S" content of 47%)	0.95 (or a re- duction in "S" content of 56%)

REMARKS:

In all experiments we could detect in the Residue, described in the text of this presentation, corresponding values of Sulphur which were scavenged with the Iron Powder.

TABLE III

Used Grinding Oil	Fuel Oil No. 6
Analyzed Total Sulphur Content in the Oil-Coal mixture after attritional grinding with the steel balls.	0.95 (or a reduction in "S" content of 56%)
The Iron powder was activated.	
Analyzed Total Sulphur Content in the Oil-Coal mixture after attritional grinding with the steel balls.	1.20 (or a reduction in "S" content of ONLY 44%)
The Iron powder was NOT activated.	

Some Pumping Characteristics of Coal Char Slurries

M. E. Sacks, M. J. Romney, and J. F. Jones

FMC Corporation, Chemical Research and Development Center
Princeton, New Jersey

As part of the program sponsored by the Office of Coal Research for increasing coal markets, Project COED (Char Oil Energy Development) is aimed at 1) developing an economic process for upgrading coal energy by converting coal to an oil, a gas, and a fuel char, and 2) decreasing the delivered cost of coal energy (1). One possible method for lowering the delivered cost of coal energy is to transport the char in a slurry to market. The pumping of solid fuels in a slurry is not new. Consolidation Coal Company demonstrated the feasibility of pumping coal-water slurries in a 108-mile coal pipeline (2). Char from a COED plant could be conveyed either in a water or oil slurry. Alternately, the char could be pumped in a water slurry with intermittent slugs of COED oil. The objective of this study was to obtain preliminary data in order to evaluate the technical feasibility of transporting char in a pipeline as a slurry.

The viscosity of char slurries was measured to determine the effects of char loading and size distribution. This survey was followed by extensive testing in an experimental pipeline.

Slurry Material

Water and two different oils--mineral oil and a petroleum recycle oil--were used as slurry media. The latter oil was used because it was similar to the product oil from a COED plant. The viscosities of the two oils were 36 and 8 cp at 100°F.

The char used for the slurries was obtained from pyrolysis of Utah A-seam coal in a multistage fluidized-bed process developed under Project COED (1). Its properties are listed in Table I.

Initial Viscosity Measurements

A rotating-spindle viscometer, Brookfield Model RVT, was used in these studies. The depth to which the spindle was inserted into the slurry, the time required for the measurement, and the temperature of the slurry were duplicated for each test. Slurry viscosities were determined at 100°F.

For char loadings higher than 25 weight percent, the viscosities of the two char-oil slurries were nearly the same, although the viscosities of the pure slurry media differed by a factor of 3.5 (Figure 1). The viscosities for the water slurries were lower at the same solids concentration.

The size consist of the char has a large effect on the observed viscosity of the slurry. Size consists for eight slurries are shown in Table II. The size distributions have two distinct peaks. One occurs between 16 and 100 mesh, and the other below 325 mesh. The average particle size was changed by varying the relative size of these two peaks. Test No. 8 is different from the others in that a large proportion of plus 16-mesh char is present with little material between 48 and 325 mesh. This slurry had a viscosity of 184 cp,

while the slurry in Test No. 4, which had the same average particle size, had a viscosity of 288 cp. Thus, a size distribution containing large and small particles, but no intermediate ones, may be desirable. This confirms the conclusions of Moreland (3) and Reichl (4).

Tests made on a 50 percent char-water slurry indicated that a minimum viscosity occurs when about one half of the char is minus 325-mesh material.

Some results of tests made employing different rotational speeds of the viscometer are given in Table III. These indicated that concentrated slurries exhibit non-Newtonian behavior. Further aspects of this non-Newtonian behavior will be discussed later.

Experimental Pipeline

A sketch of the pipeline used for testing the pumpability of char slurries is shown in Figure 2. The major components are:

1. A centrifugal pump with an open impeller and a 15 hp motor.
2. A 150-gallon slurry tank with an attached mixer for agitation.
3. A 55-gallon weigh drum for determining volumetric flow rates.
4. About 100 feet of 1-inch schedule 40 pipe arranged for recycle to the weigh tank or slurry tank.
5. Pressure-measuring devices consisting of diaphragm pressure seals, 6-inch dial gauges, and mercury manometers.

Known weights of char and slurry media were charged to the slurry tank and allowed to mix at least one hour before taking measurements to allow for absorption of the media in the pores of the char. Flow rates in the test section were controlled by by-passing a portion of the flow from the pump back to the slurry tank. Flow rates were determined by diverting the flow from the test section to a weigh tank. Average linear velocities ranged from 1 to 20 feet per second.

The pressure drop was measured over a 20-foot section with dial gauges and manometers. Pressure drops varied from 1 to 10 psi over the 20-foot section.

Pipeline Results

Figure 3 shows the effect of char concentration on pressure drop for char-mineral oil slurries at two linear velocities. Similar curves were obtained with char-water slurries. At low char loadings, the pressure drop increased only slightly over that of the liquid. After a certain loading was reached, however, the pressure drop rose very rapidly with further increases in char loading. The two oil slurries could no longer be pumped above a solids loading of 44 weight percent.

At low char loadings, the pressure drop obeyed the relationship:

$$\frac{\Delta P}{L} = k \bar{V}^a \quad (1)$$

The exponent was 1.72 for the two oil slurries, and 1.92 for the water slurries. This relation held for concentrations up to 25, 30, and 40 weight percent for the mineral oil, recycle oil, and water slurries, respectively, and for velocities as low as 3 ft./sec. The experimental data illustrating this relationship are shown in Figure 4. At higher concentrations the pressure drop was dependent on a smaller power of the velocity. This is an indication of the transition region between laminar and turbulent flow. However, dilute slurries could not be pumped in the laminar regime and concentrated slurries could not be pumped in the fully turbulent regime with the existing experimental equipment.

The effect of particle size on pressure drop was determined for char-water slurries. The addition of large amounts of minus 325-mesh char caused a marked decrease in the pressure drop, compared to that of a slurry with equal total solids loading but no fine material. Slurries with solids concentrations up to 50 percent were easily pumped. The quantitative effect of this fine material is shown in Figure 5 for two velocities at a total solids loading of 50 percent.

Discussion

An attempt was made to correlate the pipeline data on a friction factor-Reynolds number plot using the viscosity determined on the Brookfield viscometer. Such a correlation would be expected to exist, provided that the slurry can be described in terms of the properties of an equivalent fluid. The general shape of these plots were characteristic of the well known correlations for Newtonian fluids. The transition from laminar to turbulent flow was readily apparent. However, the quantitative results were not satisfactory. The transition to turbulent flow occurred at a Reynolds number of 1200 for char-mineral oil slurries and at a value of 600 for char-water slurries. In addition, the laminar data for the char-water slurries were not correlated by a single line. There was a definite trend towards higher friction factors with decreasing particle size (increasing minus 325-mesh). Hence, the effect of the size distribution was not completely accounted for by the equivalent Newtonian fluid properties of viscosity and density. This confirmed the non-Newtonian behavior indicated by the viscometer results.

A possible non-Newtonian model is the two-parameter Bingham fluid (5). This model gives the following relation between the shear stress and the shear rate:

$$\tau = -\eta \frac{du}{dr} + \tau_y \quad \tau > \tau_y \quad (2a)$$

$$\frac{du}{dr} = 0 \quad \tau < \tau_y \quad (2b)$$

This equation can be integrated (5) for pipe flow to give

$$q = (\bar{V}S) = \frac{\pi \Delta P R^4}{8\eta L} \left[1 - \frac{4}{3} \frac{\tau_y}{\tau_w} + \frac{1}{3} \left(\frac{\tau_y}{\tau_w} \right)^4 \right] \quad (3)$$

If the yield stress is small compared to the wall stress, the last term in the brackets may be neglected. Rearrangement and the insertion of $(\Delta P/L) R/2$ for the wall shear transforms Equation (3) into

$$\frac{\Delta P}{L} = 8 \left[\frac{\eta \bar{V}}{R^2} + \frac{\tau_y}{3R} \right] \quad (4)$$

The laminar data for char-water slurries are in agreement with this model. Pressure drop-velocity data were fitted to Equation (4). The resulting values of yield stress and plasticity are tabulated in Table IV.

The failure of the friction factor-Reynolds number plot to correlate the data can now be explained. The dimensional analysis leading to this correlation was based on only one rheological parameter, the Newtonian viscosity. If the two Bingham parameters are taken into consideration, a third dimensionless group is required (6, 7, 8). This is the Hedstrom number:

$$N_{He} = \frac{\rho \tau_y D}{\eta^2} \quad (5)$$

The Reynolds number is now based on the plasticity instead of the Brookfield viscosity:

$$N'_{Re} = \frac{\rho \bar{V} D}{\eta} \quad (6)$$

The data for char-water slurries in laminar flow were plotted using these dimensionless parameters in Figure 6. One set of data for char-oil slurries and a set for coal-oil slurries (9) are included. This correlation indicates that the Hedstrom number is about 1000, which is consistent with the value calculated from experimental yield stresses.

Some assumptions were required to obtain the curve for the turbulent region in Figure 6. At high shear rates, corresponding to turbulent flow,

$$-\eta \frac{du}{dr} \gg \tau_y$$

and Equation (2a) can be approximated by

$$\tau = -\eta \frac{du}{dr} \quad (7)$$

The slurries in turbulent flow can now be treated like Newtonian fluids.

An equation of the Blasius (5) form

$$f = k'' (N_{Re}')^b$$

was assumed for turbulent flow. Forcing Equation (1) into this form yields:

$$f = k' (N_{Re}')^{a-2} \quad (8)$$

Data from Figure 4 were transformed from the coordinates of head loss versus velocity to those of f versus N_{Re}' by using Equation (8). The error introduced by these approximations was never more than 20 percent. The result is a reasonable representation of the turbulent regime in Figure 6.

The most significant aspect of this correlation is the predicted suppression of turbulence at high Hedstrom numbers. Since the Hedstrom number is proportional to the square of the pipe diameter, it becomes increasingly important when attempting scale-up.

Economics

From the predictions of the correlation in Figure 6 and the properties of the slurries studied, a preliminary estimate of pumping cost was obtained. Figure 7 shows the estimated cost on a cents per ton per mile basis as a function of pipe diameter. Only those costs which are dependent on pipe diameter are included. At the diameter corresponding to the minimum in the total cost curve, the pumping cost is 0.16 cents per ton per mile. This is comparable to the operating costs of other commercial slurry pipelines (2).

In the final economic evaluation, several other factors need to be considered. The costs in Figure 7 do not include terminal facilities. These include not only capital investment in pumping stations, but slurry preparation and separation facilities as well. The effect of the extra fine material, which must be added, on product value has not been determined.

Acknowledgment

The authors thank the Office of Coal Research, Department of the Interior, and the FMC Corporation for permission to publish this paper. The authors also thank C. R. Allen for performing the initial work, and C. A. Gray for counsel during the investigation.

References

1. Jones, J. F., Eddinger, R. T., and Seglin, L., CEP, 62, 2, 73-79 (1966).
2. Reichl, E. H. and Thager, W. T., "Economics and Design Requirements of Pipeline Transport for Coal Slurry", Paper No. CPA 62-5113, National Power Conference, September, 1962.
3. Moreland, C., "Viscosity of Suspensions of Coal in Mineral Oil", The Canadian Journal of Chem. Engr., February, 1963.
4. Reichl, E. H., "Transportation of Coal by Pipelines", U. S. Patent No. 3,073,652 (1963).
5. Bird, R. B., Stewart, W. E. and Lightfoot, E. N., Transport Phenomena, John Wiley and Sons, Inc., New York-London (1960).
6. Thomas, David G., Ind. Eng. Chem., 55, 11, 18-29 (1963).
7. Ibid, 55, 12, 27-35 (1963).
8. Michiyoshi, I., Matsumoto, R., Mizuno, K., and Nakai, W., International Chemical Engineering, 6, 2, 383-8 (1966).
9. Berkowitz, N., "Some Newer Concepts in Solids Pipelining", Contribution No. 199 from the Research Council of Alberta, Edmonton, Canada (1963).

Nomenclature

a	Constant defined in Equation (1). Dimensionless
b	Constant
D	Pipe diameter, ft.
f	Fanning friction factor = $\frac{D}{4} \frac{\Delta P / L g_c}{1/2 \rho V^2}$ Dimensionless
k	Constant defined in Equation (1)
k'	Constant defined in Equation (8)
k''	Constant
L	Pipe length, ft.
N_{He}	Hedstrom number = $\frac{\rho \tau_y D^2}{\eta^2}$ Dimensionless
N'_{Re}	Modified Reynolds Number = $\frac{\rho \bar{V} D}{\eta}$ Dimensionless
ΔP	Pressure drop, psi
q	Volumetric flow rate, cu.ft./hr.
r	Radial distance, ft.
R	Pipe radius, ft.
S	Pipe cross sectional area, sq.ft.
u	Linear velocity, ft.sec. ⁻¹
\bar{V}	Average linear velocity, ft. sec. ⁻¹
$\frac{du}{dr}$	Shear rate, sec. ⁻¹
η	Plasticity defined by Equation (2a), lb _f sec.ft. ⁻²
ρ	Density, lb _m ft. ⁻³
τ	Shear stress, lb _f ft. ⁻²
τ_w	Shear stress at the wall = $\frac{P(R)}{L(2)}$ lb _f ft. ⁻²
τ_y	Yield stress defined by Equation (2a) lb _f ft. ⁻²

TABLE I
Physical Properties of Char

Properties	Before Pumping	After Pumping	
		Mineral Oil	Recycle Oil
Slurry Medium			
Density			
Bulk, lb./cu.ft.	27	34	-
Packed, lb./cu.ft.	31	41	-
Particle, g./cc.	0.79	-	-
Sieve Analysis, Tyler Mesh, cum. wt. %			
14	4	1	3
28	27	11	25
48	60	41	58
100	82	68	83
200	95	80	95
325	98	85	99
Average Particle Diameter, in.	0.009	0.005	0.009

TABLE II
Effect of Minus 325-Mesh Char Content on the Viscosity of a Char-Oil Slurry

Test No.	Char Size Consist. wt. % on Tyler Screen							Average Particle Diameter, in.	Viscosity of a 44 wt. % Char-Oil Slurry at 100°F., cp.
	16	28	48	100	200	325	Minus 325		
1	5.6	21.2	36.8	23.4	10.8	1.3	0.9	0.00739	616
2	5.1	19.3	33.4	21.2	9.8	1.2	10.0	0.00447	344
3	6.0	19.0	30.0	14.0	9.0	4.0	17.0	0.00344	328
4	4.5	17.1	29.7	18.9	8.7	1.1	20.0	0.00323	288
5	4.0	15.0	26.0	16.5	7.6	0.9	30.0	0.00252	250
6	3.4	12.8	22.3	14.2	6.5	0.8	40.0	0.00205	180
7	0.3	11.0	26.4	17.6	10.6	6.6	27.5	0.00245	202
8	31.0	20.5	12.0	6.1	2.6	1.1	26.5	0.00310	184

TABLE III

Viscosity of a 40 Weight Percent Char-Water Slurry
at Different Rotational Speeds of Viscometer

<u>Rotational Speed, rpm</u>	<u>Apparent Viscosity Measured With a Brookfield RVT Viscometer Using Spindle No. 2</u>
100	132
50	260
20	455

TABLE IVRheological Parameters

<u>Nominal Total Solids Concentration, wt. %</u>	<u>Minus 325- Mesh Char Concentration, wt. % of total solids</u>	<u>Yield Stress, τ_y lb_f/sq.ft. $\times 10^2$</u>	<u>Plasticity or Limiting Viscosity, η lb_f.sec./ sq.ft. $\times 10^4$</u>	<u>Measured Total Solids Concentration, wt. %</u>
50 char in water	47.5	4.13	5.84	50.4
	41.9	6.42	5.85	51.6
	36.9	2.53	8.02	47.4
	34.8	7.01	7.67	48.9
	28.6	5.27	10.52	52.3
45 char in water	28.6	5.49	6.55	45.4
38 char in recycle oil	-	(-6.96)	21.8	-
55 coal in oil	-	0.276	11.88	-

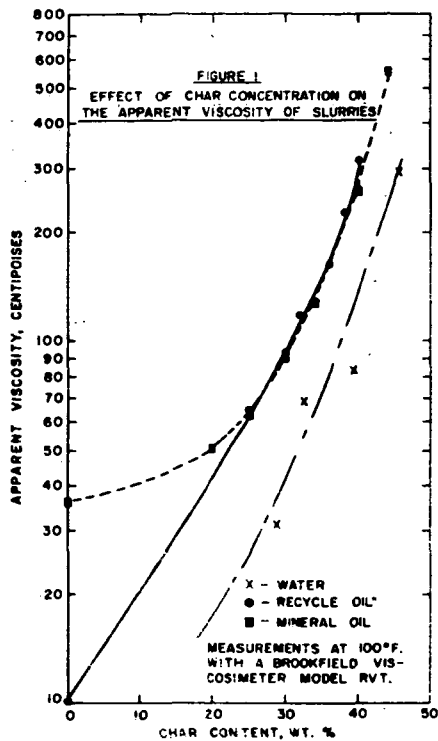
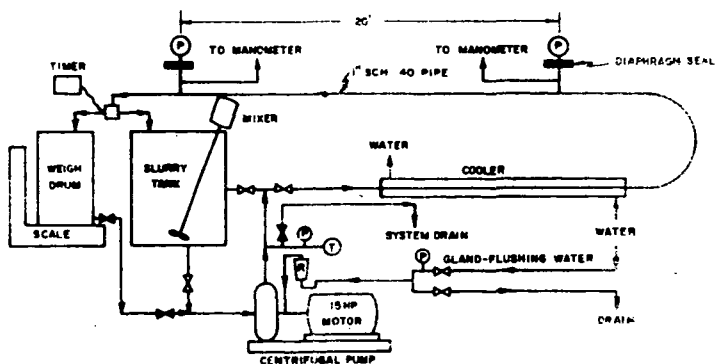


FIGURE 2
PIPELINE TEST SYSTEM



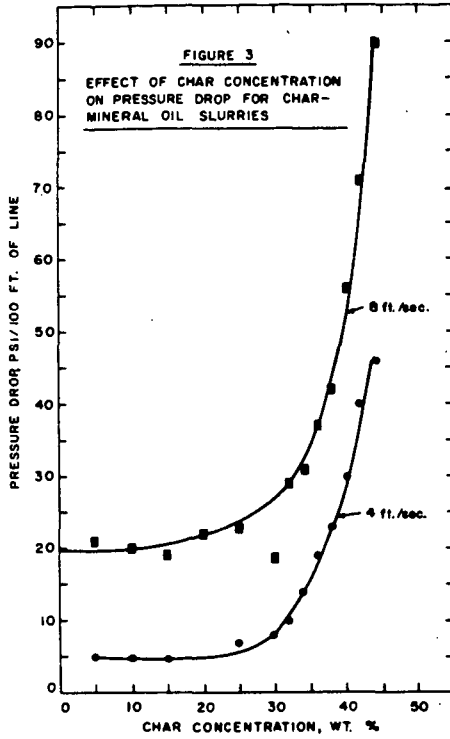


FIGURE 4
HEAD LOSS VERSUS VELOCITY FOR CHAR-WATER SLURRIES WITH SOLIDS CONCENTRATIONS FROM 21 TO 39 WEIGHT PERCENT

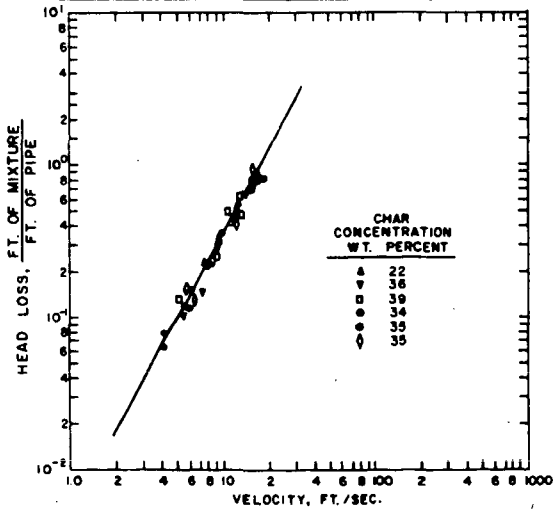


FIGURE 5
 EFFECT OF CONTENT OF MINUS 325-MESH
 CHAR ON PRESSURE DROP
 FOR A 50-50 CHAR-WATER SLURRY

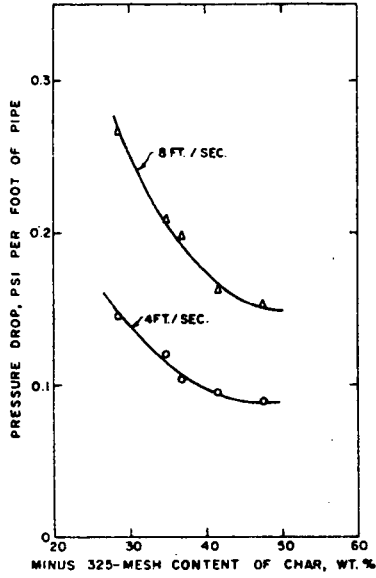


FIGURE 6
 MEDSTROM NUMBER-REYNOLDS NUMBER-FRICTION FACTOR PLOT

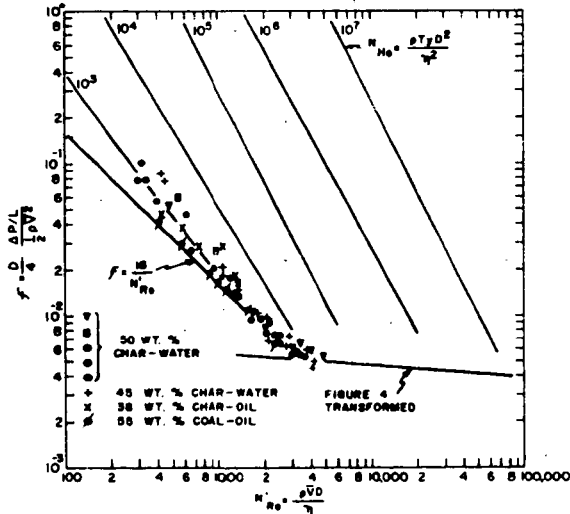
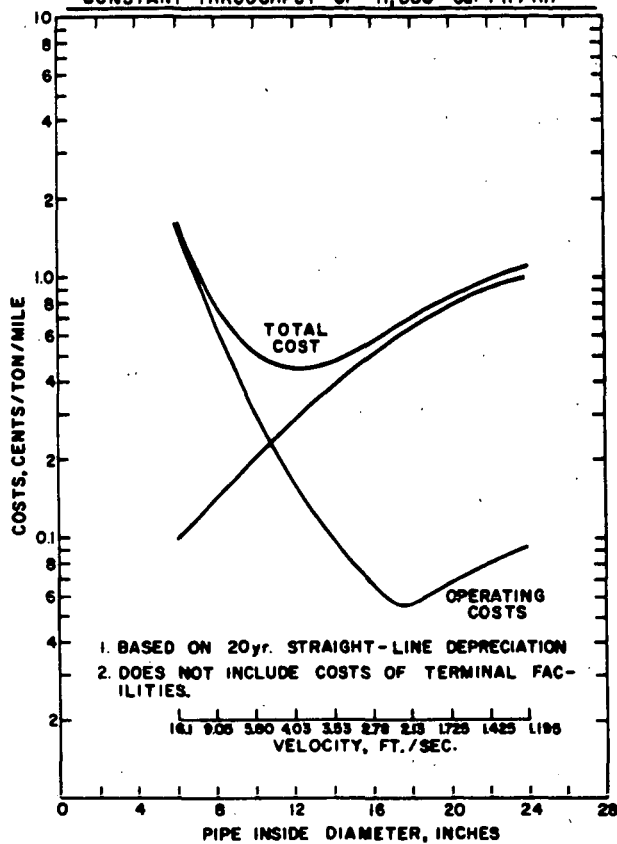


FIGURE 7
PIPE DIAMETER VERSUS COST OF PIPELINING FOR A
CONSTANT THROUGHPUT OF 11,380 Cu. Ft./Hr.



CONTROLLED LOW-TEMPERATURE PYROLYSIS OF BENZENE-EXTRACTED GREEN RIVER OIL SHALE

J. J. Cummins and W. E. Robinson

Laramie Petroleum Research Center
Bureau of Mines, U.S. Department of the Interior
Laramie, Wyoming 82070

INTRODUCTION

The present study was undertaken to determine the rate at which oil-shale kerogen decomposes and to determine the composition of the pyrolytic products formed at 300° and 350° C in a helium atmosphere at atmospheric pressure. A study of the thermal reaction at these low temperatures (150° to 200° C below normal retorting temperatures) is important because of the current interest in the in situ retorting processes of converting oil shale to shale oil. During in situ retorting it may take long periods of heating to raise the temperature of the oil shale from ambient temperature to the final retorting temperature, thus thermal reactions at intermediate temperatures may become important. The present study was made to investigate some of the possible variables in the thermal behavior of the oil-shale organic material as a function of time and temperature.

A number of investigators have studied the conversion of oil shale to pyrolytic products. Hubbard and Robinson⁶ investigated the oil-shale decomposition rates from 350° to 500° C. Dinneen³ studied the effect of various retorting temperatures on the composition of shale oil. Allred¹ presented some considerations on the kinetics of oil-shale pyrolysis. Hill and co-workers⁵ studied the thermal decomposition of kerogen in the presence of methane.

The present study extends the published data to a lower temperature range by discussing the kinds of products obtained at pyrolysis temperatures of 300° and 350° C and at pyrolysis times ranging from 12 to 96 hours.

EXPERIMENTAL

One-hundred-gram samples of benzene-extracted oil shale were heated at 300° or 350° C for selected periods of 12, 24, 48, 72, or 96 hours in a helium atmosphere at atmospheric pressure. The amounts of pyrolytic products that formed during the heating process (except gas and carbon residue) were determined. No attempt was made to determine the amount of gas and carbon produced because only small amounts are formed at these temperatures. The pyrolytic product that volatilized during the heating is called oil. The pyrolytic product that did not volatilize was recovered by extracting the heated residue and is called bitumen.

Oil-Shale Sample. The sample of Green River oil shale used in this study was obtained from the Bureau of Mines demonstration mine near Rifle, Colorado. The sample assayed about 66 gallons of oil per ton of shale, contained 30.2 percent organic carbon, and contained 7 percent benzene-soluble bitumen. Prior to heating, the shale was crushed to pass a 100-mesh sieve and then benzene extracted five times, each time with fresh solvent, until it was essentially free of soluble organic material. This was demonstrated by the decreasing recovery with each successive extraction. The extracted sample was then dried at 60° C under reduced pressure until free of benzene.

The percent organic carbon in the extracted oil shale and in the pyrolytic residues was determined by combustion analysis. The results were used as a measure of the kerogen decomposition.

Apparatus. The pyrolysis apparatus used in this investigation is capable of heating a 100-gram sample of oil shale. Weighed samples were pyrolyzed in a stainless-steel boat housed in a Pyrex combustion tube 800-mm long x 50-mm o.d. One end of the combustion tube was equipped with a metal cap having a sliding metal bar through the middle of the cap and a gas inlet tube in the side of the cap. The metal bar was used to move the boat in or out of the hot zone of the furnace. The other end of the combustion tube was connected to two traps in series, a water-cooled trap followed by a Dry Ice trap.

Recovery of the Products. The volatile product (oil) that condensed in the water-cooled trap was recovered with benzene. After the benzene was removed, the product was dried and weighed. The heated residue was cooled in the outer end of the combustion tube in the presence of helium. After cooling, the heated residue was placed in a Soxhlet extractor and extracted with benzene for 16 hours. The nonvolatile product (bitumen) recovered from the benzene solution by evaporation of the benzene, was dried and weighed. The residue was dried under vacuum at 60° C and weighed. The percent organic carbon remaining in the heated residue was determined, and the percent unconverted organic carbon was calculated from this determination and from the results of a similar determination on the starting material. Most of the pyrolytic gases were trapped in the Dry Ice trap. The trap was allowed to warm to room temperature. The weight of the product was used to estimate the amount of gas formed.

Fractionation of the Oil and Bitumen. Each oil and each bitumen were fractionated using standard procedures.² The product was allowed to stand in pentane at 0° C for 16 hours thereby separating the material into pentane-soluble and pentane-insoluble fractions. After the pentane was removed, the pentane-soluble material was placed on an alumina column using a 1 to 25 ratio of sample to alumina and was fractionated by elution chromatography into hydrocarbon concentrate and resin fraction. The hydrocarbon concentrate was placed on a silica-gel column, using a 1 to 25 ratio of sample to silica gel, and separated into an alkanes-plus-olefins fraction and an aromatic-oil fraction. The alkanes plus olefins were placed on a silica-gel column using a 1 to 60 ratio of sample to silica gel and fractionated into alkane and olefin fractions using a method developed by Dinneen and co-workers.⁴ The alkanes were placed on 5 Å molecular sieves and separated into an n-alkane fraction and a branched-plus-cyclic alkane fraction. The n-alkanes were fractionated using a programmed GLC at a heating rate of 7.5° C min⁻¹ and using a 5-foot, 1/4-inch SE 30 column.

RESULTS AND DISCUSSION

The results of this study will be discussed in terms of the amount of pyrolytic products formed, the conversion of kerogen to oil and bitumen, and the order of thermal reactions. In addition, the distribution of individual components of the thermal products and their rates of formation will be discussed. As an aid to planning future studies, the conversion of kerogen to pyrolytic products at temperatures lower than 300° C was estimated.

At low temperatures kerogen is converted mainly to oil and bitumen. The amount of gas formed at 300° and 350° C was less than 1 percent of the total pyrolytic products. The amount of carbon residue formed at 300° and 350° C, although not determined, was assumed to be less than 1 percent of the pyrolytic product. Thus, the pyrolytic gas and carbon residue formed were

not considered separately in this report. Any carbon residue formed was included in the unconverted kerogen value and any gas formed was included in the kerogen converted value.

The amounts of pyrolytic products formed at 300° and 350° C at different time intervals appear in table 1. The percent of the kerogen converted to pyrolytic products is based on the

TABLE 1. - The amount of pyrolytic products formed

Time, hours	$(100X)^{1/2}$	1-X	Log (1-X)	Weight percent of pyrolytic products	
				Oil	Bitumen
300° C					
12	5.4	0.946	-0.0241	73	27
24	7.4	.926	- .0334	69	31
48	8.6	.914	- .0391	77	23
72	9.7	.903	- .0443	78	22
96	11.0	.890	- .0506	76	24
350° C					
12	34.9	.651	- .1864	62	38
24	40.2	.598	- .2233	63	37
48	51.4	.486	- .3134	72	28
72	61.8	.382	- .4179	77	23
96	64.3	.357	- .4473	94	6

$1/2$ Kerogen converted, weight percent of total kerogen.

difference between the organic carbon content of the sample before heating and the organic carbon content of the heated residue after the removal of the volatile and soluble products. At each temperature, the amount of kerogen converted to pyrolytic products doubled when the heating time was increased from 12 to 96 hours. Approximately a sixfold increase in the amount of kerogen converted was obtained when the temperature was increased from 300° to 350° C.

The kerogen is converted to a volatile oil product and to a nonvolatile bitumen during pyrolysis. At both temperatures the amount of volatile oil formed is greater than the amount of bitumen formed. A large decrease in the amount of bitumen was obtained at 96 hours over that obtained at 72 hours at 350° C. This indicates that the bitumen degraded and volatilized as oil.

The conversion of kerogen to oil and bitumen at 300° C is shown in Figure 1 where concentration is plotted against time. The oil-plus-bitumen curve rises sharply for the first 24 hours, then tends to level off from 24 to 96 hours. Similar trends are apparent in the oil and bitumen curves. These trends suggest that the conversion of bitumen to oil is negligible at 300° C. In contrast, a similar plot of the 350° C data (Figure 2) shows that the bitumen curve decreases after 72 hours and tends toward zero at 96 hours. The oil curve continues to rise between 72 and 96 hours. The latter results support the findings of Allred¹ and Hubbard and Robinson⁶ who suggest that kerogen is converted to bitumen and the bitumen is in turn converted to oil.

To determine the order of the thermal reaction of kerogen at 300° and 350° C, the log of the kerogen concentration [$\log(1-X)$ shown in table 1] was plotted against time for each temperature. Reasonably straight line relationships were obtained for the 300° C data (Figure 3) and the 350° C data (Figure 4) showing that the overall thermal conversion of kerogen at these temperatures is probably first order.

The specific reaction rates at each temperature were calculated from the slope of the curves in the log concentration-time plots and equal 2.303 times the slope of the curve. The determined specific reaction rate (k) of the total thermal product at 300° C equals 0.7×10^{-3} hour⁻¹ and at 350° C equals 7.6×10^{-3} hour⁻¹. From this, it appears that the reaction rate at 350° C is about 11 times the rate at 300° C. The calculated activation energy between 300° and 350° C is about 33 kilocalories mole⁻¹.

Each oil and each bitumen were fractionated to ascertain any existing differences in their compositions. The oils and bitumens were fractionated into the following type components: n-Alkanes, branched-plus-cyclic alkanes, olefins, aromatic oil, resins and pentane-insoluble material. The distribution of these fractions appears in table 2 where the results obtained for

TABLE 2. - Distribution of components present in the thermal product

Time, hours	Weight percent of kerogen					Pentane- insoluble material
	n-Alkanes	Branched-plus- cyclic alkanes	Olefins	Aromatic oil	Resins	
300° C						
12	0.17	0.30	0.05	0.17	4.00	0.71
24	.11	.71	.17	.17	2.93	3.31
48	.13	.79	---	.43	7.05	.20
72	.15	1.00	.15	.61	7.14	.65
96	.26	1.02	.19	1.02	8.01	.50
350° C						
12	.80	2.48	.56	1.95	25.93	3.18
24	2.17	3.70	.64	3.38	25.97	4.34
48	1.39	3.86	.36	1.75	35.87	8.17
72	2.72	3.52	.80	1.17	35.98	17.61
96	3.02	4.82	1.22	4.24	48.24	2.76

the volatile oil and the nonvolatile bitumen were calculated as one pyrolytic product. In general, the thermal products from both temperatures contained more polar materials (resins plus pentane-insoluble materials) than hydrocarbons.

The data from the fractionation of the oils and bitumens prior to combining showed the oil fractions to contain more hydrocarbons than did the bitumen fractions. The hydrocarbon content of the oil fractions ranged from 20 to 26 percent of the total fraction, and the hydrocarbon content of the bitumen fractions ranged from 1 to 7 percent. These results show that during oil-shale

pyrolysis the high-molecular-weight nonvolatile polar bitumen degrades to a less polar and lower-molecular-weight oil. These results are different than those from a previous study⁶ where kerogen was pyrolyzed at 350° C in tetralin to soluble products. In that study more than half of the products remained as high-molecular-weight pentane-insoluble material. This indicated that further degradation to volatile products is not a major factor when kerogen is converted to pyrolytic products in the presence of tetralin.

The specific reaction rates were calculated for the individual components of the pyrolytic products using the method previously described. The results are shown in table 3. At

TABLE 3. - Reaction rates for the production of the individual components present in the thermal products

Fraction	k, hours ⁻¹		$\frac{350^\circ \text{ C rate}}{300^\circ \text{ C rate}}$
	300° C	350° C	
n-Alkanes	3×10^{-5}	6×10^{-4}	20
Branched-plus-cyclic alkanes	1×10^{-4}	3×10^{-4}	3
Olefins	1×10^{-4}	7×10^{-4}	5
Aromatic oil	9×10^{-5}	4×10^{-4}	4
Resins	5×10^{-4}	4×10^{-3}	8
Pentane-insoluble material	2×10^{-4}	2×10^{-3}	9
Total product	1×10^{-3}	8×10^{-3}	7

300° C the n-alkanes are formed at the slowest rate while the resins are formed at the fastest rate. At 350° C the branched-plus-cyclic alkanes are formed at the slowest rate while the resins are formed at the fastest rate. The total product rate agrees favorably with the overall rate given previously. The 350° C rate divided by the 300° C rate shows the proportional rate of increase of the individual components between 300° and 350° C and their relationship to the overall rate. Normal alkanes formed 20 times as fast at 350° C as at 300° C. Branched-plus-cyclic alkanes formed three times as fast at 350° C as at 300° C. The change in production of the other fractions is not much different from the change in the total product rate.

The n-alkanes from the oil fractions were separated by GLC and chromatograms were obtained for each fraction. Plots of carbon numbers of the n-alkanes versus concentration were made to determine the effect of pyrolytic time and temperature on the composition of the n-alkanes. The data from the 300° C n-alkanes produced envelopes at C₁₃ to C₂₆ and envelopes at C₂₇ to C₃₅. The data from the 350° C alkanes produced envelopes at C₁₂ to C₂₆ and C₂₇ to C₄₀. In general, the percent of n-alkanes in the C₁₂ to C₂₆ range increased with increase in heating time at both temperatures. Also, the percent of n-alkanes in the C₂₇ to C₄₀ range decreased with increase in heating time at both temperatures. These results indicate that more low-molecular-weight n-alkanes than high-molecular-weight n-alkanes are thermally degraded from the kerogen or degraded from the bitumen with increased time and temperature.

A plot of percentage of kerogen converted, in terms of the yearly rates ($R \times 10^2$), versus the reciprocal of absolute temperature was made to determine if it is practical to study the thermal reaction rate of kerogen at temperatures lower than 300° C. The plot (Figure 5), based on the thermal reaction rate per year at 300° and 350° C, is extrapolated to 50° C. The figure shows that 100 percent of the kerogen would be converted to soluble products in 1 year at 265° C.

About 30 percent of the kerogen would be converted to soluble products in 1 year at 250° C while about 1 percent would be converted in 1 year at 200° C. It is evident from this plot that extended periods of time would be required to study the rate of conversion at temperatures lower than 300° C. One interesting aspect of this plot is the indication that about 6 percent of the kerogen should be converted to soluble products at 50° C in 100 million years. This suggests that the soluble bitumen present in the oil shale could have been derived from the kerogen at temperatures as low as 50° C during the life span of the Green River Formation (Eocene, 60 million years).

SUMMARY

A twofold increase was obtained in the amount of pyrolytic product at constant temperature (300° or 350° C) when the length of heating time was increased from 12 to 96 hours. A sixfold increase was obtained in the amount of pyrolytic product at constant heating time when the temperature was increased from 300° to 350° C.

The overall thermal decomposition of kerogen at 300° and 350° C appears to be a first-order reaction. The specific reaction rate constant at 300° C was determined as 0.7×10^{-3} hour⁻¹ and at 350° C as 7.6×10^{-3} hour⁻¹.

Differences in the rate of formation of individual type components of the pyrolytic product are apparent. Between 300° and 350° C, n-alkanes formed faster than the overall average rate of product formation while the branched-plus-cyclic alkanes formed slower than the overall average rate. Rate of formation of the other fractions was nearly equal to the average rate.

The average molecular weight of the n-alkane fraction decreased with increase in heating time and heating temperature.

Extrapolation of the rate data to temperatures below 300° C indicated that the amount of natural bitumen present in oil shale could have been thermally degraded from kerogen at 50° C in a period of time equivalent to the estimated age of the Green River Formation.

ACKNOWLEDGMENT

The work upon which this report is based was done under a cooperative agreement between the Bureau of Mines, U.S. Department of the Interior and the University of Wyoming.

REFERENCES

1. Allred, V. D. Some Considerations on the Kinetics of Oil Shale Pyrolysis. Presented at the Symposium on Oil Shale and Shale Oil Processing, Fifty-Eighth National A.I.C.E. Meeting, Dallas, Texas, February 1966.
2. Cummins, J. J., and W. E. Robinson. Normal and Isoprenoid Hydrocarbons Isolated from Oil-Shale Bitumen. *J. Chem. Eng. Data*, v. 9, No. 2, 1964, pp. 304-307.
3. Dinneen, G. U. Effects of Retorting Temperature on the Composition of Shale Oil. *Chem. Eng. Progr.*, v. 61, No. 54, 1965, pp. 42-47.

4. Dinneen, G. U., J. R. Smith, R. A. Van Meter, C. S. Allbright, and W. R. Anthony. Application of Separation Techniques to a High Boiling Shale-Oil Distillate. *Anal. Chem.*, v. 27, 1955, p. 185.
5. Hill, G. R., D. J. Johnson, L. Miller, and J. L. Dougan. Direct Production of a Low Pour Point High Gravity Shale Oil. *Ind. and Eng. Chem., Product Research and Development*, v. 6, No. 1, 1967, pp. 52-59.
6. Hubbard, A. B., and W. E. Robinson. A Thermal Decomposition Study of Colorado Oil Shale. *BuMines Rept. of Inv. 4744*, 1950, 24 pp.
7. Robinson, W. E., and J. J. Cummins. Composition of Low-Temperature Thermal Extracts from Colorado Oil Shale. *J. Chem. Eng. Data*, v. 5, 1960, pp. 74-80.

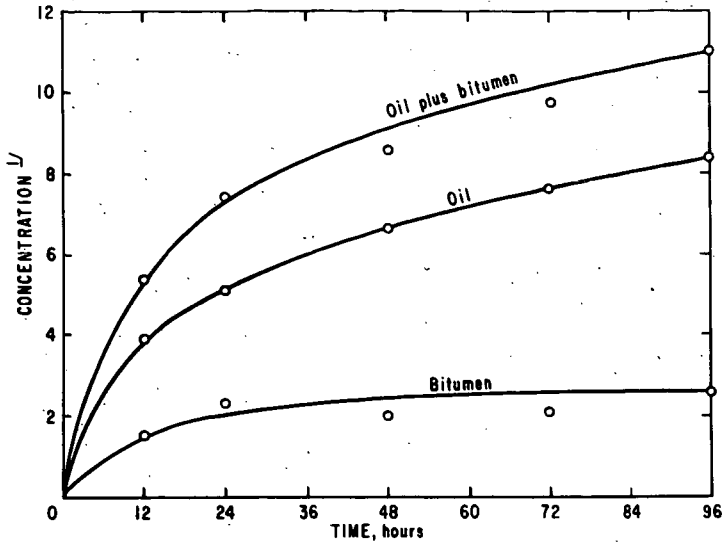


FIGURE 1.-Conversion of Kerogen to Oil and Bitumen at 300 °C.
(% Kerogen converted, wt pct of total kerogen)

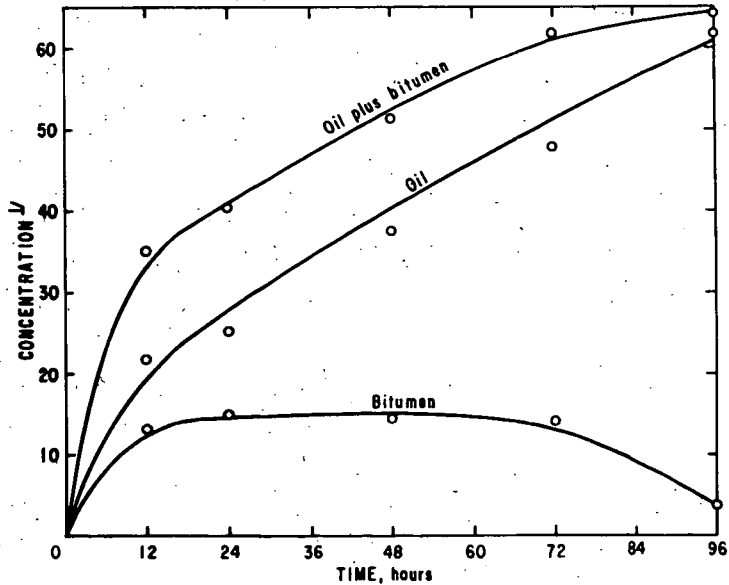


FIGURE 2.-Conversion of Kerogen to Oil and Bitumen at 350 °C.
(% Kerogen converted, wt pct of total kerogen)

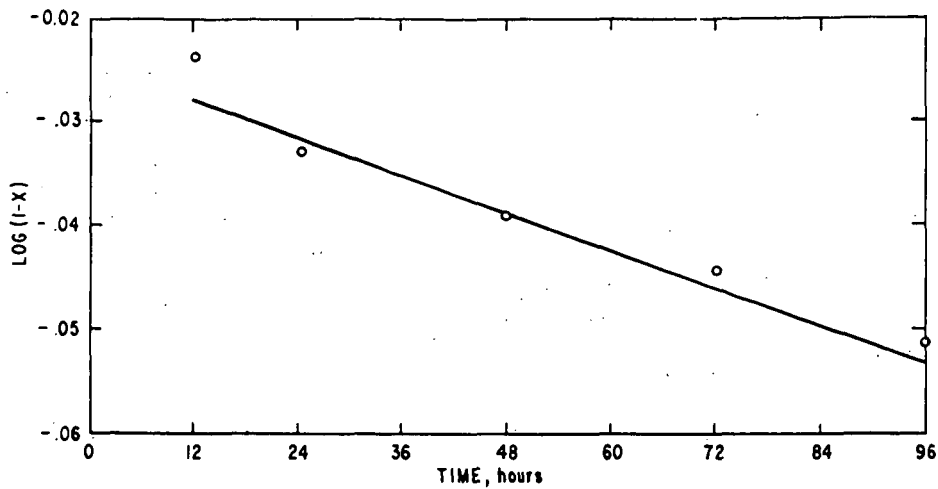


FIGURE 3.-First-Order Plot of Kerogen Conversion at 300 °C.

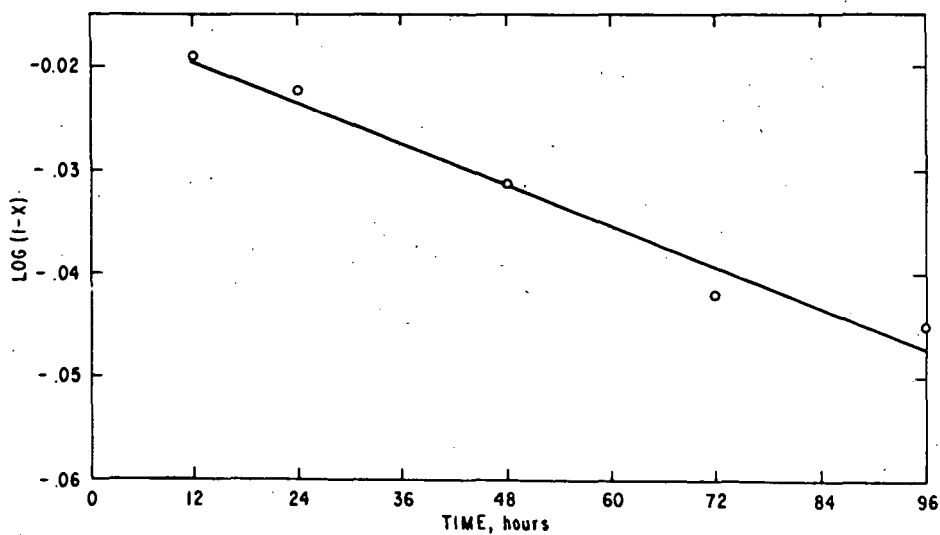


FIGURE 4.-First-Order Plot of Kerogen Conversion at 350 °C.

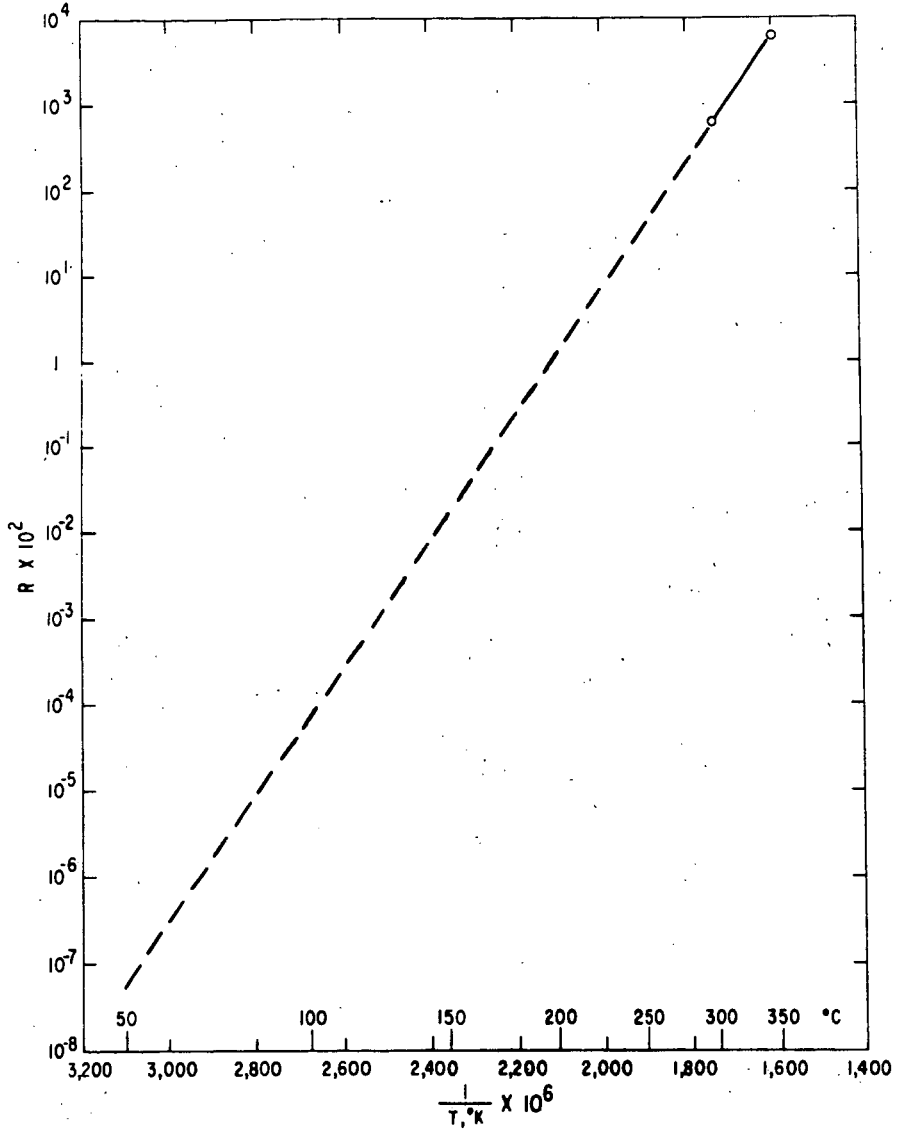


FIGURE 5.- Percent Conversion of Kerogen to Pyrolytic Products in One Year at Various Temperatures.

PREPARATION OF CARBON METALLURGICAL ELECTRODES FROM LOW-TEMPERATURE LIGNITE COKE AND LIGNITE PITCH BINDER

John S. Berber and Richard L. Rice

U. S. Department of the Interior, Bureau of Mines,
Morgantown Coal Research Center, Morgantown, West Virginia 26505

INTRODUCTION

Low-temperature carbonization of coal produces char and coal tar. Char is potentially useful as powerplant fuel, as smokeless fuel for domestic uses, for synthesis gas production, and for blending with other coals to make metallurgical coke. Low-temperature tar is a potential source of organic chemicals and other products, including materials for making carbon electrodes. Large quantities of carbon in the form of petroleum coke are used to make carbon electrodes for the aluminum, steel, electrochemical, and electrothermal industries.

Two methods were developed for producing carbon electrodes from low-temperature lignite tar. Electrodes were then made by these methods and evaluated by comparing their properties and performance with those of commercial grade electrodes. This paper presents preliminary results of the comparison.

ELECTRODE PRODUCTION AND SPECIFICATIONS

Carbon and graphite manufacture was developed by the end of the 18th and the beginning of the 19th century. The earliest use of carbon in an electrical application is attributed to Sir Humphrey Davy in 1800. His carbon material was charcoal. The need for stronger carbon materials, which could resist heat and have higher electrical conductivity, enhanced the carbon industry for its manufacture. The first baked carbon composition from coke, lampblack, and sugar syrup, is credited to a French scientist, Carré, in 1876. The graphite industry started 20 years later, in 1896, with the development of the resistance type electric furnaces.

Carbon electrodes for metallurgical purposes today are made by mixing petroleum coke, graphite, anthracite, or coal with a coal pitch, placing the mix in a mold, then baking for about 24 hours to about 2,000° F. Baking converts the pitch into coke which serves as a binding skeleton between filler particles, resulting in a strong finished product (7). Theoretically, about 0.3 ton of carbon is required to produce a ton of aluminum, however in practice about 0.6 ton of carbon of which 0.2 ton is pitch is required (3, 8, 11). About 400,000 tons of coal tar pitch is used annually in the United States for aluminum production. The U. S. market for carbon electrodes is about 2.5 million tons per year.

The characteristics of the coal tar pitch determine the stability and tensile strength of finished electrodes (5). The amount of binding coke formed during the baking operation depends to a large extent on the percentage of medium molecular weight tar resins contained in the coal pitch. The higher the amount of these resins in the pitch binder, the greater will be the binding effect. Alpha resins contained in pitch have high molecular weight, however, and do not enhance

binding of the electrodes; therefore their content in the pitch should be as low as possible. Contrarily, the beta resins, being in colloidal form in the pitch, have a great binding power, so their content in the electrode pitch binder should be as high as possible. Since the value of the resins is determined by its free carbon, the free carbon characterizing the total pitch unity should be as high as possible. The pitch binder coke produced during baking is an all-important factor in bonding coke aggregate particles into an overall structure possessing high compressive strength, high apparent density, and low electrical resistivity. A good pitch binder should have a carbon-hydrogen ratio of 1.20 to 1.80, ash content less than 1%, softening point of about 105° to 120° C, and coking value of at least 60% (9). For many purposes, a density approaching the theoretical maximum of 2.6 g/cc is highly desirable, yet in practice it is difficult to exceed 2.0 g/cc (4, 6, 10).

EXPERIMENTAL EQUIPMENT AND PROCEDURE

Materials used to produce electrodes in this investigation were derived from low-temperature lignite tar except for the petroleum coke and bituminous binder. The latter two were obtained from commercial suppliers.

Coke and binder for the electrodes were obtained from low-temperature lignite pitch by two methods--thermal cracking (1) and delayed coking (2). Both thermal cracking and delayed coking produce an oily liquid and coke. The liquid is distilled into a distillate and a residue. The residue shows suitable specifications for use as an electrode binder. Coke from both processes is leached, calcined, and screened for electrode aggregate as shown in Figure 1.

Coke is leached by digesting it in a 50% hydrochloric acid solution for 2 hours. After filtration and washing until neutral, the leached coke is dried at 212° F and then calcined for 12 hours in nitrogen atmosphere at 2,500° F. Calcination of green coke is necessary for several reasons. First, the green coke when ground cannot be bound together to give a proper density. Second, electrodes are difficult to mold or extrude from green coke. Third, the electrodes give off volatile matter during baking, thus resulting in a very porous electrode. Finally, electrodes are poor conductors and have a high resistivity when made from green coke. The green and leached coke, both calcined at 2,500° F, were analyzed for iron, sulfur, ash content, and electrical resistivity.

Two systems were used for making electrical resistivity measurements. A Wheatstone bridge galvanometer was capable of measuring 0.001 ohm. The other system (Figure 2) impresses a 2 ampere current through the electrode and then measures the voltage drop across a 2.01 inch length. From this measurement and the diameter, the electrical resistivity is calculated.

The preparation of test electrodes involves making the green mix (or paste), molding, and baking. The pitch is placed in an oil heated sigma-blade mixer which has been preheated to about 300° F. After the pitch has melted, the mixer is started and different size coke fractions are added one at a time, starting with the largest size (minus 10 plus 20 mesh). About 5 minutes is allowed between the addition of each size fraction (the timing of the addition is recorded) to assure wetting of the coke by the binder. When the mixing of the paste is completed, it is transferred still hot to the molds, which have been preheated to about 250° F. The paste is tamped into stainless-steel molds and pressed. At first graphite

molds were used, but later stainless-steel molds were found more practical. Two sizes of molds were used, 1-1/4 inches diameter by 5 inches long and 1-3/4 inches diameter by 5 inches long. The larger electrodes were required for use in the metallurgical reduction cell.

The upper one-half inch of the mold is filled with powdered dry coke and the molds are placed in the baking jig. The jig is then placed in a crucible type furnace and baked (in a nitrogen atmosphere) to 1,850° F at a heating rate of 90° F per hour.

After baking, the electrodes are allowed to cool in the furnace for 24 hours and then removed for testing. The density is determined by carefully measuring a section of the electrode and then weighing it. The resistivity and strength of the section are then measured and the remains are used for the reactivity test. The electrodes were also evaluated in an electrical reduction cell used for reduction of alumina.

RESULTS AND DISCUSSION

Calcination. A study on the effect of calcination of coke at different temperatures on the electrical resistivity and density gave interesting results, as shown in Table 1. Calcination causes shrinkage with the expulsion of volatile matter and effects an increase in the specific gravity or real density of the electrode. The photomicrographs (Figure 3) compare the appearance of coke particles after calcination at increasing temperatures from 1,850° to 4,800° F. The particles calcined at 1,850°, 2,500°, and 3,000° F show little change in appearance from the original coke. At 3,175° F the appearance begins to change from the asymmetric oblong grains to the irregular grains with rough edges that are highly branched and are the predominant shapes of the particles calcined at 4,800° F.

Table 2 shows the analytical differences between the green and the leached coke, which influence the qualitative specifications of a carbon electrode. The green coke showed a much higher electrical resistivity and iron content than the leached coke.

Product Specifications. When a coke is mixed with a binder and the mix extruded or molded, a structure is formed that is similar in many aspects to a compressed powder. During the mixing of the pitch with the coke, the degree of wetting is of considerable importance, because it is desirable to obtain nonporous and very compact electrodes of low specific resistivity, high compressive strength, low reactivity, and low ash and sulfur content. Low electrical resistivity avoids waste of electric power, which is one of the largest costs in electrolytic processes. High compressive strength requires that the electrodes be sturdy when subjected to tension, compression, and shear and twist; otherwise they fail, disrupting furnace and cell operation and increasing overall cost. High reactivity destroys the electrodes by oxidation. Some elements in the ash, for example, iron, vanadium, boron, and alkalis, by acting as catalysts, can affect the reactivity of the electrode with certain gases present during operations. Ash is especially undesirable in electrolytic operations that use consumable electrodes, since the ash can contaminate electrolyte and, in some operations, can be reduced and contaminate the product. For applications where these conditions apply, the ash content of binder pitches and electrode aggregates should be as low as possible. A high

sulfur content in pitches used for electrodes can contribute to the formation of a layer of iron sulfide on the metallic contact pins, thus changing the electrical resistance at the interface. Sulfur can have harmful effects on carbon products during graphitization. The fumes of sulfur are also objectionable. The sulfur content of most coal tar pitches ranges from 0.35 to 0.50 percent.

The pitch binder has a tendency to penetrate deep into the voids of the coke aggregate. Photographs of the electrode sections (Figure 4) show the poor condition that occurs inside some of the electrodes and serve as the first step in photomicrographic studies to determine wetting of the coke by the binder and the quality of calcination during the baking cycle. All the electrodes shown in Fig. 4 were made with about the same amount of binder, except the one labeled "thermally cracked lignite binder," having 25% of binder. The preferred weight-percentage of low-temperature lignite pitch binder for the green mix was found to be 25 to 27%, varying in relation to the density of the calcined coke. The higher the calcination temperature, the higher is the density of the coke, as shown in Table 1, consequently the amount of binder should be proportionately increased to avoid higher porosity of an electrode.

Calcined coke prepared by thermal cracking of lignite is compared with petroleum coke in Figure 5. The coke particles differ, lignite particles being much more angular in appearance than the petroleum particles that have a more uniformly rounded appearance. The wetting property of the binder is of equal value using both cokes. The finished baked electrodes using lignite coke have more and larger void spaces than the ones using petroleum coke. Sections of coke particles exposed in the baked electrode show the lignite coke to be denser in appearance with thicker cell walls, whereas the petroleum coke has a more striated appearance in section.

Electrodes having about 400 kg/cm^2 of compressive strength and 0.007 to 0.009 ohm/cm^3 of electrical resistivity, Table 3, have been prepared totally from materials derived from lignite tar.

The characteristics of the binder pitch are given in Table 4. The better electrodes were prepared with a binder content less than 27%, and a binder having a hydrogen content less than 5%. The effect of the coking value and the benzene- and quinoline-insoluble contents are completely overshadowed by the large variation in binder percent in the electrodes.

Product Evaluation. Results of tests performed on our electrodes at the College Park Metallurgy Research Center showed that the surface of anodes prepared from our electrodes, Figure 6, after electrolysis were very similar to anodes made from commercial materials. The surfaces were uniformly eroded and the electrolyte covers the entire surface, indicating good wettability.

CONCLUSIONS

Results of replacing petroleum coke with lignite coke to produce an entire lignite electrode were very encouraging. Lignite coke produced from thermal cracking and delayed coking of lignite pitch was calcined at $2,500^\circ \text{ F}$ in a nitrogen atmosphere. This coke, after being calcined to $2,500^\circ \text{ F}$, showed a density of 1.96 g/cc and an electrical resistivity of 0.045 ohm/in^3 .

Evaluation of electrodes (prepared from lignite coke and lignite binder) in an alumina reduction cell, showed them to be more susceptible to the Boudouard reaction ($C + CO_2 \longrightarrow 2CO$) than electrodes made from bituminous binder and petroleum coke, resulting in higher anode consumption. However, electrodes with higher compressive strength and higher densities were found to be less reactive.

Many factors affect the characteristics of electrodes, and it is difficult to isolate any one factor as being most important in regard to performance of electrodes in reduction cells. However, two factors seem to be involved more than others noted. Coke that had been calcined to 3,175° F, as opposed to the usual 2,500° F, performed best in a reduction cell. Also, binder with a hydrogen content of less than 5 percent gave a higher compressive strength and lower porosity.

ACKNOWLEDGMENTS

Appreciation is expressed to: Dr. V. L. Bullough, Director, Applied Research, Reynolds Metals Company, and Mr. J. J. McGahan, Manager, Development Department, The Carborandum Company, for their advice and help in high-temperature calcination of our lignite coke; Dr. T. Henrie, Research Director, Reno Metallurgy Center, Dr. D. Schlain, Project Coordinator, and Mr. V. A. Cammarota, Jr., Project Leader, of the College Park Metallurgy Research Center, for their help in evaluating our electrodes.

REFERENCES

1. Berber, John S., Richard L. Rice, and Delmar R. Fortney. Thermal Cracking of Low-Temperature Lignite Pitch. *Ind. Eng. Chem., Prod. Res. Develop.*, v. 6, No. 3, September 1967, pp. 197-200.
2. Berber, John S., Richard L. Rice, and Robert E. Lynch. Delayed Coking of Low-Temperature Lignite Pitch. *Preprints, Am. Chem. Soc., Div. of Fuel Chem.*, v. 12, No. 2, March 31-April 5, 1968, pp. 47-55.
3. Domitrovic, R. W., R. M. Stickel, and F. A. Smith. Rapid Test Method for the Determination of the Benzene- and Quinoline-Insoluble Content of Pitches. *Symp. on Tars, Pitches and Asphalts. Preprints, Am. Chem. Soc., Div. of Fuel Chem.*, Sept. 9-14, 1962, pp. 54-64.
4. Hoiberg, Arnold J., ed. *Bituminous Materials, Asphalts, Tars and Pitches. Vol. III, Coal Tars and Pitches.* Interscience Publishers, New York, 1966, 585 pp.
5. Jones, H. L., Jr., A. W. Simon, and M. H. Wilt. A Laboratory Evaluation of Pitch Binders Using Compressive Strength of Test Electrodes. *J. Chem. Eng. Data*, v. 5, No. 1, January 1960, pp. 84-87.
6. Kuvakin, M. A., and N. D. Bogomolova. New Types of Coke for Carbon Electrodes. *Coke Chem. (USSR) (English Transl.)*, No. 12, 1965, pp. 23-28.

7. Lauer, G. G., and K. P. Bonstedt. Factors Influencing the Performance of Pitch Binders in the Baking of Small Carbon Electrodes. *Carbon*, v. 1, No. 2, February 1964, pp. 165-169.
8. Martin, S. W., and H. W. Nelson. Carbon Materials Required in Electrolytic Reduction of Alumina. *J. Metals*, v. 7, No. 4, April 1955, pp. 540-543.
9. Morgan, M. S., W. H. Schlag, and M. H. Wilt. Surface Properties of the Quinoline-Insoluble Fraction of Coal-Tar Pitch. *J. Chem. Eng. Data*, v. 5, No. 1, January 1960, pp. 81-84.
10. Stepanenko, M. A., N. I. Matusyak, A. T. Movchan, and P. L. Saltan. Electrode Pitch Manufacture by Thermal Treatment. *Coke Chem. (USSR) (English Transl.)*, No. 12, 1965, pp. 20-23.
11. Thomas, B. E. A. Electrode Pitch. *Gas World*, v. 151, No. 3946, Coking Suppl., v. 56, No. 564, April 2, 1960, pp. 51-64, 66.

TABLE 1. - Electrical resistivity and density of coke at different calcination temperatures

Calcination temp., °F	Resistivity, ohm/in ³	Density, g/cc
1,850	0.0940	1.83
2,200	0.0640	1.95
2,500	0.0450	1.96
3,000	0.0081	1.97
3,175	0.0075	1.97
4,800	0.0053	2.00

TABLE 2. - Analytical differences between green and leached coke

	Green	Leached
Percent:		
Ash	1.15	0.75
Iron	0.11	0.03
Sulfur	0.82	0.83
Resistivity, ohm/in ³	0.051	0.035
Calcination temperature, °F	2,500	2,500

TABLE 3. - Properties of electrodes from coke produced by delayed coking and thermal cracking

Batch No.	Coke			Electrodes		
	Method	Calcining temp., °F	Resistivity, ohm-cm	Resistivity, ohm-cm	Strength, kg/cm ²	Density, g/cc
87	Delayed	2,000	0.163	0.013	284	1.31
89	do.	2,500	0.122	0.010	363	1.32
105	do.	2,500	0.122	0.011	258	1.36
106	do.	2,500	0.122	0.0088	315	1.43
90	Cracked	2,500	0.089	0.012	274	1.23
92	do.	2,500	0.089	0.011	321	1.37
93	do.	2,500	0.089	0.012	208	1.25
95	do.	2,500	0.089	0.013	205	1.22
100	do.	2,500	0.089	0.012	225	1.27
111	do.	2,500	0.089	0.0080	393	1.45
113	do.	2,500	0.089	0.0070	413	1.46
101	do.	3,175	0.038	0.0052	237	1.47
94	Petroleum ¹	Unknown	0.088	0.0087	254	1.28

¹ Coke obtained from a commercial supplier. Lignite pitch used as binder.

TABLE 4. - Characteristics of pitch binder from lignite

Batch No. EB	Processing conditions			Characteristics of binder						
	Coking method	Binder, pct	Softening point, °C	Carbon, wt pct	Hydrogen, wt pct	C-H ratio	Coking value	Benzene insolubles, pct	Quinoline insolubles, pct	
106	Delayed	26.3	106	88.16	5.20	1.41	60.5	27.9	20.1	
105	do.	27.6	106	88.16	5.20	1.41	60.5	27.9	20.1	
113	Cracked	25.5	105	89.17	4.89	1.51	58.0	36.7	25.1	
111	do.	26.0	105	89.17	4.89	1.51	58.0	36.7	25.1	
89	do.	28.0	110	88.25	4.72	1.56	61.5	39.9	23.7	
90	do.	28.0	118	89.09	4.94	1.50	61.4	51.4	16.8	
102	do.	28.0	110	88.73	5.14	1.44	70.1	29.9	15.6	
95	do.	29.0	106	86.90	5.98	1.21	49.8	38.2	10.7	
87	do.	30.0	110	82.25	4.72	1.56	61.5	39.9	23.7	
93	do.	30.0	106	86.90	5.98	1.21	49.8	38.2	10.7	
94	do.	30.0	106	86.90	5.98	1.21	49.8	38.2	10.7	
101	do.	30.0	112	90.89	5.04	1.50	67.3	34.0	25.2	

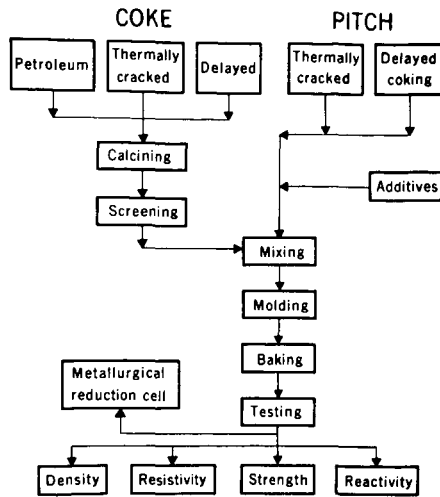


FIGURE 1. - Flowsheet for preparation of coke and pitch for carbon electrodes.

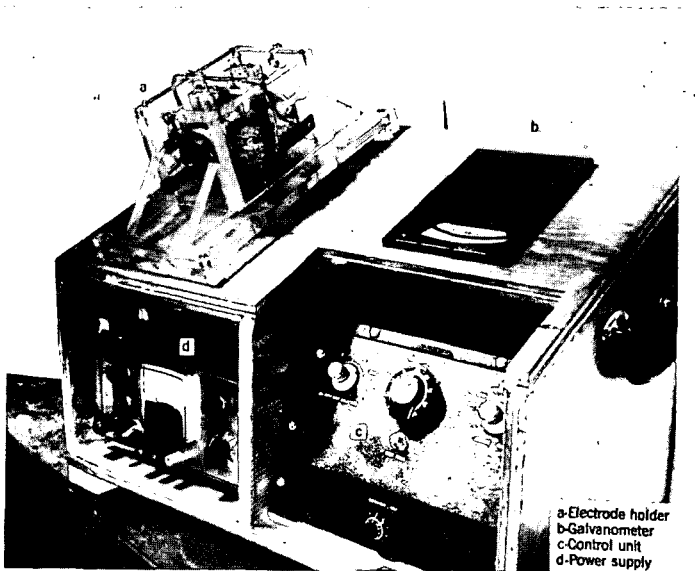


FIGURE 2. - Electrical resistivity apparatus.

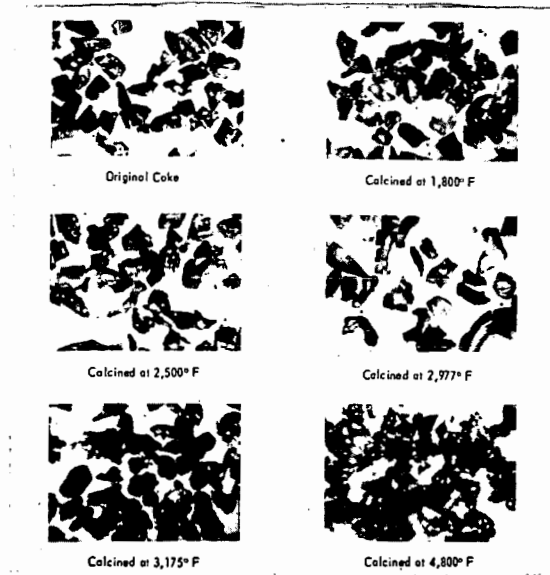


FIGURE 3. - Coke from low-temperature lignite pitch calcined at 1,800° to 4,800° F (X 50).

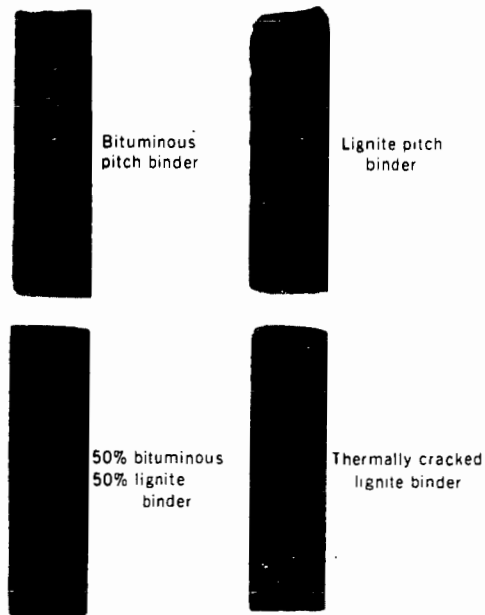


FIGURE 4. - Longitudinal cuts of electrodes from bituminous and lignite binders.

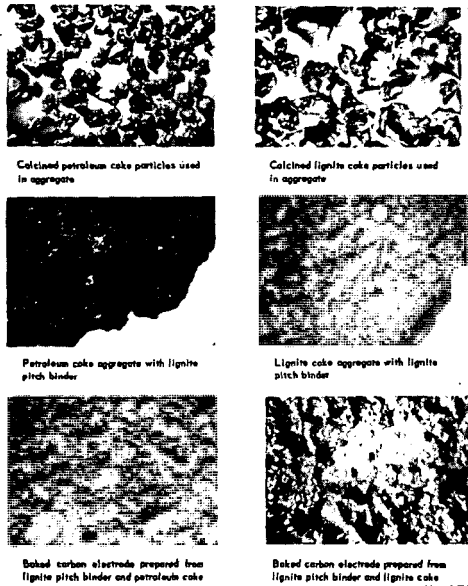
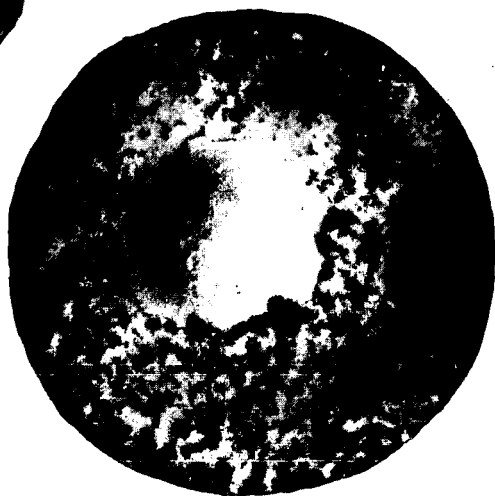


FIGURE 5. - Photomicrographs of carbon electrodes and their components (X 30).



Anode B-11-0 2.2x magnification.

1. Anode B-111 2.2x magnification.



3. Anode B-113-0 2.2x magnification.

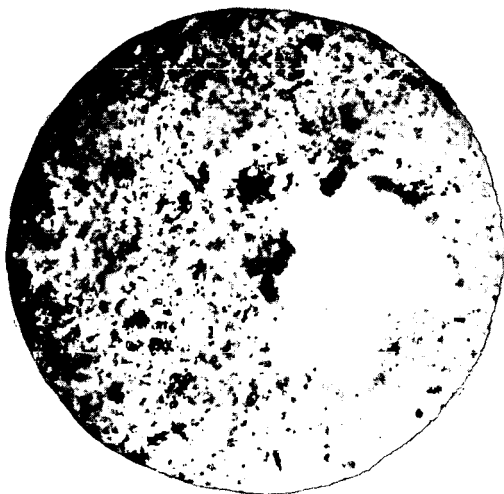


FIGURE 6. - Anodes, machined from electrodes prepared from low-temperature lignite coke and lignite pitch binder, after use in an alumina reduction cell.

THE EFFECT OF PITCH QUINOLINE INSOLUBLES ON GRAPHITE PROPERTIES

James Jerauld Ferritto

Airco Speer
A Division of Air Reduction Co., Inc.
Electrode & Anode Development Dept.
Niagara Falls, New York 14302

Joseph Weiler

Allied Chemical Company
Plastics Division
Edgewater, New Jersey

INTRODUCTION

For several years Airco Speer has been working with raw materials suppliers in order to characterize or better define these raw materials, in terms of their effects on final graphite properties. In particular, Airco Speer's work with Allied Chemical Company, a major pitch supplier, was directed toward the development of a better electrode binder, through a clearer definition of their process parameters (such as column atmospheres, distillation temperatures, tar sources and other feed stream variables), as they affect pitch characteristics, hence, graphite properties.

Of the many pitch characteristics specified by the graphite electrode industry,^{1,2,3} the Q.I. content was chosen the subject of this investigation. The Q.I.'s consist primarily of solid particles^{4,5,6} ranging in size from colloidal to coarse⁷. The colloidal particles are mostly complex hydrocarbons of high molecular weight. They are derived from the decomposition of coal directly or may be derived indirectly from the condensation and dehydrogenation of small aromatic molecules coming from the coal. The coarse particles can be any insoluble "dirt", such as coal or coke dust. The function of the Q.I. is to provide sites for crystallite growth (nucleation) during carbonization or graphitization.⁸

Many investigators feel that the Q.I. of coal tar pitch is important in determining graphite quality.^{9,10} It is known, for example, that the higher the Q.I., the higher will be the graphite strength, density and conductivity. However, Q.I. levels of over 16 to 18% generally have no beneficial effect and, in fact, may be detrimental. Not as well known, but perhaps more important, is the type of Q.I., vis., the process parameters by which certain levels are attained, affect not only those levels, but also the nature of the Q.I., and, consequently, may affect the nature of the graphite.

EXPERIMENTAL

After managerial approval of both Companies, the basic plan was formulated. A 3 x 4 factorial-type experiment was proposed in which Allied would process one low (~5%) Q.I. tar by filtration, distillation, two heat treatments, addition of Thermax (a thermostatically decomposed "black") and blending. Four different pitches would initially be made. Each would be modified by the processes described,

to contain three levels of Q.I. --about 7, 14 and 21%. Twelve (12) pitches in all would result.

In the preparation of the raw materials and the blend components (Figure 1), the starting material was feed Tar "A", with a low (5%) Q.I. This tar was filtered to yield low (4%) Q.I. Pitch "Z". This, in turn, was used as the blending pitch for Processes I through IV. The residue from feed Tar "A" was used to make the high (12%) Q.I. Tar "B", which was used as the raw material in Processes I and II.

In the preparation of natural Q.I. pitches (Process I), the high Q.I. Tar "B" was distilled (Figure 2) to yield a high Q.I. Pitch "Y", raising the Q.I. from 12 to about 21%. This pitch was blended with low Q.I. Pitch "Z" to give Pitches "X" and "W", thus lowering the Q.I. to about 7 and 14%, respectively.

The pitches in Process II were produced from the high Q.I. Tar "B" in Process I (Figure 3). This pitch was distilled to yield Pitch "U", with a Q.I. of 21%. As in Process I, this pitch was blended with low Q.I. Pitch "Z" to give Pitches "T" and "S", again, lowering the Q.I. to 7 and 14%, respectively.

The high Q.I. tar from Experimental Process II was used in preparing the pitches in Process III (Figure 4). This tar was distilled to yield Pitch "P", with a Q.I. of about 21%. Pitch "P" was blended with Pitch "Z" to give Pitches "Q" and "N", with Q.I. 's of 7 and 14%, respectively.

Process IV pitches were prepared by starting with one of the original raw materials, low Q.I. Tar "C", which was feed Tar "A" with the insolubles removed by filtration. The low Q.I. Tar "C" then had Thermax dispersed in it, thus raising the Q.I. from 2 to about 12% (Figure 5), resulting in high Q.I. Tar "E". By distillation, the Q.I. was increased to about 21% and was now called Pitch "M". The Q.I. content of Pitch "M" was lowered to 7 and 14%, by blending with Pitch "Z" to yield Pitches "L" and "K", respectively.

The characteristics of all these pitches, as received by Airco Speer, is shown in Table 1. Since Allied used new or modified polymerization techniques, it proved difficult to make some of the pitches with specific Q.I. values. In particular, Pitch "P" was considerably lower in Q.I. than predicted. To be consistent with their process scheme, it would have been economically impractical or technically impossible for them to change their processing to raise the Q.I.

When Airco Speer received the pitches, they were extruded in an electrode formulation in the Pilot Plant, in five inch diameter rods. Concurrently, a control lot, using a standard binder pitch, was also extruded.

It was the intention to extrude all pitches at three binder levels, according to standard Pilot Plant operating procedures. However, Pitches "K", "M" and "P" were non-extrudable at the lower binder level. The as-formed rods were then baked to about 800 C in the Pilot Plant furnace, then graphitized to about 2800 C. All stock was tested by the Chemical and Physical Measurements Group of the Research Department.

RESULTS AND DISCUSSION

Table 2 summarizes all of the pertinent graphite data and also gives the relative

Table 1

CHARACTERISTICS OF 12 ALLIED EXPERIMENTAL PITCHES

Pitch Type	Softening	Q.I.	Q.I.	Q.I.	Carbon
	Point	(Predicted)	(Airco Speer)	(Allied)	Disulfide Insoluble
	C	%	%	%	%
Y	102	21.0	20.5	20.0	34.1
W	104	14.0	14.6	14.5	32.9
X	103	7.0	9.9	8.6	29.2
M	103	21.0	20.8	21.7	38.4
K	104	14.0	15.6	15.0	34.2
L	102	7.0	9.4	8.9	28.1
U	105	21.0	17.4	18.9	37.1
S	105	14.0	13.8	12.0	33.8
T	105	7.0	9.4	7.3	29.8
P	105	21.0	12.3	10.9	35.5
N	105	14.0	10.7	9.7	32.6
Q	105	7.0	7.7	7.2	28.5

binder levels at which the formulations were extruded. Since these were electrode formulations, it is reasonable to assume that the spread in binder levels, 2 pph, can result in significant differences in graphite properties. The actual binder levels and formulations are proprietary. It should also be noted that the graphite properties are coded. Though the actual values are not represented, they do show the true, relative differences in values, which correctly shows the change in effects due to the different pitches.

A portion of the data is graphically represented in Figures 6, 7 and 8. Only the optimum values for some of the most important properties were plotted. These values are: transverse coefficient of thermal expansion (T-CTE), flexural strength and apparent density. Thus, for the T-CTE's (Figure 6), only the binder levels that resulted in the lowest CTE, were considered. Those binder levels are not necessarily the same ones that resulted in optimum flexural strengths (Figure 7) or apparent densities (Figure 8), and vice versa. In determining the suitability of a particular pitch for further evaluation, a compromise is sometimes necessary in considering which binder levels merit most attention.

On this basis, the most important process, in terms of T-CTE, is Process III. In particular, Pitch "P", at its optimum value (Figure 6), had a T-CTE of about $0.54 \times 10^{-6}/C$, which was substantially lower than the standard. However, the flexural strengths (Figure 7) were also lower, but could be increased, if required, through impregnation. It is of further interest to note that all of the T-CTE's were either lower or equivalent to the standard, with no apparent degradation of structural integrity.

Pitch "Y", from Process I, is also important, not only because of its low graphite T-CTE, but also because the flexural strengths and apparent densities (Figure 8) were at least equivalent to the standard. From the same standpoint, but to a somewhat lesser degree, Pitches Q, N and W were also important because of their low T-CTE's. Graphite strengths were equivalent to the standard.

From the longitudinal electrical resistivity data (Table 2) it can be seen that all the values were higher than the standard, with the exception of graphites from Pitches "T", "U" and possibly "L" and "N", which were about equivalent. However, even those with equivalent resistivities were no better than the standard, in terms of apparent density, flexural strength or transverse CTE.

CONCLUSION

The most significant fact to arise out of our research is that graphite physical properties, such as CTE, flexural strength, apparent density and electrical resistivity, are apparently unrelated to pitch Q.I. levels, alone, but to the nature or type of Q.I. This, in turn, is directly related to the method of preparation, i. e., process route, by which specific Q.I. levels are attained.

GRAPHITE PROPERTIES OF 12 ALLIED EXPERIMENTAL PITCHES

Pitch Type	Pitch Process	AD	Long. Resist.	Trans. Resist.	Long. CTE	Trans. CTE	FS	Binder Level
		g/cc	$\times 10^{-5}$ ohm-in	$\times 10^{-5}$ ohm-in	$\times 10^{-6}/C$	$\times 10^{-6}/C$	psi	
K	IV	1.23	7.8	18.1	0.59	1.32	499	M
K	IV	1.15	9.5	10.9	0.57	1.14	211	H
L	IV	1.17	4.9	6.2	0.57	0.99	311	L
L	IV	1.15	7.6	10.9	0.61	1.18	344	M
L	IV	1.15	8.9	13.3	0.61	1.18	309	H
M	IV	1.21	10.3	29.2	0.68	1.04	307	M
M	IV	1.19	10.5	32.2	0.61	1.04	291	H
N	III	1.12	5.0	20.6	0.49	0.83	235	L
N	III	1.10	8.5	31.8	0.58	1.13	292	M
N	III	1.12	5.4	23.2	0.53	0.94	269	H
Q	III	1.13	10.1	31.2	0.49	0.99	189	L
Q	III	1.14	9.3	22.6	0.55	1.04	202	M
Q	III	1.13	7.7	29.6	0.55	0.91	222	H
P	III	1.01	14.8	32.2	0.65	0.67	28	M
P	III	1.08	9.0	31.9	0.61	1.11	201	H
S	II	1.18	8.4	11.6	0.58	1.18	232	L
S	II	1.19	6.8	13.8	0.57	1.52	430	M
S	II	1.12	8.8	14.5	0.54	1.33	227	H
T	II	1.17	2.9	16.3	0.48	0.96	306	L
T	II	1.15	4.2	18.9	0.51	0.99	281	M
T	II	1.13	6.8	25.0	0.49	1.00	239	H
U	II	1.14	8.8	24.7	0.58	0.99	295	L
U	II	1.17	4.0	26.1	0.69	1.13	332	M
U	II	1.12	7.4	29.9	0.65	1.00	263	H
W	I	1.18	7.9	9.6	0.60	0.90	323	M
W	I	1.15	9.2	9.8	0.59	0.92	334	H
X	I	1.18	9.4	11.9	0.56	1.20	290	L
X	I	1.16	9.2	30.9	0.57	1.17	366	M
X	I	1.17	8.6	15.8	0.45	1.13	412	H
Y	I	1.19	7.1	28.5	0.66	1.11	280	L
Y	I	1.19	7.6	24.4	0.57	0.91	347	M
Y	I	1.17	7.9	24.4	0.59	1.00	245	H
Standard		1.21	2.4	16.4	0.68	1.21	375	M

Note: Binder Level--H - high, M - medium, L - low. There is a difference of 2 pph of binder (based on the weight of filler) between each binder level; thus, there is a spread of 4 pph between the highest (H) and lowest (L) level.

REFERENCES

- 1 M. B. Dell, "Characterization of Pitches for Carbon Anodes", presented before the Division of Gas and Fuel Chemistry, American Chemical Society, Urbana, Illinois (May 15 & 16, 1958).
- 2 D. McNeil and L. J. Wood, "The Use of Coal Tar Pitch as an Electrode Binder", Coal Tar Research Association, Gomersal, Leeds, Industrial Carbon and Graphite, Society of Chemical Industry, paper read at the conference in London (September 24 - 26, 1957).
- 3 P. L. Walker, Jr., C. R. Kinney, D. O. Baumbach, and M. P. Thomas, "The Relationship of the Chemical and Physical Properties of Coal Tar Pitches to Their Carbonization and Graphitization Character", Fuel Technology Department, The Pennsylvania State University, University Park, Pennsylvania.
- 4 S. J. Green and S. G. Ward, "The Insolubles Matter of Coal Tar", Journal of the Society of the Chemical Industry (London), 67, 422 (1948).
- 5 J. O'Brochta, Koppers Company, Inc., "The Composition and Properties of Coal Tar Pitches", presented April 13, 1956, at Dallas, Texas, before the Gas and Fuel Division of the American Chemical Society.
- 6 A. J. Lindsay, et al, "Polycyclic Aromatic Hydrocarbons in Carbon Blacks", Chemical and Engineering (London), pp. 1365-66 (1958).
- 7 S. S. Pollack and L. E. Alexander, Journal of Chemical Engineering Data, 5, 88 (1960).
- 8 J. Taylor and H. Brown, "Carbon Obtained from Thermal and Catalytic Cracking of Tars", Japan Carbon Conference (1964).
- 9 M. S. Morgan, W. H. Schlag, and M. H. Wilt, "Surface Properties of Quinoline Insolubles Fraction of Coal Tar Pitch", Journal of Chemical Engineering Data, 5, No. 1, pp. 81 - 84 (1960).
- 10 S. W. Martin and H. W. Nelson, Industrial Engineering Chemical, 50, 33 (1958).

FIGURE 1
 PREPARATION OF RAW MATERIAL
 AND BLEND COMPONENTS

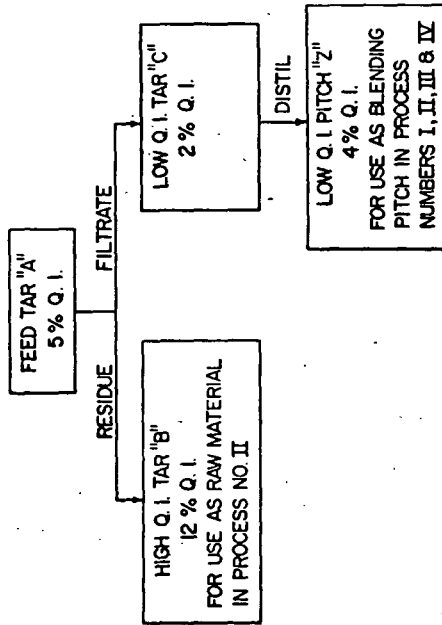


FIGURE 2
 PROCESS NO. I
 PREPARATION OF NATURAL Q. I. PITCH

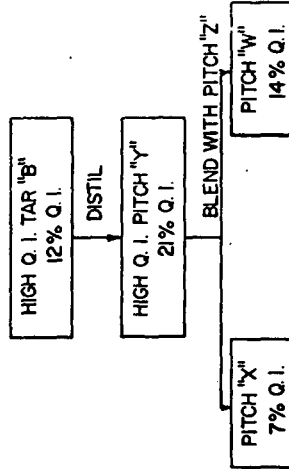


FIGURE 3
PROCESS NO. II
PREPARATION OF PITCH USING
EXPERIMENTAL PROCESS TYPE I

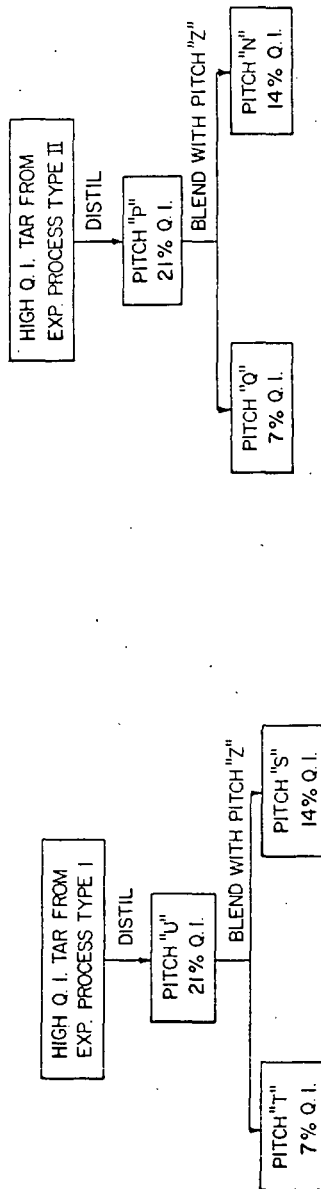
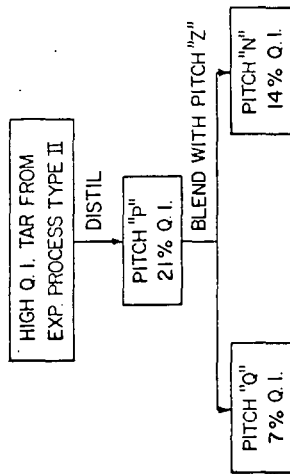


FIGURE 4
PREPARATION OF PITCH USING
EXPERIMENTAL PROCESS TYPE II



ACTUAL Q.I. LEVELS vs T-C.T.E. LEVELS

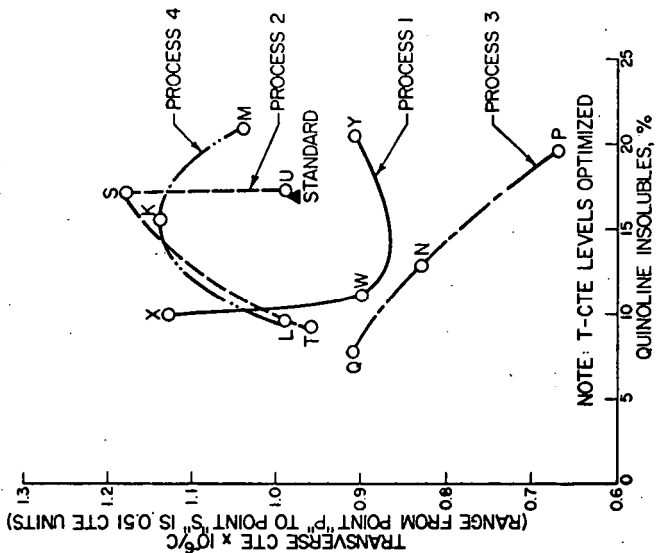
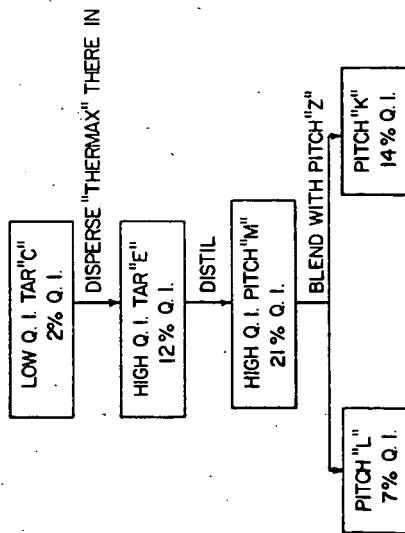


FIGURE 6

FIGURE 5
PREPARATION OF "THERMAX"-
MODIFIED Q. I. PITCH



ACTUAL Q. I. LEVELS vs FLEXURAL STRENGTH LEVELS

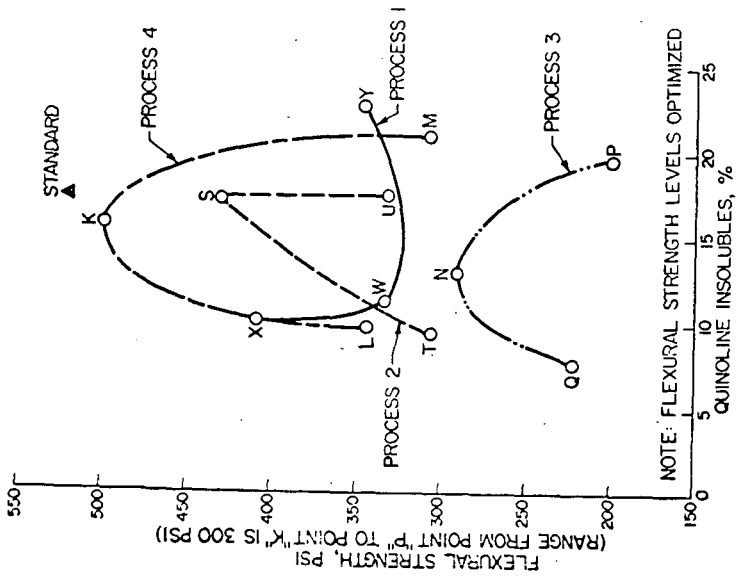


FIGURE 7

ACTUAL Q. I. LEVELS vs APPARENT DENSITY LEVELS

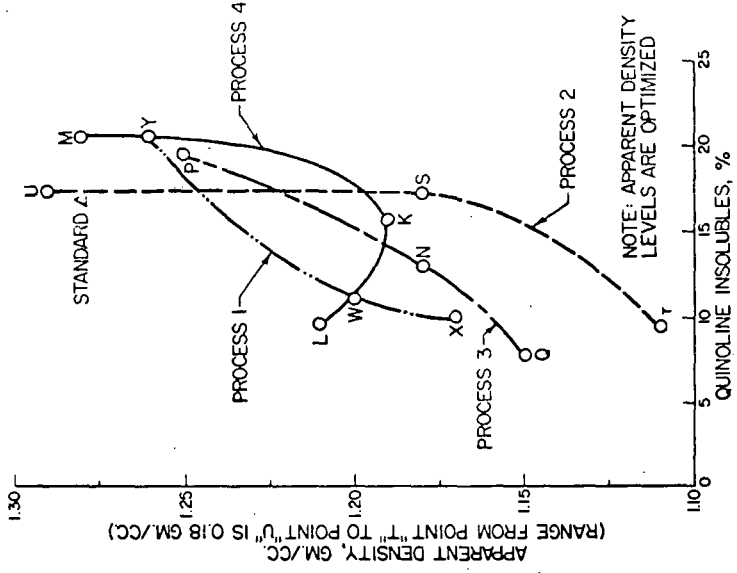


FIGURE 8

ELECTRODE TESTS OF PURIFIED COKE FROM
COAL IN ALUMINUM MANUFACTURE

V. L. Bullough, L. O. Daley, W. R. Johnson and C. J. McMinn

Reduction Research Laboratory, Reynolds Metals Company, Sheffield, Alabama

During the electrowinning of aluminum from aluminum oxide by the Hall process nearly 0.5 pounds of high grade carbon is consumed for each pound of aluminum produced. The raw materials making up this carbon must, of necessity, be of high purity because many metallic impurities in the carbon are transferred to the aluminum produced, and affect the metallurgical properties of the aluminum. For this reason raw materials used in anode manufacture for the aluminum industry have stringent purity specifications.

In addition to the specifications of purity, coke used in the manufacture of electrodes for aluminum production must be heat treated to temperatures of about 1300°C to insure the high temperature dimensional stability of the electrode. It must also contain about 25 percent of particles larger than 1/4 inch to allow for a graduated aggregate in electrode manufacture that is needed to prevent the propagation of stress cracks in large carbon masses.

Because petroleum coke represents a large volume source of relatively pure carbon, it is used almost exclusively for anode manufacture by the aluminum industry in the United States. Some coal tar pitch coke is used in Europe to supplement the supply of petroleum coke.

Coke derived from coal is not used in alumina reduction cell anodes because of the high ash content. Several investigators¹⁻⁶ have studied methods of removing the mineral matter from coal for the purpose of making purified coke for electrode use, and coke from purified coal has been used in Europe on a commercial scale in at least two cases.^{7,8} These were wartime uses, however, and were not competitive when adequate supplies of high grade petroleum coke were available.

Possible future shortages of electrode grade petroleum coke have encouraged the continued investigation of methods of producing high purity coke from coal as a substitute and competitive material for use in electrodes. This report will be concerned primarily with a performance test of electrodes made from a purified coke from coal in pilot plant and commercial alumina reduction cells.

Process Description

Figure 1 is a diagram of the major steps of a process for manufacturing high grade coke from coal. In a pilot plant operated by Reynolds Metals Company for the production of coke, a mixture of high volatile bituminous coal and a solvent oil was digested in a continuous pressure digester to a temperature slightly above the temperature of maximum solubility of the coal.⁹ The coal solution from the pressure digester was charged to centrifuges where the

suspended mineral matter and fusain were separated from the coal solution. This solution from the centrifuge was charged to a continuous distillation still where the solvent was separated and returned to the mixing cycle. The still bottoms which contained the purified coal were charged directly to a coke oven where a purified coal was converted to coke and heat treated to a temperature that would assure dimensional stability at the operating temperature of an alumina reduction cell.

Coal from two sources was run in the pilot plant — the Black Creek seam in North Alabama and the No. 9 seam in Western Kentucky. Typical analyses of these coals are shown in Table I. Typical properties of cokes made from these coals compared with an electrode grade petroleum coke are shown in Table II. Electrical resistivity was determined by the Great Lakes Carbon Company Method, C-12, and the Hardgrove grindability index was determined by ASTM Method No. D409-51. The coke prepared from these coals had a grey metallic luster and was more resistant to grinding than regular petroleum coke. The iron content was the only property of this coke that was inferior to electrode grade petroleum coke and did not meet specifications imposed by aluminum producers. Since the iron content of the coke produced in the pilot plant was about three times higher than coke produced from the same coals in laboratory scale equipment, it is believed that this difference represents iron pickup from the pilot plant processing equipment and is not an inherent limitation of the process.

Two types of carbon anodes are used in the aluminum process. In the prebaked anode type cell, electrode blocks are fabricated from a graded carbon aggregate and coal tar pitch. This mixture is pressed into blocks by large hydraulic presses, and the resulting blocks are heated in furnaces to about 1200°C. The baked block is suspended in the molten salt electrolyte by the electrical connection which is usually made with a steel pin held in a specially molded well in the carbon block by cast iron. In the other type of anode system, which is known as the continuous electrode or Soderberg system, heat from the electrolytic process is used to bake a carbonaceous paste prepared from a graded coke aggregate and coal tar pitch. This paste is added to the top of the anode casing as carbon is consumed by the process from the bottom of the anode. Electrical connections are made through steel pins embedded in the carbon.

Approximately 6000 pounds of coke from purified coal were processed into electrode blocks at the carbon plant of a commercial aluminum plant for tests in a 10,000 ampere scale alumina reduction cell. These blocks were 20 x 16 x 13 inches and each weighed about 200 pounds.

There are two major sources of anode carbon consumption in an alumina reduction cell. These are electrolytic reaction with oxygen released from the aluminum oxide at the working face of the anode and reaction with oxygen from the air on the sides and top of the anode in the area not wet by the molten salt electrolyte. To determine the amount of carbon lost to oxygen from each of these sources, a number of the anodes were capped with an alumina cap prepared from a tabular alumina castable refractory. The rest of the blocks were run without a cap to protect against air burning which is the normal practice in an alumina reduction plant. To provide experimental control and comparison against regular electrode materials, half of the anodes in the cell at any time were prepared from petroleum coke.

Each anode was weighed before being placed in the test cell. After seven days of electrolysis the unburned portion was removed from the cell and weighed. The difference between the initial and the final weights was taken to be equal to the carbon consumed during the test period. The anodes that were capped with an alumina refractory were weighed before capping and after test the remaining cap was broken from the block before the stub was weighed. Each individual anode position on the test cell was equipped with electrical shunts and the current passing through the block during the test period was recorded with integrating ammeters. Results of the test are summarized in Table III. Approximately 30 anode blocks made from the coke from purified coal were tested as were a like number of control blocks made from petroleum coke. This number of blocks was established by statistical treatment of data from previous experiments as being the number required to distinguish a carbon consumption difference of 0.5 gms. /amp. hr. in this type of test cell.

The anode stubs from the coke from coal blocks removed from the test cell were hard and dense and showed no tendency for coke particles to dust from the electrode surface.

In a second test, more than 20,000 pounds of coke made from purified coal were made into a carbon paste and tested in a 45,000 ampere Soderberg type reduction cell. Mechanical properties of electrode specimens prepared from samples of the carbon paste that were baked to about 1,000°C in a laboratory furnace are shown in Table IV with the mechanical properties of specimens from comparable paste made from electrode grade petroleum coke. One notable characteristic of the paste prepared from coke from purified coal was that about two percent less pitch was required than was normally used to prepare paste of comparable viscosity from petroleum coke.

Midway through the test the anode was raised from the electrolyte and inspected. The working face of the anode was flat and smooth and the anode was free of large cracks indicating that the coke from the pilot plant was thermally stable for use at the anode operating temperatures. Cell operation was smooth and efficient and the anode generally could not be distinguished from anodes made from petroleum coke.

Discussion

Examination of the test results summarized in Table III indicate that the consumption of carbon blocks was nearly the same for the coke from coal anodes as it was for the petroleum coke anodes. The difference in consumption between capped and uncapped anodes shows that 20 percent of the carbon in the petroleum coke anodes was lost to air burning compared to 16 percent for the anodes made with coke from coal. This is an indication that the coke from coal electrodes were less susceptible to attack by oxygen in the air. This indication is supported by observations made while determining the ash content that the cokes made from coal required considerably longer time to burn away than did petroleum cokes.

The performance testing of electrodes made from coke from purified coal in both prebaked and Soderberg type anodes indicated that the coke was satisfactory and could meet the specifications for anode grade coke for the aluminum industry.

ACKNOWLEDGMENT

The permission of Reynolds Metals Company to publish the results of this investigation is gratefully acknowledged.

LITERATURE CITED

1. Selvig, W. A., W. H. Ode, and F. H. Gibson, "Coke From Low-Ash Appalachian Coals for Carbon Electrodes in Aluminum Industry," Bureau of Mines Report of Investigations 3731, 1943, 188 pp.
2. Graham, H. G., and L. D. Schmidt, "Methods of Producing Ultra-Clean Coal for Electrode Carbon in Germany," Bureau of Mines Information Circular 7481, 1948, 13 pp.
3. Campbell, R. J., Jr., R. I. Hilton, and C. L. Boyd, "Coal As a Source of Electrode Carbon in Aluminum Production," Bureau of Mines, Report of Investigations 5191, 1956, 53 pp.
4. Klemgard, E. N., "Electrode Carbon From Washington State Coal," Bulletin No. 218, Washington State Institute of Technology, Pullman, Washington, 1953, 37 pp.
5. Bloomer, W. I., and F. L. Shea, "Coal Deashing and High-Purity Coke," American Chemical Society, Division of Fuel Chemistry, Preprints, 11 No. 2, 378-392 (April 1967).
6. Kloepper, Dean L., Thomas F. Rogers, Charles H. Wright, and Willard C. Bull, "Solvent Processing of Coal to Produce a De-ashed Product," Research and Development Report No. 9, Office of Coal Research.
7. Nelson, H., "The Selective Separation of Super Low Ash Coal by Flotation, Gas World," Vol. 127, 1947, pp 125-130-132.
8. Lowry, H. H., and H. J. Rose, "Pott-Broche Coal Extraction Process and Plant of Ruhrol G. M. B. H., Bottrop-Wilhelm, Germany," Bureau of Mines Information Circular 7420, 12 pp.
9. U. S. Patent 3,240,566.

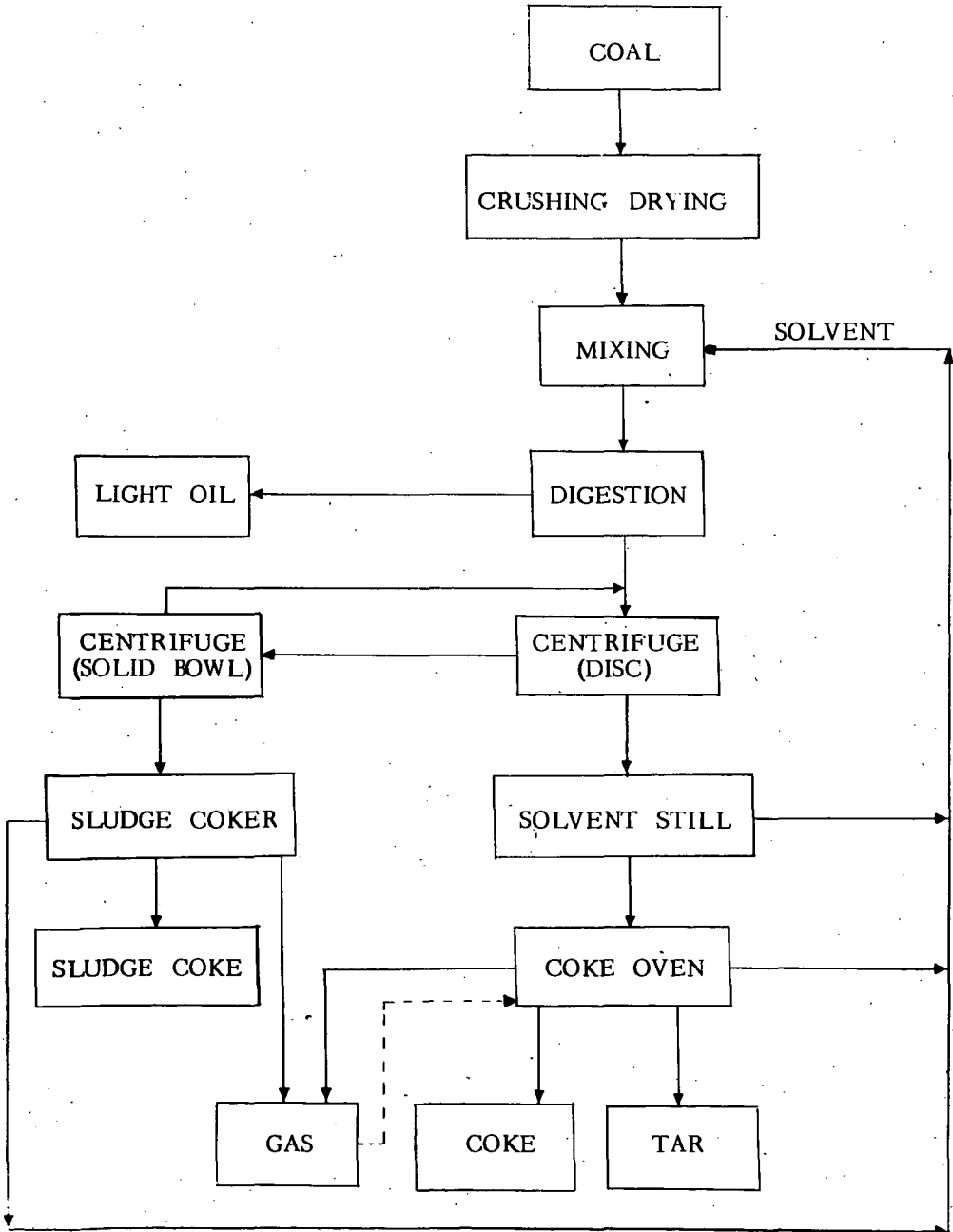


FIGURE 1. DIAGRAM OF A COKE-FROM-COAL PROCESS

TABLE I
ANALYSES OF COALS USED IN INVESTIGATION
OF ELECTRODE COKE FROM COAL.

	Black Creek Coal Seam		Kentucky No. 9 Coal Seam	
	As Received %	Dry Ash-free %	As Received %	Dry Ash-free %
Moisture	2.7	----	----	----
V. M.	35.4	37.4	40.5	45.0
Ash	2.8	----	9.9	----
H ₂	5.4	5.7	5.1	5.6
C	79.8	84.4	72.5	80.5
N ₂	1.7	1.8	1.5	1.7
O ₂	9.5	7.6	7.9	8.8
S	.8	.8	3.1	3.4

TABLE II

PROPERTIES OF COKES FROM KENTUCKY COAL AND
ALABAMA COAL AFTER CALCINING TO 1340°C

	Alabama Coke	Kentucky Coke	Typical Petroleum Coke
Specific Gravity	2.02	2.01	2.03
Electrical Resistivity, ohm-in.	0.029	0.034	0.034
Hardgrove Grindability Index	22	22.5	37
Sulfur, Percent	0.46	0.67	0.8 - 1.65
Silicon, Percent	0.04	0.09	0.03
Iron, Percent	0.07	0.08	0.05
Aluminum, Percent	0.09	0.09	0.02
Ash, Percent	0.58	0.76	0.34

TABLE III
 CONSUMPTION OF CARBON IN A 10,000
 AMPERE PREBAKE ALUMINUM CELL

	Electrode Consumption, gms. /amp. hr.			
	Coal Coke		Petroleum Coke	
	Result	σ	Result	σ
Capped Carbons	0.121	± 0.002	0.118	± 0.003
Uncapped Carbons	0.144	± 0.004	0.147	± 0.004

TABLE IV
 PHYSICAL PROPERTIES TEST RESULTS OF
 SODERBERG ELECTRODE SPECIMENS WITH
 COKE-FROM-COAL AGGREGATE

	Aggregate			
	Coke-From-Coal		Petroleum Coke	
	Result*	σ	Result*	σ
Apparent Density, gms. /cm. ³	1.58	$\pm .03$	1.56	$\pm .02$
Electrical Resistivity, ohms/m/mm ²	53	± 2.2	60	± 1.6
Compression Strength, Kg. /cm. ²	601	± 56	436	± 35

* Average of eight determinations.

THE IRREVERSIBLE EXPANSION OF CARBON
BODIES DURING GRAPHITIZATION

M. P. Whittaker and L. I. Grindstaff

Great Lakes Research Corporation
Elizabethton, TennesseeINTRODUCTION

The formation of synthetic graphite from amorphous carbon should theoretically be accompanied by a continuous shrinkage of material. However, in many instances an irreversible volume expansion, commonly referred to as puffing, is actually observed to occur at some point in the transformation. The addition of certain metals, particularly iron and calcium or their compounds, is known to inhibit or eliminate this expansion. Although "puffing" has generally been associated with the sulfur content of the petroleum coke, very little information has actually been published concerning this phenomenon. Based largely upon analogies found in the puffing behavior of sulfur-containing petroleum cokes and of carbon-bromine lamellar residue compounds, H. C. Volk¹ advanced the theory that puffing resulted from the decomposition of carbon-sulfur lamellar residue compounds. The formation of a thermally stable carbon-sulfur-metal ternary lamellar compound was proposed as an explanation for the inhibition mechanism. However, the existence of these compounds has not been convincingly established and our results are certainly difficult to reconcile with lamellar compound formation.

EXPERIMENTAL

The carbon bodies were made from a standard mixture of calcined petroleum coke, particle sizes ranging from -35 mesh to -100 mesh, and a coal tar pitch binder by hot pressing in an electrically heated mold at 12,500 psig for thirty seconds at 100°C. The cylindrical plugs were baked to a temperature of 850°C.

The extent of irreversible expansion exhibited by the baked carbon bodies as a function of heat treatment was measured with a graphite dilatometer. The dilatometer holding the carbon plugs was heated in a graphite tube furnace to temperatures as high as 2900°C at a rate of 14°C/min. A nitrogen atmosphere was maintained throughout the heating period.

A 15,000 psi mercury porosimeter was used to obtain micropore volume distribution in the heated carbon plugs. The plugs were crushed to -35/48 mesh and pore volume determinations made on 0.400 g. samples of this material.

X-ray diffraction examinations were made with a recording diffractometer using monochromatic Cu $\text{K}\alpha$ radiation at room temperature.

The sulfur in the carbon samples was determined by igniting the sample in an oxygen atmosphere at 1400°C. The SO_2 formed was titrated continuously by iodometry in the presence of starch indicator. Good agreement was found between this method and the method using the Parr-peroxide bomb combustion technique.

RESULTSCause of the Deformation

The petroleum cokes studied which were subject to deformation could be separated roughly into two broad groups according to their puffing characteristics. Typical dynamic elongation curves of the two groups are compared in Figure 1 and Figure 2. It can be seen that there exists a difference of 300°C between the two groups of carbons with respect to the temperature at which the deformation begins. The cokes which deform at the lower temperature do not respond well to puffing inhibitors and generally have a higher concentration of sulfur, oxygen and nitrogen.

The loss of the volatile constituents of a large number of carbons as a function of heat treatment was determined. In all cases oxygen and nitrogen were lost at temperatures below 1000°C. The sulfurous gases, however, were evolved over precisely the same temperature range as that at which the deformation occurred. The sulfur evolution from the samples was followed by heating the bodies at the same rate, 14°C/min., as was used in the dynamic puffing test to various temperatures before the desired analyses were made. The composition of the samples was compared and correlated with the dynamic puffing characteristics. An example of such a correlation is presented in Figure 3. The rate of sulfur evolution in the carbon samples in which the initial decomposition and corresponding deformation occurred at the lower temperature, 1400°C, was ten to twenty times greater than the rate observed in samples with the more thermally stable sulfur.

The escaping gas from several carbons was carefully trapped and analyzed. The gas was found to be essentially hydrogen sulfide. Unfortunately, all of the carbons studied with a high enough sulfur content to permit meaningful gas analysis puffed in the low temperature range.

If a sample is heated to the temperature at which the sulfur first begins to evolve and is held at that temperature until the desulfurization is essentially complete, deformation of the sample occurs only at this temperature, see Figure 4. There is little doubt that puffing results from internal pressures generated by the sudden expulsion of H₂S.

By carefully measuring the crystallite dimensions during the course of the deformation by means of x-ray diffraction, it becomes apparent that the puffing is an inter-crystalline phenomenon. However, in one experiment in which a sample made from a coke having an unusually high sulfur content was pushed directly into a furnace at 1400°C, an anomalous x-ray pattern was obtained from the sample. The 00 ℓ diffraction peaks were split, one portion of the peak being located at the expected 2 θ angle and the other occurring at a slightly higher angle, see Figure 5. Upon further heat treatment a coalescence into a single peak occurs, the lower angle portion of the peak overtaking the other. One possible explanation is that the high internal pressure generated within the sample has actually forced part of the sample to a more graphitic state. It is certainly well known that externally applied pressure facilitates graphitization.²

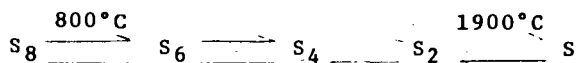
The pore structure of the samples during puffing was evaluated by means of mercury porosimetry. Typical pore size distribution curves are presented in Figure 6. Puffing is characterized by an increase in

pores having diameters in the 0.1-.015 μ range. The total deformation of the sample can be accounted for by the creation of this additional porosity resulting from the hot expanding gas channeling its way to the sample surface.

The magnitude of the deformation does not depend entirely upon the sulfur content of the coke. The microstructure of the coke is also important. As would be expected, hard carbons characterized by a high degree of cross-linking between crystallites are much more resistant to deformation than the more graphitic "softer" type carbons. For this reason there are several cokes which do not puff although they have a sulfur content comparable to that of a puffing softer type coke and the sulfur is evolved over the same temperature range at the same rate. This microstructural dependence was further illustrated by producing a softer type carbon from a feedstock which ordinarily forms a relatively hard carbon by making certain changes in processing and comparing the puffing characteristics of the two cokes. The sulfur content of the more graphitizable carbon exhibiting a linear CTE of $5.0 \times 10^{-7}/^{\circ}\text{C}$ was exactly the same as the less graphitizable carbon having a CTE of $23.0 \times 10^{-7}/^{\circ}\text{C}$. The softer carbon, however, puffed while the other coke exhibited no measurable deformation.

Mechanism of Puffing Inhibition

As illustrated in Figure 7 for the case of iron oxide, certain materials when added to the carbon sample eliminate or at least diminish in magnitude the puffing effect. The temperature required to initiate the volatilization of sulfur is higher and the rate of the subsequent gaseous evolution is lower in the samples containing an inhibitor, see Figure 8. An analysis of the effluent gas reveals that the sulfur is principally in the form of elemental sulfur rather than H_2S . The composition of the sulfur vapor at these temperatures is governed by the following equilibria:



Even above 1900°C the sulfur vapor is 55% associated.³ An increase in association of the sulfur atoms would, of course, result in a decrease in gas volume. By following the composition of the inhibitor as a function of temperature by means of x-ray diffraction, the mechanism of inhibition becomes apparent. This type of analysis for iron oxide is given in Figure 9. The inhibitor reacts with the sulfur to form a sulfide which subsequently decomposes at a higher temperature liberating sulfur in its elemental form and at a reduced rate. The effectiveness of the metal in preventing puffing is a function of the stability of its sulfide. Sodium, for example, forms a sulfide which is expelled rapidly at a relatively low temperature resulting in distortion of the sample, see Figure 10.

A secondary deformation of reduced magnitude was observed to occur at around 2500°C in the most graphitic or needle type carbons studied upon inhibition with iron oxide, see Figure 11. A gaseous evolution resulting from the decomposition of the iron sulfide is occurring at this temperature, however, the rate of volatilization at 2500°C is not substantially different from that at temperatures immediately below this delayed puffing range. This indicates that structural changes must be occurring in the carbon body which

effectively reduce its resistance to puffing. It is well known that the mechanical strength of graphite increases with temperature to about 2500°C and then decreases sharply with temperature above 2500°C.⁴ A substantial amount of creep occurs in graphite at 2500°C and higher. This sudden decrease in strength of the body coupled with the internal pressure generated by the decomposition of the metal sulfide provides a logical explanation for the observed delayed puffing.

Lamellar Residue Compounds

Lamellar and lamellar residue compounds are known to have a pronounced effect on the resistivity of the carbon. Dilute residue compounds with a composition $C_{100}X$ (X = intercalated species) are reported to decrease the resistivity of graphite to between 1/2 to 1/10 of its original value, both for n- and p-type compounds.¹ The resistivity of a sample heated to a temperature at which puffing is initiated should increase with time as the residue compound decomposes. We have not found this to be the case. In some carbons, in fact, the resistivity as illustrated in Figure 12 in which the weight percent sulfur loss and resistivity are plotted against holding time actually bears a direct relationship to sulfur evolution. In these materials a decrease in d-spacing and rapid crystallite growth accompanied the decrease in resistivity, see Figure 13. This is additional evidence that premature graphitization is induced by the high internal pressure of the sulfurous gases.

The presence of sulfur per se does not affect the d-spacing in carbon. Therefore, the proposed carbon sulfur lamellar residue compounds cannot be located between the layer planes since a difference in d-spacing would be observable due to their presence. However, residue compounds located at imperfections in the graphite structure would be unlikely to cause a change in the c axis of the graphite if the imperfections are randomly distributed. The diffraction pattern would either not be changed or else only a slight line broadening would occur due to the enlargement or creation of new random imperfections. The existence of the parent lamellar compounds would be expected to be detectable by means of x-ray diffraction except for the fact that the x-ray pattern of carbon heated only to the low temperatures, below 1200°C, at which they are thought to exist is quite diffuse.

Similarly, the resistivity of an inhibited sample is not adversely affected by the removal of the sulfur and inhibitor by heat treatment. Volk noted that the resistivity of the sample was apparently independent of the inhibitor concentration. For this reason, he postulated that the carbon-sulfur-iron compounds were ternary lamellar compounds in which iron functions as a spacer and is therefore not ionized. However, a lamellar compound such as this should be easily detectable by x-ray diffraction analysis. The x-ray spectra of an inhibited carbon is essentially the same before elimination of inhibitor by means of heat treatment alone or with the aid of a purifying gas as after removal. In addition, the diffraction pattern of an inhibited puffing carbon is not significantly different from that of a non-puffing carbon with the same metal concentration. The existence of a ternary lamellar compound is, therefore, certainly doubtful.

CONCLUSIONS

Puffing of carbon bodies results from internal pressure generated by the sudden formation of sulfurous gases, primarily hydrogen sulfide. This pressure is sufficient, in some cases, to cause premature graphitization. The increased volume of the body is in the form of small micropores 0.1 to .015 μ in diameter. Various metals act as inhibitors by reacting with sulfur to form sulfides which subsequently decompose at a temperature and with a rate which is dependent upon the stability of the sulfide. The magnitude of the deformation is also a function of the coke structure. The hard, cross-linked carbons are much more resistant to deformation than the softer, more graphitic carbons. No evidence was found for the existence of lamellar or lamellar residue compounds involving sulfur or the inhibitor.

REFERENCES

1. H. C. Volk, "Lamellar Compounds of Non-Graphitized Petroleum Coke", WADD Tech. Report 61-72, Vol. XXV, (August, 1963).
2. T. Noda, "Graphitization of Carbon under High Pressure", Paper presented at Eight Biennial Conference on Carbon, June 19-23, 1967, Buffalo, N. Y.
3. R. C. Brasted (ed.), Comprehensive Inorganic Chemistry, Vol. 8, D. Van Nostrand Co., Inc., Princeton, N. J., 1961, p-29.
4. S. Mrozowski, "Mechanical Strength, Thermal Expansion and Structure of Cokes and Carbon", Proceedings of the First and Second Conferences on Carbon, Univ. of Buffalo (1956) p-31.

Figure 1.

**DYNAMIC ELONGATION OF A
PETROLEUM COKE (RATE 14°C/min)**

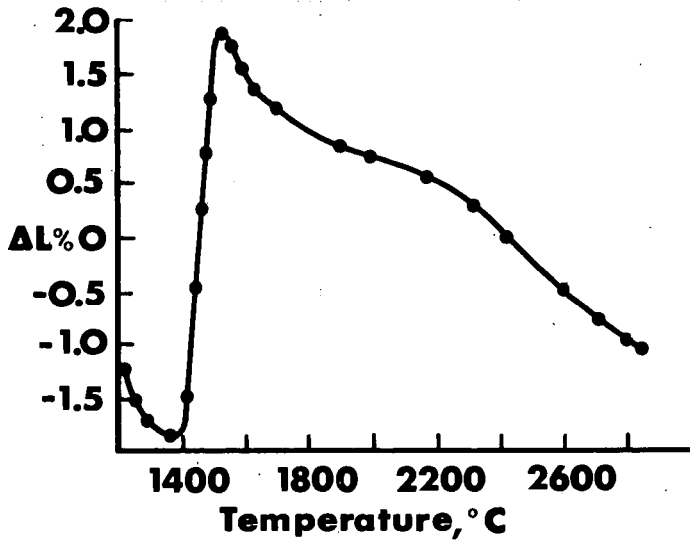


Figure 2.

**DYNAMIC ELONGATION OF A
PETROLEUM COKE (RATE 14°C/min)**

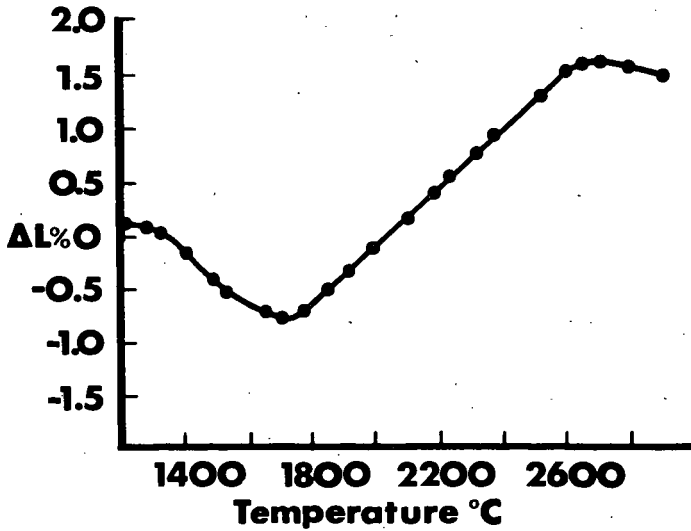


Figure 3.

**EVOLUTION OF SULFUR AND DYNAMIC
ELONGATION OF PETROLEUM
COKE VS. TEMPERATURE**

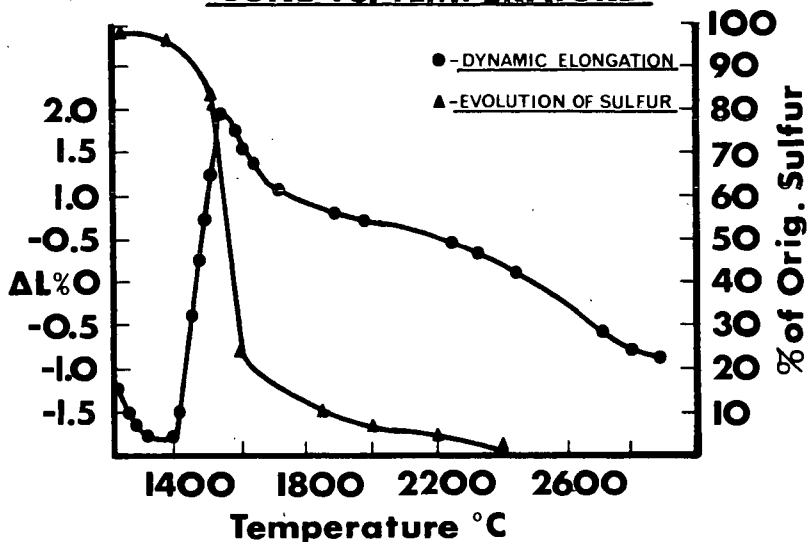


Figure 4.

**DYNAMIC ELONGATION OF PETROLEUM
COKE AT CONSTANT TEMP.**

(Held at 1400°C 3.5 hrs, then to 2900°C @ 14%/m)

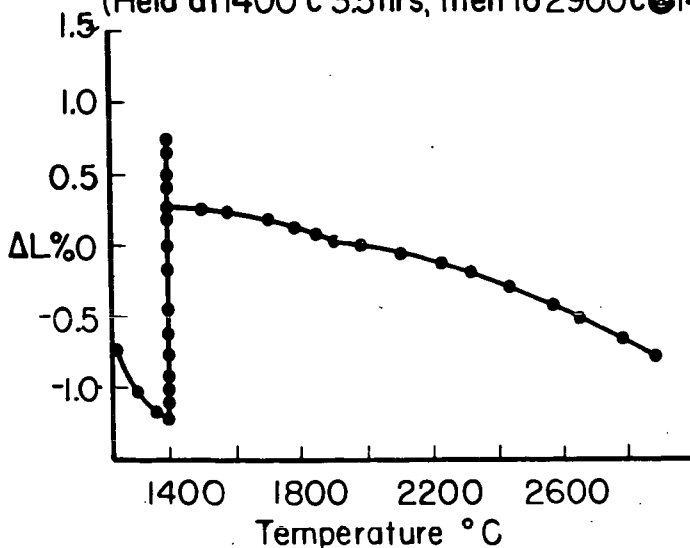


Figure 5. .002 X-RAY DIFFRACTION PEAK

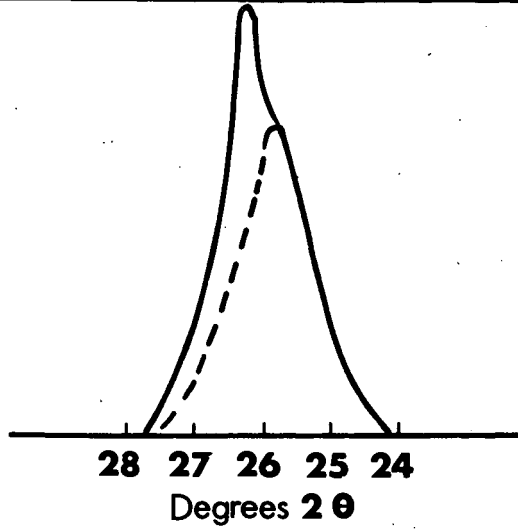


Figure 6. PORE SIZE DISTRIBUTION IN PETROLEUM COKE HEATED TO VARIOUS TEMPERATURE

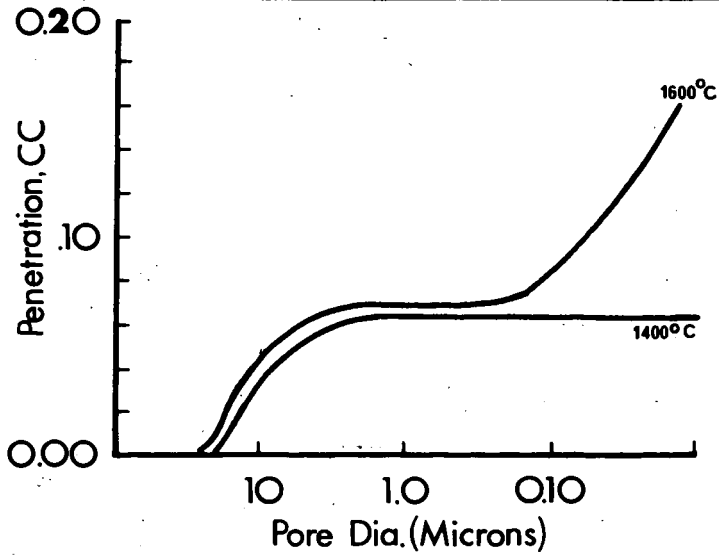


Figure 7. DYNAMIC ELONGATION OF A PETROLEUM COKE CONTAINING Fe_2O_3

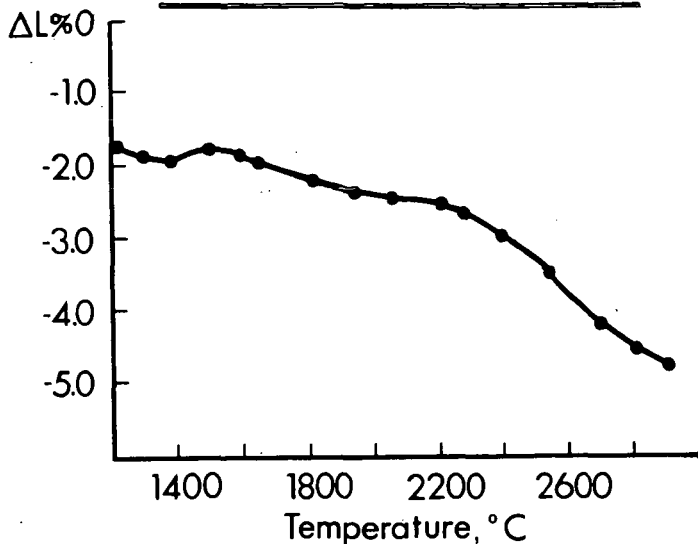


Figure 8. EFFECT OF ADDED Fe_2O_3 ON THE THERMAL STABILITY OF SULFUR IN PETROLEUM COKE

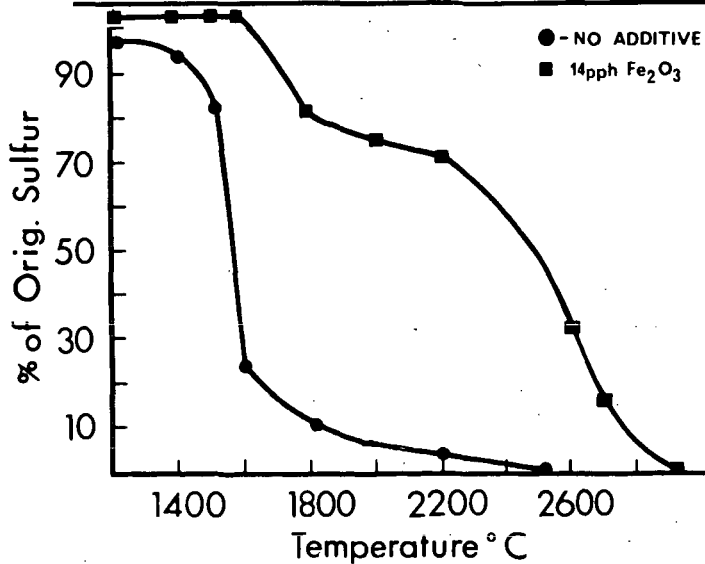


Figure 9.

BEHAVIOR OF IRON OXIDE IN CARBON BODY ON HEATING

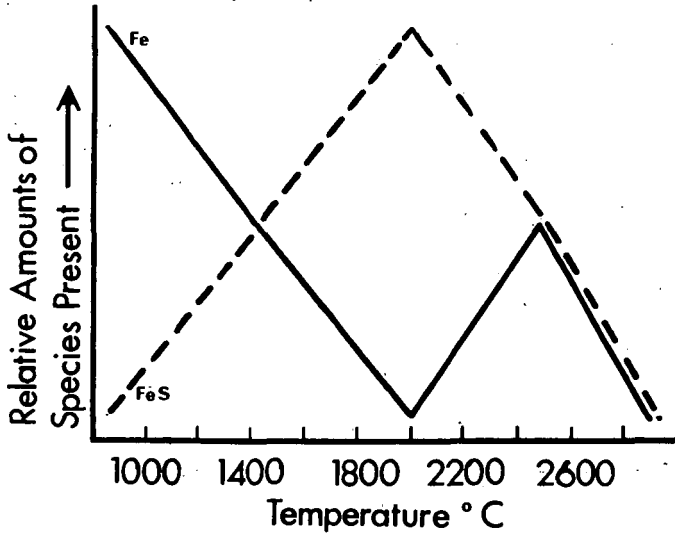


Figure 10.

DYNAMIC ELONGATION OF A PETROLEUM COKE CONTAINING Na_2CO_3

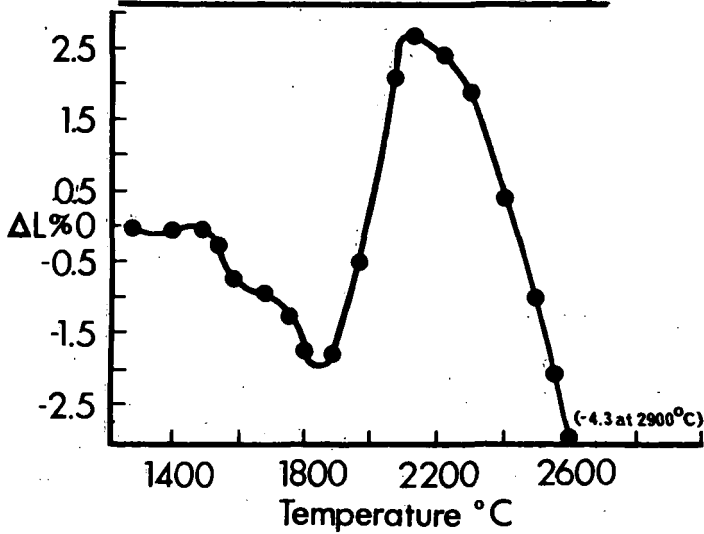


Figure 11. DYNAMIC ELONGATION OF A PETROLEUM COKE CONTAINING Fe_2O_3

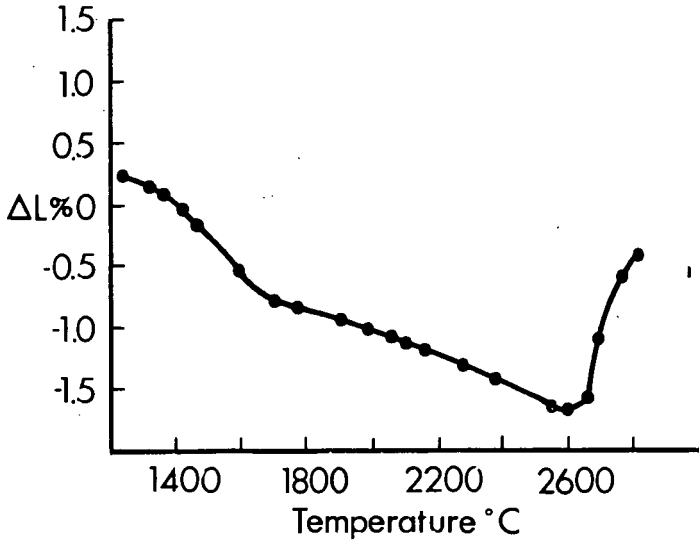


Figure 12. EFFECTS OF HEATING A PETROLEUM COKE AT 1400°C

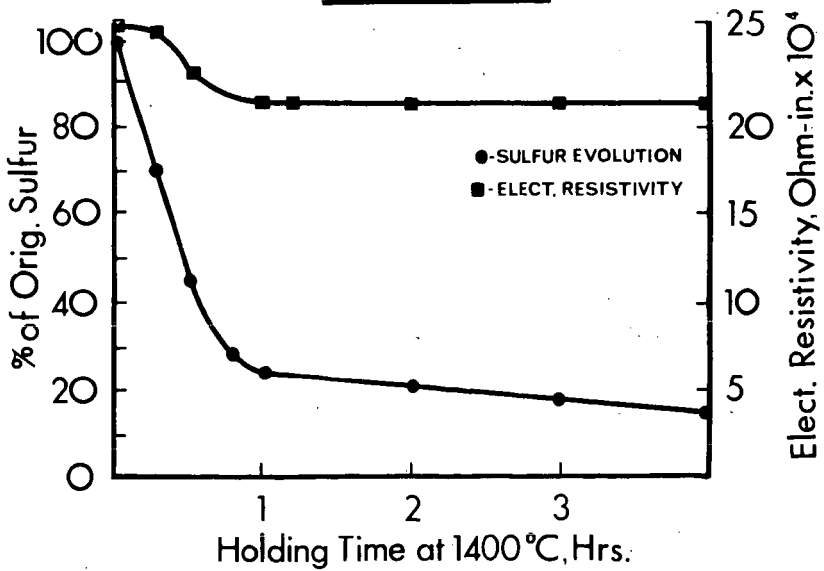
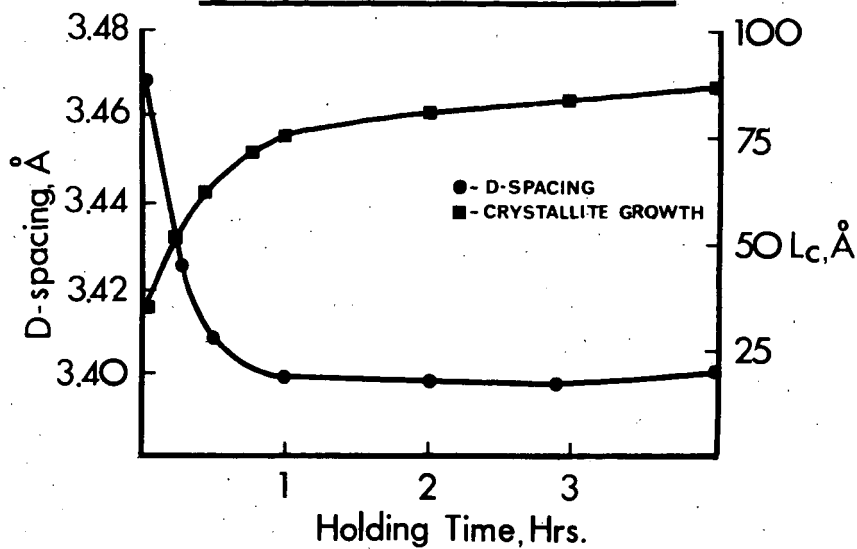


Figure 13.

D-SPACING AND CRYSTALLITE GROWTH IN COKE HEATED AT 1400°C



"Grafoil" Graphite Tape - Its Manufacture, Properties and Uses

Joseph F. Revilock

Union Carbide Corporation, Carbon Products Division, New York, N. Y.

SUMMARY

This paper will describe a new form of graphite - GRAFOIL graphite tape, paper-like in structure and having unusual properties including a high degree of flexibility and compressibility. The paper will discuss briefly the manufacture of GRAFOIL tape products, their properties and their uses in research and development and in chemical and other industrial applications.

MANUFACTURE

GRAFOIL is Union Carbide's trade mark for graphite tape which is made up of interlocking and self-adhering graphite particles. The tape contains no bonding agents such as adhesives, resins or rubber compounds. The particles and the layers which give the tape a laminar structure through its thickness are held together by Van der Waal forces. GRAFOIL graphite tape is manufactured by a patented process in which graphite particles are rolled into sheets .005 or .010 inches in thickness. These 5 and 10 mil thick tapes are flexible as can be seen by the spiral in Figure 1. The normal density of the tape is 70-75 pounds per cubic foot, and by varying the rolling pressure, the density of the tape can be controlled down to 12 pounds per cubic foot.

From these basic graphite tape forms, GRAFOIL laminates (Figure I) are made by cementing layers of tape together with a resin cement which is then carbonized while the laminate is held under pressure. As the thickness of these laminates increase, the flexibility characteristic of the GRAFOIL tape decreases. However, they are still flexible compared to solid graphite and they are still compressible.

Two other forms of GRAFOIL tape illustrated in Figure I are foam and molded forms, made by compressing graphite particles in a mold under pressure. Again the bond is strictly a particle surface phenomenon, no bonding agents being used. Foam materials are light, having a density in the range of 3 to 6 pounds per cubic foot, whereas the molded materials have densities in the range of 70 to 100 pounds per cubic foot, depending on their configuration and end use.

PROPERTIES

The physical properties of GRAFOIL tape are shown in Table I. As can be seen from the data, GRAFOIL tape has a relatively high tensile strength for graphite material. Compressive strength is more than adequate for most applications. The low permeability of GRAFOIL tape is shown by its helium admittance of 2×10^{-4} sq. cm./sec., which is comparable to that of cast brass. (Conventional extruded graphites have admittances of 10^2 to 10^3 sq. cm./sec., while premium graphites have helium admittances in the range of 10^{-2} sq. cm./sec.)

TABLE I
PROPERTIES OF "GRAFOIL" TAPE

<u>Property</u>	<u>Approximate Value</u>
Bulk Density (lb./cu.ft.)	60-80
Ash Content (Weight %)	0.1
Melting Point	Does not melt; sublimes at 6600°F
Tensile strength (surface plane or "a" direction) (lb./sq.in.)	1500-2500
Elastic Modulus, Tensile (10^6 lb./sq.in.)	0.2
Ultimate Compressive Strength (lb./sq.in.)	15,000
Helium Admittance: 0.005 in. thick foil (sq. cm./sec.)	2×10^{-4}
laminated bodies (sq. cm./sec.)	5×10^{-5}
Coefficient of Friction (against stainless steel @ 8 lb/sq.in.)	0.05

The material is very anisotropic and this is shown by the directional nature of the electrical resistances, which are given in Table II. In this respect, GRAFOIL material is similar to pyrolytic graphite.

Table II.

ELECTRICAL RESISTANCE OF "GRAFOIL" TAPE

<u>Form</u>	<u>Surface Plane or "a" Direction</u>	<u>Across Surface Plane or "c" Direction</u>	<u>Ratio "c" to "a" Direction</u>
Tape	.00046 ohm-cm	70 ohm-cm	150,000
Laminate	.0008 "	0.4 "	500

The thermal conductivity of GRAFOIL graphite tape in the surface plane or "a" direction is similar to that of most graphite materials in that it decreases with increasing temperature. Table III shows thermal conductivities at various temperatures for a GRAFOIL graphite tape laminate with a density of 70 lbs/cu.ft.

TABLE III
THERMAL CONDUCTIVITY OF "GRAFOIL" LAMINATE

<u>Temperature</u>	<u>Surface Plane or "a" Direction</u>	<u>Across Surface Plane or "c" Direction</u>
70°F	100 BTU/hr./sq.ft./°F/ft.	3.0 BTU/hr./sq.ft./°F/ft.
900°F	50 "	1.8 "
1800°F	25 "	1.7 "
4000°F	11 "	2.0 "
4500°F	11 "	"

Table IV shows data on compressive load deflection characteristics of GRAFOIL laminates as a function of starting density. The data were taken at a load of 250 lbs./sq.in. With a density of 43 pounds/cu.ft., a load of 250 lbs./sq.in. produced a 22.8% deflection of which 13.6% was permanent set. The resiliency was 7.4% and there was no hysteresis. At densities of 73 and 90 pounds per cubic foot, deflections were 5.5% and the resiliencies were 2.6%. The permanent sets were 2.7% and 2.2%, respectively. These data show the ability of the GRAFOIL material to be cold worked to a higher density at relatively low loads. The material retains resiliency at the higher densities. With the range of densities available, material can be fabricated to a specified low deflection characteristic over a wide range. In one instance, GRAFOIL laminates were made to a specification of 67% deflection at 11 psi load.

TABLE IV
COMPRESSIVE LOAD DEFLECTION OF "GRAFOIL" LAMINATE

<u>Starting Density - lbs/cu.ft.</u>	<u>Deflection-% of Original Thickness</u>	<u>Permanent Set-% of Original Thickness</u>	<u>Resilience-% of Final Thickness</u>
44	22.8	13.6	7.4
73	5.5	2.7	2.6
90	5.5	2.2	2.6

As GRAFOIL graphite tape is all graphite without any binders, its corrosion and temperature resistance are those of graphite. It can be used at temperatures from those of cryogenic liquids, such as liquid oxygen, to those of molten metals, such as molten aluminum and steel. It can be used in any chemical environments other than those of a highly oxidizing nature, such as air above 740°F, hot concentrated nitric acid and hot wet chlorine. In neutral and reducing atmospheres, the material has been used at temperatures up to 3000°C. Table V is a brief list of corrosives to which GRAFOIL materials are resistant. The corrosion resistance at higher temperatures is illustrated by the references to molten caustic, high pressure steam and molten aluminum.

TABLE V
CORROSION RESISTANCE OF "GRAFOIL" MATERIAL

	<u>Conc.</u>	<u>Temp.</u>
Hydrochloric Acid	All	All
Sulfuric Acid	To 95%	300°F
Phosphoric Acid	All	All
Hydrofluoric Acid	All	All
Nitric Acid	To 60%	70°F
Caustic Soda	All	750°F
Aluminum	-	1350°F
Steam	-	1000°F
Chlorinated Organics	All	All
Organic Alcohols	All	All
Organic Esters	All	All
Benzene	All	All
Air	-	740°F

APPLICATIONS

Corrosion and temperature resistance combined with their resilience and compressibility make GRAFOIL materials outstanding as gaskets for flange joints and as packings for seals in rotating and reciprocating equipment. Typical gaskets and packings are shown in Figure II. GRAFOIL tape's sealing characteristics are similar to those of rubber-like materials. Neither cold flow nor creep are experienced with the material and no special flange face conditions are required. Table VI shows applications in which GRAFOIL gaskets give excellent service.

TABLE VI

"GRAFOIL" GASKET APPLICATIONS

<u>Chemical Environment</u>	<u>Temperature-°F</u>	<u>Pressure-Lbs/Sq.In.</u>
Molten Aluminum	1350	5000
Molten Polyester Resins	600	6000
Dowtherm	660	80
Anhydrous Hydrogen Fluoride	660	50
Molten Caustic	650	25
Anhydrous Hydrogen Chloride	1000	Atmospheric
Steam	490	600
Hydrogen Chloride;Chlorine;Organics	100	25
Chlorine plus Organics	650	10
Titanium Tetrachloride	1800	10
Chlorinated Hydrocarbons	212	200

Of even greater importance to the Chemical Process Industries is the use of GRAFOIL packings in pumps, valves, mixers, etc. To take advantage of the material's directional thermal conductivity, the packing is fabricated with the high 'a' direction thermal conductivity perpendicular to the shaft so that frictional heat developed in the stuffing box is transmitted rapidly away from the shaft, preventing overheating and possible impairment of the strength and corrosion resistance of the shaft. Conversely if the stuffing box must be heated, GRAFOIL packing will rapidly conduct the heat throughout the box. As there are no binders or additives in GRAFOIL packing, thermal breakdown, chemical attack, leaching or squeezing out of additives commonly used in other types of packings can not degrade performance. GRAFOIL packing is self-lubricating, has a low coefficient of friction and prevents shaft, stem or plunger scoring.

Figure III illustrates equipment in which GRAFOIL packing is giving extended packing life without shaft damage in a wide variety of corrosive environments. Table VII lists some of the results obtained in commercial installations of GRAFOIL packing.

TABLE VII

"GRAFOIL" PACKING APPLICATIONS

<u>Equipment</u>	<u>Corrosive</u>	<u>Temp.-°F</u>	<u>Pressure-lb/sq.in.</u>	<u>Comments</u>
Plunger Pump	Acid Water	200	1,500	Life up 50 times. No scoring.
Plunger Pump	Organics	70	2,500	Life up 10 times. No lubrication required.
Centrifugal Pump	Organics	100	80	Out-performed mechanical seal; leak- free operation
Centrifugal Pump	Pitch	340	50	Life up 12 times. No scoring.

TABLE VII (Continued)

"GRAFOIL" PACKING APPLICATIONS

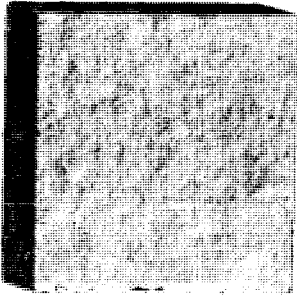
<u>Equipment</u>	<u>Corrosive</u>	<u>Temp.-°F</u>	<u>Pressure-lb/sq.in.</u>	<u>Comments</u>
Centrifugal Pump	Mobiltherm-600	400	50	No leakage after 6 months.
Control Valve	Chlorinated Organics	350	100	Life up 9 times. No scoring.
Control Valve	Dowtherm	660	80	Life up 4 times.
Pressure Control Valve	Steam	490	600	Life up 3 times.

Other uses of GRAFOIL tape take advantage of its flexibility together with its electrical conductivity, its chemical inertness and its low thermal conductivity in the "c" direction at extremely high temperatures. Thin film batteries designed for high power outputs use GRAFOIL tape as internal conductors and anodes. GRAFOIL is an excellent separator in multiple hot pressing of refractory metal compounds and ceramic items since its laminar construction allows easy separation of adjacent pressed parts.

The low "c" direction thermal conductivity and dimensional stability at extremely high temperatures of GRAFOIL materials are being put to use in insulating barriers used in missiles, nuclear reactors, and high temperature vacuum furnaces. GRAFOIL tapes cut into narrow strips are used as electric resistance heating elements. Research and development laboratories throughout the country stock GRAFOIL tape for use in high temperature experimental work.

In conclusion, GRAFOIL tape is a unique form of graphite. Properties such as directional thermal and electrical conductivities, excellent corrosion resistance, low permeability and temperature stability are available in a thin, flexible, compressible, easily fabricated form for a wide range of demanding chemical, metallurgical, nuclear and aerospace uses.

FIGURE I

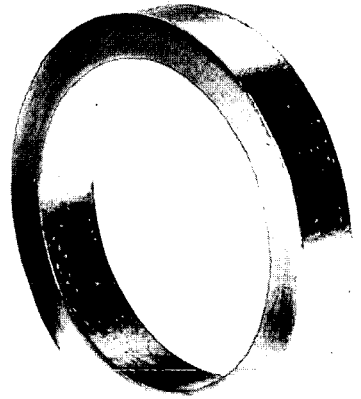


LAMINATE



TAPE

FOAM



MOLDED RING

FIGURE II

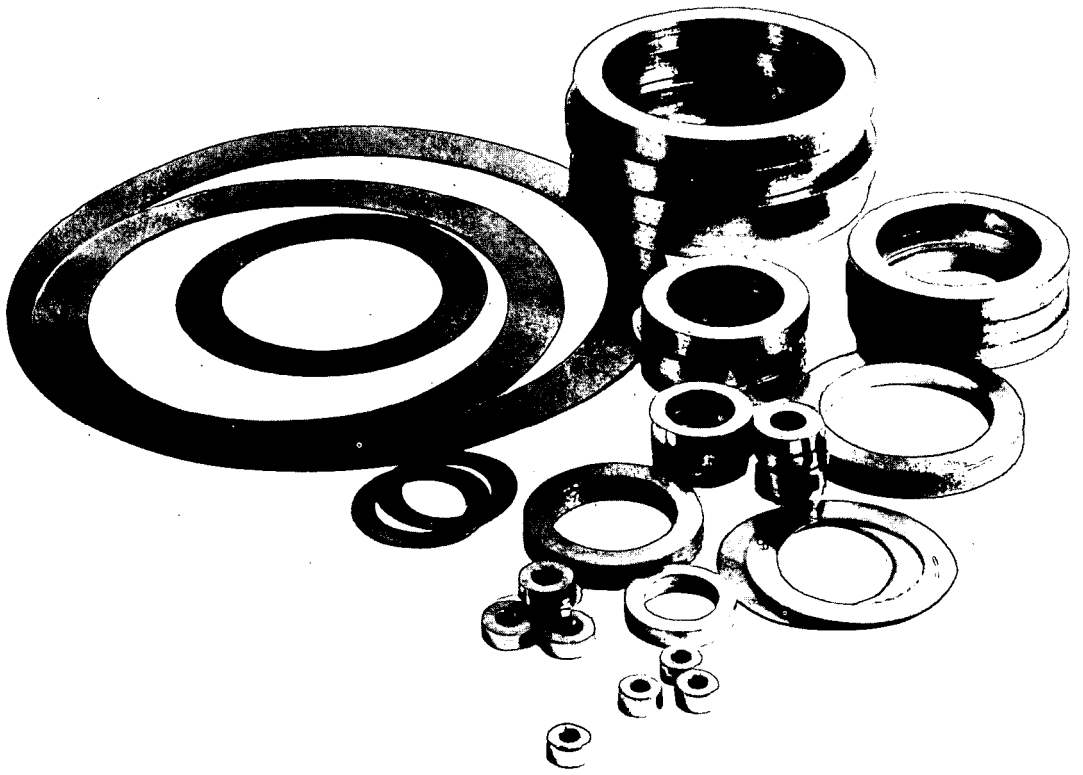
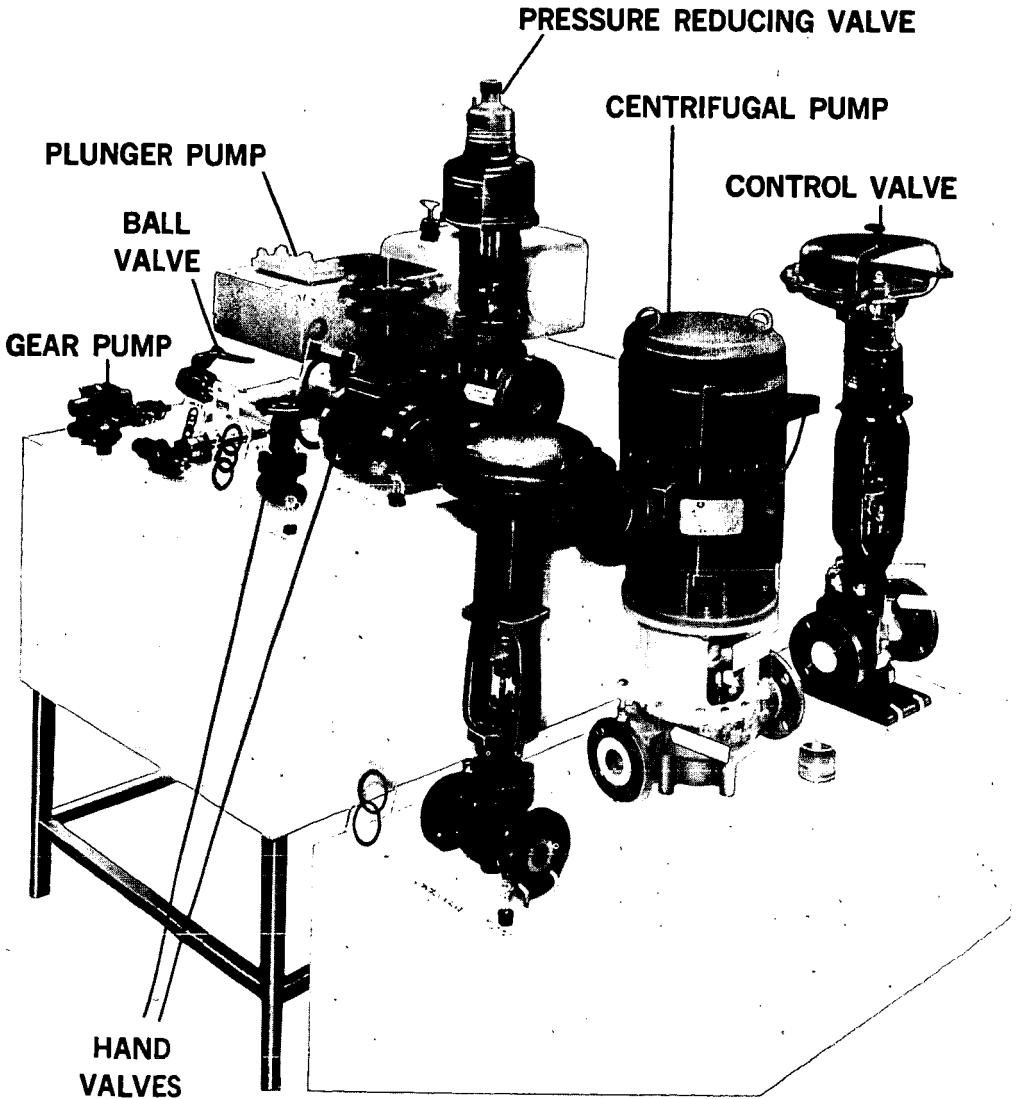


FIGURE III



CARBON FOAM - ITS PREPARATION AND PROPERTIES

R. A. Mercuri, T. R. Wessendorf, and J. M. Criscione

Union Carbide Corporation
Carbon Products Division
Parma Technical Center
Parma, Ohio 44130

I. INTRODUCTION

Light weight cellular carbons are widely used in many industrial and aerospace applications as high temperature thermal insulators and as structural support materials. The Carbon Products Division of Union Carbide Corporation has for many years been engaged in the research and development of carbon foams made by means of the pyrolysis of thermo-setting organic foam precursors. This paper describes the preparation and properties of two types of carbon foams, one based on a phenolic foam and the other on a polyurethane foam precursor. By varying the conditions of preparing the precursor foams and also the rate of pyrolysis, a very broad range of product properties can be obtained.

II. PREPARATION OF CARBON FOAMS

Many factors determine the density and suitability of an organic foam as a carbon precursor; the density of the resins, the temperature and resin balance of the formulation, the molding procedures, and various post curing operations are important examples. A typical foam formulation contains four components: the resin; a surfactant to maintain cell integrity during the foaming process; a foaming aid to obtain a smooth even foaming action starting at low temperatures; and, finally, a catalyst, which is used to initiate the resin polymerization reaction.

The organic foam is converted to cellular carbon by heating in a controlled environment. The heating rate depends on both the precursor thickness and formulation. If the foam is heated improperly, the structure may melt, rupture, or even explode.

A. PYROLYSIS OF PHENOLIC FOAM

The pyrolysis of the phenolic foam is accomplished in a nonoxidizing environment which may be provided by the product gases. Heating rates from 1° to 200°C/hour have been employed in the pyrolysis of phenolic foams. The rate depends on sample size, density, and the strength requirements of the products carbon. For example, samples of low density (0.05 g/cc) phenolic foam with dimensions of 16" x 16" x 2" may be heated at a rate of 100°C/hour to 1000°C to effect the conversion to carbon.

The preferred pyrolysis schedule for any starting foam represents a compromise between product yield and properties. When 0.25 g/cc carbon foams were prepared from phenolic foam at a heating rate which gave a 90 percent yield of crack-free pieces, the compressive strength ranged from 500 to 820 psi. When the heating rate was extended over twice that period of time, the yield of crack-free pieces was increased only slightly but the compressive strength was nearly doubled, to 1000 - 1480 psi. On the other hand, when the original heating rate was doubled, the yield was less than 50 percent acceptable pieces.

The weight and volume changes which occur during pyrolysis vary with the density of the precursor foam. The high density phenolic foams lose 60 percent of their weight and 70 percent of their volume when heated to 2600°C. The shrinkage is anisotropic to the extent that the change in length is usually 3 or 4 percent greater than the change in diameter. Table I shows the changes in weight and density for high density phenolic foam (0.25 g/cc) at various temperatures from 100° to 2600°C. The cyclic behavior of the density indicates that the major weight and volume losses do not occur at the same temperatures. Most of the work was done with semi-cylindrical phenolic foam samples approximately 19" diameter and 7" long; but the trends have been verified with samples as long as 24". The results at 2000°C and higher are averages of at least 30 semi-cylindrical samples 19" diameter and 7" long. The lower temperature studies involved no fewer than four samples.

TABLE I
Heat Treatment of 0.25 g/cc Phenolic Foam

Temperature °C	Weight Loss, %	Density Change, %
100	2.7	- 1.4
200	5.6	+ .6
300	14.1	- 4.7
400	26.8	- 2.9
500	44.2	-12.8
600	50.0	- 8.2
700	54.9	- 4.2
800	54.4	- 1.2
900	56.0	- 0.9
1000	56.1	0.1
2000	60	- 3.0
2200	61	- 1
2400	61	+18
2600	61	+26

The data in Table I are characteristic of phenolic foam over the entire range of densities; however, low density foam tends to shrink slightly more at treatment temperatures above 700°C.

B. PYROLYSIS OF URETHANE FOAM

The heat treatment of the urethane foams involves a two-step oxidation prior to pyrolysis in an inert atmosphere. The specific temperature and dwell time used in the polymerization-oxidation step varies with the size and density of the urethane precursor. Typically, the foam is held at 150°C and again at 250°C for 24 hours to prevent fusion during pyrolysis. The weight and volume changes which occur during pyrolysis to 1000°C are about 55 and 60 percent respectively. There is a density increase of about 10 percent for the low density, and 20 percent for the high density carbonized urethane foam.

Union Carbide has patents (2) granted and pending which describe in detail the preparation of organic precursor carbon foam.

III. PROPERTIES OF CARBON FOAM

The physical properties of the product carbon foams are dependent on the type, quality, and treatment of the precursor. The major apparent difference among the types of organic precursor is the average cell size of the product carbon (see Table II). The cell size of the carbonized urethane foam is 8 to 32 mils for the 0.05 g/cc density and approximately 8 to 16 mils for the 0.25 g/cc density; the phenolic precursor carbon has a 2 to 6 mil cell size in the low density foam and approximately 1 to 3 mils in the high density material.

TABLE II
Cell Size of Carbon Foam

Foam Precursor	Density	Cell Diameter
Urethane	0.05 g/cc	8-32 mils
	0.25 g/cc	8-16 mils
Phenolic	0.05 g/cc	2-6 mils
	0.25 g/cc	1-3 mils

The cell structures of these carbon foams are shown in Figure 1. The cells are football shaped with the major axes parallel to the foaming directions. The pyrolyzed foams are pseudomorphs of the parent foam.

The compressive strengths, defined as the point at which a change in slope of the stress-strain curve occurs; of properly prepared 1000°C carbon foam from phenolic and urethane precursors are given in Figure 2, for foams in the density range of 0.15 to 0.35 g/cc. The strength of the phenolic precursor carbon varies from 500 to 1900 psi over the density range; the strength of urethane precursor carbon is about one-half these values.

The ultimate compressive strength of the 0.35 g/cc phenolic precursor carbon foam is usually above 3000 psi. The strength of low density foam exhibits a greater degree of anisotropy than high density foam. The strengths of 0.05 g/cc carbon perpendicular and parallel to the foaming direction are 30 and 50 psi, respectively. Subsequent heat treatment of carbon foam to 2800°C results in no change in strength for the phenolic precursor carbon but does result in as much as a 70% reduction in strength for urethane precursor.

The thermal conductivity of the foam, determined by the Fitch method, is quite low, approximately 0.1 and 0.2 BTU/ft-F°-hr for 0.05 and 0.25 g/cc carbon, respectively. The high temperature thermal conductivity was determined by the cyclic phase shift⁽¹⁾ technique for a sample of 0.27 g/cc density phenolic precursor carbon foam. The data are shown in Table III. The thermal conductivity parallel to foaming is 10 to 25 percent higher than the conductivity perpendicular to foaming. In the direction of high thermal conductivity, the range is 0.5 to 0.8 BTU/ft-F°-hr in the temperature range of 1400° to 2100°C. Other properties of material from the same sample are shown in Table III.

TABLE III

Properties of 0.27 g/cc Phenolic Precursor Carbon Foam

Property	Direction Perpendicular	Direction Parallel
Density, lb/ft ³	0.27 g/cc	0.27 g/cc
Compressive Strength, psi	1,350	2,150
Shear Strength, psi	725	570
Thermal Conductivity, BTU/ft-F°-hr		
RT →100°C	0.18	0.20
1400°C	0.47	0.53
1800°C	0.45	0.57
2100°C	0.60	0.75

Of particular interest is the high shear strength which demonstrates that when the material is used as an insulator, it can be firmly bonded to the surface to be insulated.

The permeabilities of various carbon foams are shown in Table IV along with the permeabilities of graphite and PC-45 a high density porous carbon. The best commercial grades of graphite with densities in the range of 1.6 to 1.73 g/cc have permeabilities in the range of 0.5 to 0.02 Darcy's. The permeability of phenolic carbon foam is in the range of 1.9 to 0.36 Darcy's, roughly an order of magnitude greater than that of graphite; the permeability of the urethane precursor carbon foam is in the range of 22.6 to 71.5 Darcy's, two orders of magnitude greater than that of graphite. Porous carbon, PC-45, has a porosity almost identical with that of the high density urethane precursor carbon, approximately 22 Darcy's.

TABLE IV

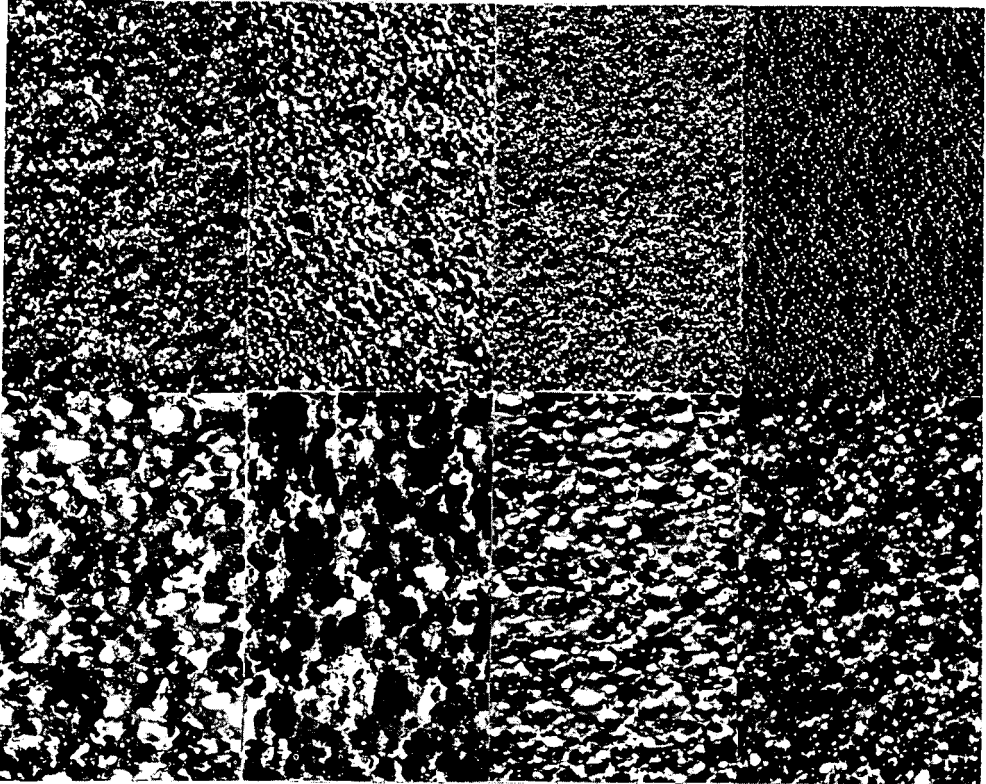
Permeability of Carbon Foam

Precursor Material 1000°C Treat	Density, g/cc	Permeability in Darcy's	
		Parallel to Foam	Perpendicular to Foam
Urethane	0.05	71.5	31.0
Urethane	0.30	24.3	22.6
Phenolic	0.08	1.9	1.1
Phenolic	0.30	0.95	0.36
PC-45	1.04	20	20
ATL Graphite	1.78	0.068	0.064

In summary, carbon foam is a light weight, high strength material which is stable above 2800°C. It may be used as an insulator, filter, or structural support material and is presently available in sizes as large as 14" diameter by 18" long.

Figure 1

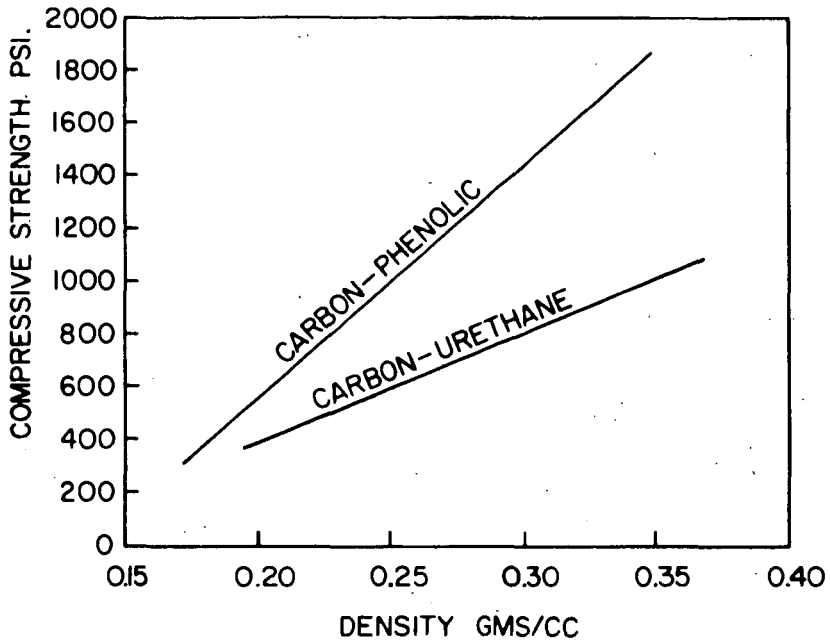
CARBON FOAM 1000°C HEAT-TREAT



The upper row is phenolic precursor carbons in both directions of 0.05 and 0.25 g/cc density. The lower row is corresponding urethane precursor carbons.

Figure 2

COMPRESSIVE STRENGTH VS. DENSITY
FOR CARBON FOAM



References

- (1) "Measurements of Thermal Diffusivity and Thermal Conductivity of Graphite with Carbon Arc Image Furnace," M. R. Null and W. W. Lozier, 5th Thermal Conductivity Conference, Denver, Colorado, October 20, 1965.
- (2) U. S. Patent 3, 121, 050; U. S. Patent 3, 302, 999; U. S. Patent 3, 387, 940.

Some Experimental Techniques Used in Carbon Reaction Studies

L. Kurylko, Stackpole Fellow
Combustion Laboratory, The Pennsylvania State University
University Park, Pennsylvania

R. W. Froberg, Research Scientist
Stackpole Carbon Company, St. Marys, Pennsylvania

R. H. Essenhigh, Associate Professor
Combustion Laboratory, The Pennsylvania State University
University Park, Pennsylvania

1. INTRODUCTION

Although research on carbon has proliferated unbelievably in the last decade, there are indications of a growing dichotomy between two somewhat disparate points of view regarding the objectives of the research. On the one hand, university-oriented work has tended to be of the so-called "pure" or "fundamental" variety, often concentrating on small, very specialized points and utilizing many highly-elaborate techniques of an impressive level of sophistication. Industrial research on the other hand has, of necessity, to be of an applied nature, and often contains a high component of empiricism. These latter are sometimes referred to as engineering studies. The two respective points of view can be summed up in the phrases "Know Why" and "Know How."

It is a truism to say that the Know Why ought to illuminate the Know How, but recently there has been increasing skepticism of the part of some investigators that this is possible, and in this lies the source of the dichotomy. The problem is best seen by way of an example. In the measurement of activation energies, for instance, it seemed possible at one time that if the energies could be measured for different carbons under known conditions then the value, or range of values for the different carbons, was likely, to imply a particular mechanism. However, recent work [1] on the adsorption isotherms at low temperatures have shown the evident existence of a range of possible and overlapping alternate steps in the reaction each with its own individual energy. Therefore, it would seem that any activation energy not determined by these very precise methods must be only an average with an evident ambiguity of interpretation. The problem is then compounded when we consider that, when the detailed mechanisms were elucidated, this was by using ultrapure, highly specialized "research" carbons, such as Spheron 6, whereas industrial carbons have the additional complexities of different degrees of graphitization, accessibility, and reactivity, of binder and filler, together with modifying factors due to ash, permeability, porosity, isotropism or lack of it, etc. It is, therefore, a very real question whether the "pure" and so-called "engineering" studies really have sufficient in common to make attempts at cross-correlations and interpretations worthwhile.

As we have ourselves been concerned primarily with more "engineering" studies, we have therefore been somewhat exercised by this very question. Whilst not finding the description sufficiently important to quarrel about, it does nevertheless seem to us that our studies do in fact lie more or less between the two (what might therefore legitimately be called technological studies if one looks for a name). Our conclusions are that cross-correlations between studies of different levels of fundamentality are in fact possible, if applied with caution; and also that the unfortunate dichotomy that has started to develop will have to be closed.

The first consideration to be examined was whether the lack of interpretation in terms of fundamental mechanisms actually mattered. After all, the carbon industry has existed quite successfully for decades (centuries if one includes charcoal burning) without access to the information now being developed. However, the last 10 or 20 years has been an increasing sophistication in carbon manufacture, paralleled by much more varied and extreme uses, which has been itself largely the stimulus for the increased research; and it is clear that we now require a matching sophistication in knowledge of reaction behavior of actual carbons as manufactured for industrial processes.

Now, when we consider the behavior of industrial carbons with the attendant complexity of reaction in real situations, it seems to us that, so long as we can unravel the complexity due to the real situation, the only factor likely to disturb any mechanistic interpretation is the parameter modification due to the presence of two or more components (such as filler, binder, ash, etc.). Here it is true that kinetic parameters such as frequency factors, activation energies and so on will be averages of some sort; but this does not seem to be an insuperable objection since all it means is that behind the average we measure is some (unknown) statistical distribution of the parameter values. Any such statistical distribution must itself be determined by composition and other material properties; and the use of an average value does not seem to be any less relevant than the use, for example, of average properties of gasses such as velocity, or energy, or temperature. In the case of carbon studies, the more fundamental work may in time determine the statistical distributions of the relevant parameters due to variable material compositions and properties, and this will be of immense assistance in filling out any interpretation. In the meantime, lacking such information, we may legitimately assume (till proved otherwise) that the background distributions are rather narrow, so that any kinetic constants obtained by experiment are presumed to be close to unique--and therefore mechanistically interpretable--values.

To us, the more important problem at this stage is the unambiguous experimental determination of these (statistical) property parameters, and this is primarily a matter of experimental design. The problem is that many of the more applied (engineering) methods of experimentation lack definition so that there can be considerable uncertainty what property a measured value is really related to--even before one starts to consider the problem of the statistical average. The activation energy, for example: it is true that the value measured is the weighted statistical average of all possible adsorption energies; or could it be the average of all possible desorption energies? This is typical of the type of ambiguity that can arise.

To eliminate such ambiguities requires good experimental design, and this is jointly a matter of technique and of instrumentation. Recently we described a technique, with some brief outline of the instrumentation that we were able to show did eliminate much ambiguity [2]. In this paper our purpose is to re-summarize the technique (for completeness) and to amplify the information on the instrumentation in the belief that this may be of value to those concerned with the more precise, unambiguous "engineering" values of kinetic constants, but still measured on such a basis that there is some hope of applying a valid mechanistic interpretation. This is not to say that we think this is the only technique able to develop kinetic information on the basis required, but we believe it to be the most fully developed so far. The point we are making is that the time has come to start closing the gap between the "fundamental" and "engineering" studies on carbon reactions, so that the latter are as valid as the former for obtaining kinetic data and mechanistic interpretations of behavior.

2. ESSENTIALS OF THE EXPERIMENTAL METHOD

2.1. General - In the studies of heterogeneous reactions it is of great importance that experimental data are obtained which define both the state of the reacting surface and the state of the fluid that influences the course of the reaction. This also requires a precisely known solid geometry. The need for meaningful data in research on carbon-oxygen reactions is especially acute; the reason being that within a temperature span of several hundred degrees and a pressure span of one atmosphere, many of the elementary steps of reaction change from dominant to nondominant, e.g., adsorption of reactants, desorption of products, diffusion of reactants to the surface, diffusion of reactants through the carbon, etc. Coupled with the problems of heat exchange and continuous changes in the diffusion rates and surface area that occur due to consumption of carbon, an experimenter is faced with a formidable task of analyzing the kinetics of the reaction [3]. An experimental system is thus required capable of generating data whose interpretation would be unambiguous.

To determine process kinetics of carbon reactions information is needed about the sample weight, rate of weight change, temperature of carbon and gas, sample geometry, gas composition, and the surface area and permeability of the carbon. To obtain such data we have developed a technique in which a carbon sample is suspended in a vertical furnace, continuous records of sample weight, sample geometry, and sample and gas temperatures are obtained (Fig. 1). In addition gas composition inside and around the sphere can be measured at regular time intervals. Other data which are obtainable on samples that were partially reacted then quenched at the desired level of burnout are an independent check of porosity profiles and the BET surface area.

In the experimental technique which was developed a carbon sphere is used because of its well defined geometry and symmetry during burnout. The reactant flow velocity is kept low so that the heat and mass transfer conditions are well defined. From continuous measurement of weight and diameter the average density change can be established. When temperature measurements are included, the Arrhenius plot of reaction rate can be developed, together with information about the heat release rates inside and outside the carbon sample.

2.2 Temperature Measuring System - The temperature of the carbon sphere was measured by imbedded thermocouples. A small hole about 0.3 mm. in diameter was drilled in the carbon sphere. One lead of a Pt-Pt-13% Rh Thermocouple was threaded through the hole and a butt weld was made to the other lead. Then the hot junction was pulled back to the desired location in the sphere. To insulate the thermocouple leads from the sphere, they were shielded by quartz capillary tubing or flame plated with silica prior to insertion into the sphere. As many as three thermocouples were used to record the inside temperatures at one time.

The thermocouple leads above the sphere were threaded through an eight-inch long ceramic support rod. Alternatively, a section of a metal-shielded thermocouple was stripped of its metal cladding and ceramic insulation to expose thermocouple leads ready for insertion. An ice bath was used for the cold junction.

The gas temperature was measured using shielded thermocouple assemblies with bare hot junctions. Micromanipulators were used to position the beads at precise locations around the carbon sphere.

The temperature recording system consisted of millivolt suppression circuits and amplifiers for adjustment of the recording scale, a 24 channel recording oscillograph, and a precision potentiometer for independent spot checks of thermocouple outputs.

2.3. The Weighing System - The weighing of the carbon sphere was made using a conventional analytical balance with an automatic recording attachment. A continuous record of the sample weight was obtained either on a potentiometric recorder or using one of the channels in the recording oscillograph. Typical reduced records of weight loss and temperature measurements are shown in Figure 2.

In the base of the balance a hole was drilled to receive a ceramic rod that was connected to one of the balance pans. At the other end of the ceramic rod was a small platinum wire loop to which the ceramic rod with the thermocouples and the carbon sphere was connected. The carbon sphere was thus suspended from the balance on two ceramic rods connected by hooks and loops. This arrangement permitted easy disconnection of the thermocouple assembly from the balance and allowed the furnace to be moved for insertion of a new test sample.

Prior to each run the test samples were weighed on an analytical balance to determine the exact original weight. Also with the cold sample suspended from the balance, a calibration run was made to simulate weight changes that would occur during sample burnout by adding weights to the proper pan.

2.4. The Sample Size Measuring System - The diameter of the carbon sphere was measured with a micrometer prior to placing of thermocouples in the sphere. After the insertion of the sphere in the furnace and its suspension from the balance, the size changes would be measured optically. To do this a telescope-projector was constructed through which one could measure the sphere visually or obtain a photograph at desired time intervals. Figure 1 shows the schematic of the size measuring system. Above the top of the furnace we have a 45° mirror which sends a projected light source through a transparent watch glass (with a hole to allow the ceramic rod to connect to the rod from the balance). The light passes vertically through the furnace tube exiting through a quartz window at the bottom of the furnace. A second 45° mirror connected to a movable telescope deflects the light through an iris diaphragm and focusing eye piece to a ground glass screen. After focusing, the ground glass screen was normally removed and a camera inserted in its place.

When the temperature of the carbon was less than about 800°C , a 1500 joule flash was used to project the shadow of the sphere onto the film. At higher temperatures the radiation intensity from the carbon sphere was sufficient for self-recording of the sphere image on ASA 125 film. An electric sequential timing switch was used to trigger the flash gun, camera, and a timing mark on the oscillograph. During a normal run the sphere was photographed about sixty times at X8 magnification.

2.5. The Furnace and Gas Feeding System - The electrical furnace contained a vertical tube which was two (2) inches in diameter by eighteen (18) inches long. The hot zone of nearly uniform temperature was about twelve (12) inches long located in the center of the furnace. On the bottom of the furnace was a water cooled brass cap containing various gas inlet ports and a quartz window in the center. One thermocouple extended through the brass cap to measure gas temperatures below the suspended carbon sphere. The furnace temperature-control thermocouple was located behind the heating elements. A proportional band controller was used to keep the furnace temperature constant. The top of the furnace was covered by a loose-fitting transparent glass lid. A hole was drilled in the lid to allow thermocouples as well as the carbon support rod to pass through.

The gasses were normally passed through molecular sieves and Drierite columns before being metered through rotameters and passed to the furnace. The pressure of gas entering the rotameters was also monitored.

3.6. Gas Sampling - A gas sampling system was developed in which a 0.1 mm. I.D. capillary steel tube was attached to the thermocouple assembly and suspended from the balance together with the carbon ball.

Gas was withdrawn both from the center of carbon sphere and from the vicinity of the sphere and analyzed using a Fisher gas chromatograph. By taking samples at regular intervals, changes in the gas composition inside the furnace could be established.

3. AMBIGUITIES AND FAILURES OF METHODS

3.1. Thermocouples - A thermocouple inserted in a carbon sphere or in a gas stream will under many circumstances indicate a temperature that is different from the true temperature of the solid or fluid at the hot junction. First, a large thermocouple will represent a large heat sink and, therefore, changes in the temperature of the material being measured will not be accurately reflected in changes in the thermocouple's readings. The goal therefore is to use as small a thermocouple as possible. Radiation exchange between the thermocouple and the surroundings is another source of error. A thermocouple exposed to walls which are at different temperature than the surrounding gas will indicate an intermediate temperature. Here it is also desirable to have a thermocouple as small as possible--the smaller the diameter of the hot junction the smaller will be the error. When the thermocouple leads are less than about 0.25 mm. and unsupported in the length of several centimeters, a serious error may develop due to vibration and movement of thermocouple leads. The vibrating thermocouple will indicate temperature fluctuations when in reality there are none. A good reference on thermometry in flames is "Flame Structure" by Fristrom and Westenberg [4], although they do not include discussion of the suction pyrometer (or HVT).

In measuring the internal temperature of an electrical conductor (like carbon) the thermocouple leads, except for the hot junction, have to be insulated from the conductor because the thermocouple will otherwise indicate some averaged temperature of the conductor rather than the temperature of the hot junction.

Another source of error in the measurement of temperature with very fine thermocouples are stray and induced currents due to furnace heating circuitry, on-off controller switching, starting and stopping of miscellaneous electrical equipment, etc. Here the recommendation is use grounded and shielded extension and thermocouple leads, amplifiers with high frequency noise filtering devices and constant voltage supply transformers. In our experience we had to use all these devices.

3.2 Gas Sampling - To obtain an accurate concentration profile while a gaseous chemical reaction is taking place, is quite difficult. First, the flow pattern of the gas around the sampling probe should not be significantly affected. Second, the chemical reaction must be quenched; otherwise, the composition of the gas as given by subsequent analysis will not be the same as that which enters the probe.

We found that during sampling of the gas from inside the carbon sphere, the hole through which the probe was inserted became enlarged. This indicated, of course, that, during sampling, a disturbance of the gas concentration profile occurred. Further information on gas sample probes is given in reference (4.).

3.3. Flow Pattern Inside the Furnace - The design of the gas feed system, the size of the furnace, and the gas throughput rate significantly influence the concentration and flow pattern of gases inside the furnace. Because the furnace, feed lines, tees, filters, etc., act as reservoirs, the change in gas concentration at the carbon sample surface normally does not follow a discontinuous change as one switches from inert to reacting gas or vice versa. After opening a valve, it is, therefore, most desirable to know when the concentration of the reacting gas reaches 95 or 98 percent of the desired value. Indeed, at low flow rates and with large holdup vessels it may take half an hour or longer to achieve a desired gas concentration around the sample.

To determine whether the flow pattern inside the furnace meets the desired characteristics, a plot of logarithm of concentration at the desired location versus time will indicate either the degree of back mixing, or the extent to which the reactor approaches plug flow conditions. The steeper the negative slope on the plot described, the closer the reactor approaches plug flow conditions (Fig. 3). If the concentration of the gas to be displaced, (nitrogen), approaches an asymptotic condition, then there exists the possibility of dead-end hold-up storage zones in the feed system, or of leakage of undesirable gas into the system.

4. SOME RECENT RESULTS

During the five years that the experimental technique has been in operation, and in process of gradual improvement, several significant experimental findings about carbon-oxygen reactions have been obtained.

First, the simultaneous measurement of both sample size and weight provided a direct method by which the data could be separated into the three zones of reaction. Thus, it was possible to construct an Arrhenius plot of the rate data in which the three major zones could be identified. The Arrhenius plot was constructed using the true sample temperature (not the furnace or gas temperature) which was measured by thermocouples within the carbon sphere. No meaningful analysis of the effect of oxygen concentration on the apparent reaction rate could be made without the sample temperature measurements. It was found that the apparent rate increased with increasing oxygen concentration but so did the sample temperature. The net result was that, regardless of the oxygen concentration, all data described a single rate curve at low temperatures (Zone I). It was concluded, therefore, that the chemical reaction was zero order.

In the further analysis of the data a definite conflict was apparent. If the reaction order was truly zero in the chemically dominant regime, why did the temperature of the carbon sphere reacting in oxygen exceed its temperature when reacting in air? This conflict was resolved only after temperature profile measurements were made of the sphere and of the surrounding gas. From these, heat exchange balances were made between the reacting sphere and the surrounding environment using a digital computer. These calculations revealed that in Zone I the heat release for the carbon-oxygen reaction amounted to that required to convert all carbon to CO_2 within the carbon sphere. But, for the case when oxygen concentration was low, such complete burn-up of the primary reaction product, CO, did not occur within the carbon boundaries; thus the temperature of the carbon reacting in air did not rise to as high a value as it did in pure oxygen.

In Zones II and III, the burn-up of carbon monoxide occurred outside the carbon sphere, as substantiated by gas sampling and temperature profile measurements and confirmed by heat balance calculations. It was also found that within a certain carbon porosity range a region of combustion instability existed between Zone II and Zone III during which the temperature of carbon oscillated by as much as 70 degrees and with a period of up to 100 seconds (Fig. 4).

5. CONCLUSIONS

Temperature, weight and size measurements of reacting carbon spheres can be made simultaneously in an electrically heated furnace. Combining these measurements with gas sampling, surface area, and density profile determinations, the progress and process of heterogeneous solid-gas and of subsequent gas phase reactions can be established. Measurements of atmospheric conditions gave results revealing the true

order of chemical reaction of carbon with oxygen, allowed the determination of the depth of penetration of the reaction zone into carbon, established the presence of an oscillatory combustion phenomena, etc. Problem areas to be encountered by the experimenter with the above techniques are pointed out.

These results show the importance and value of adequate experimental techniques designed to deliver results whose interpretation will be unambiguous.

REFERENCES

1. Bansal, R. C., F. J. Vastola, and P. L. Walker, Paper C130, Eighth Carbon Conference, State University of New York at Buffalo, June 19-23, 1967.
2. Essenhigh, R. H., and R. W. Froberg, Papers C111 and C112, Eighth Carbon Conference, State University of New York at Buffalo, June 19-23, 1967.
3. Wicke, E., Fifth Symposium on Combustion, New York: Reinhold, p. 245, 1955.
4. Fristrom, R. M. and A. A. Westenberg, Flame Structure, McGraw-Hill, New York, 1965.

ACKNOWLEDGMENTS

This work was carried out in the Combustion Laboratory of the Department of Fuel Science, The Pennsylvania State University, for the Office of Naval Research under Contract NONR 656-29 whose support is acknowledged. We also have pleasure in acknowledging joint support for the project from the Stackpole Carbon Company, St. Marys, Pennsylvania, by provision of Research Fellowships to the first two authors.

ON THE USE OF PHOSPHATES TO INHIBIT OXIDATION OF INDUSTRIAL CARBONS

Robert W. Froberg

Stackpole Carbon Company, St. Marys, Pennsylvania 15857

I. INTRODUCTION

The use of additives to inhibit the oxidation of carbon-graphites has been well-known in the industry for many years. Among the earliest to report on the use of phosphorus-containing additives was Wicke [1]. He studied the effect of phosphoryl chloride which was added to the gas phase during oxidation. Others who have examined the effects of oxidation-inhibiting additives include Arthur [2,3], Hadman et al [4], Day [5], and Hedden [6].

The exact mechanism by which phosphates, in particular, inhibit the oxidation of carbon is still a moot question. However, it is generally agreed that both chemical and physical processes are involved. That is, the phosphate covers potentially active sites on the carbon surface both by a strongly chemisorbed layer [7] and/or a physical barrier of either a glassy or crystalline nature as in the case of some oxides [8]. The latter would appear to be the case in the work reported by Paxton [9].

Factors which determine the effectiveness of a given phosphate treatment include the chemical composition of the impregnant, the molar concentration of the starting solution, the amount of material finally deposited within the pore system of the carbon, the distribution of the treatment within the carbon, and the reactivity of the original carbon-graphite [10-13]. Of importance also is the permeability of the original carbon to the solution or liquid used for the impregnation.

The oxidation of untreated carbon at some temperature is usually expressed as the Specific Reaction Rate [14, 15]. That is, weight loss per unit time per unit area [15]. The area used to calculate the rate may be the geometric or apparent surface area of the sample [14], the B.E.T. or nitrogen adsorption area, or some fraction of the total surface area [16]. There are certain advantages and shortcomings involved in the use of all of these [1, 17]. The rate of reaction is known to be dependent upon both chemical and diffusional mechanisms [18]. In addition, the rate of oxidation of an untreated carbon at temperature below 1800°F may be strongly affected by the nature of the carbon itself. Such variables as heat treatment history, impurity content, crystallinity, porosity, and permeability are all inherent properties of the sample material which can, in fact, influence the rate of oxidation [14, 17, 19].

In the case of a treated material, an additional set of variables (mentioned earlier) are introduced which are concerned with impregnant and its interaction with the base material. These new variables are then added to the list given above to produce the entire collection of factors which may be changed so as to affect the resulting reaction rate of treated carbon with oxygen. It is obvious that the system must be simplified greatly by making many of these quantities a constant before meaningful data may be obtained on the reaction.

The work described in this paper concerns the evaluation of phosphate impregnants for improving the oxidation resistance of commercial carbon-graphites. Impregnation of the carbon may be done by a variety of methods including molten

salts, water-or acid-based solutions, and vapor deposition. The technique used to treat the materials described was a solution impregnation via a vacuum-pressure cycle. The objective herein is to examine the experimental results and discuss some of the factors which make these phosphate treatments effective inhibitors of the oxidation of carbon.

II. EXPERIMENTAL

The TGA equipment used in this work is shown in Fig. 1. It is simply an electrobalance (Cahn RH) mounted above a vertical tube furnace. The sample is suspended within the furnace, from the balance, on a Mullite rod and the sample weight is continuously recorded as the material is burned off. The furnace control is such that the temperature may be varied with a preselected program or held constant. For the purpose of this work, the furnace temperature was held constant at 1200°F for all the runs in order to minimize the variables described earlier.

The samples were preheated in nitrogen before the oxidizing gas was admitted into the tube furnace. For this work, only air was used to burn the samples. The equipment, however, includes the necessary metering system to feed various oxygen-nitrogen mixtures into the furnace, if required.

The test data are reported as the time required for ten percent burnoff of the sample under test. With certain qualifications, the longer it takes the material to lose ten percent of its original weight, the more effective is its oxidation resistance (OR).

All samples used were in the form of 3/4-inch cubes. With a few exceptions, the same base material was used for all tests in order to minimize the variation of the data due to the reactivity of the carbon.

III. RESULTS

Table I is a compilation of the primary experimental data to be discussed in this paper. Some additional data will be presented later to clarify particular points. The base grades and treatments are given letter names because the nature of these materials is not vital to following the discussion.

TABLE I
EXPERIMENTAL RESULTS FOR 1200°F IN AIR

<u>Base Grade</u>	<u>Treatment³</u>	<u>% Treatment</u>	<u>Hours to 10% Burnoff*</u>
G ¹	None	-	0.08
G	A	10.4	54
L ²	None	-	3.4
L	A	7.5	54
L	B	4.65	103
L	C	8.2	106
L	D	9.0	134
L	E	12.6	36
Glassy Carbon	None	-	10.5

1 = graphitized material, pitch-bonded natural graphite

2 = graphitized material, pitch-bonded lampblack

3 = all treatments are metallic phosphates

*Average values

IV. DISCUSSION

The data given in Table I represent average values for a number of samples of each material. This is a point worth emphasizing since the spread in experimental data is usually about 20 percent. Therefore, a reliance upon only a few data points may be very misleading when one draws conclusions concerning the OR effectiveness of a given treatment and/or material.

A. Uniformity of Treatment:

It is usually not sufficient to know only how much of a given treatment is deposited in the carbon (percent pickup), but one should also have some information concerning the distribution of the impregnant within the carbon. To exemplify this point, data are presented in Fig. 2, which resulted from successive weighing and grinding of a number of treated cubes. It is clear from the curves in Fig. 2 that the local concentration of impregnant decreases toward the center of the cubes. Several reasons for this uneven distribution may be suggested: first, the degree to which the impregnant penetrates the sample is determined by the permeability of the carbon and the viscosity of the solution; and, second, the uniformity of the treatment may be adversely affected if the impregnant is a suspension and not a true solution. If the suspension is coarse enough, the solid particles may be filtered out and only the clear liquid may, in fact, reach the center of the sample. It is noted, however, that treatments used in this work were true solutions. Another reason suggested for this concentration gradient within the treated carbon is that when the treated material is being dried, the impregnant may migrate toward the surface of the sample. Whatever the reason, it is clear that, for the data shown in Fig. 2, there is a concentration gradient. The effect that this has on OR is obvious if the treatment is in the form of a shell and if the oxygen penetrates the pore system beyond the treated shell. Therefore, a large amount of treatment does not necessarily insure a high OR. An exception to this occurs when the pores are physically blocked as seems to be the case for the molten salt treatments described by Paxton [9].

B. Hygroscopic Behavior:

A characteristic of many phosphate treated carbons, which is undesirable from the viewpoint of product use, is the tendency to absorb moisture and ultimately exude droplets of sticky liquid from the pore mouths. It is this behavior that rules out the use of a number of treatments which are, in fact, quite effective in inhibiting the oxidation reaction. For example, the material called "Treatment D" (line 5, Table I) is quite reasonable as an OR treatment. However, the treated carbon becomes tacky and moist after several days in room air.

An improvement can be made with coatings, cure cycles, and storage conditions in that some delay can be realized in moisture pickup. These measures, however, usually do not eliminate the problem. The solution is, of course, to find a phosphate treatment which is not hygroscopic while, at the same time, it possesses excellent OR properties.

While certain phosphate compounds such as those of tungsten and molybdenum are apparently hygroscopic, it also is possible that some other treatments exhibit this behavior because of excess phosphoric acid within the finished piece. Therefore, in evaluating the moisture pickup behavior of phosphate treatments, it is advisable to consider the excess acid present, if any.

C. Glassy and Crystalline Phosphates:

Another property of the phosphate treatments which increase the OR of carbon is the structure of the material deposited on the surface of the carbon. Many treatments examined in this work were obviously glassy or crystalline (grainy) when examined visually, after cure. In general, it was found that glassy deposits offered more protection to the carbon than did those which appeared grainy and discontinuous. This fact would tend to support the view that the oxidation is inhibited by means of a physical barrier of phosphate glass between the carbon surface and the oxidizing gas. This is shown in Table I, as line 7 (glassy deposit) and line 8 (grainy deposit) with 134 and 36 hours to 10 percent, respectively.

D. Stability of the Treatment:

One of the more obvious points which can be made in this discussion is that the particular phosphate used as an impregnant must be stable at the test temperature. To prove that the interaction between the carbon surface and the phosphate material does not change the stability of the treatment, several compounds known to be unstable at 1200°F were run and the OR, measured as time to 10 percent weight loss, was very poor (less than 24 hours).

E. Reactivity of the Carbon:

The results from this work indicate that with treatment levels used in the samples tested for OR, the impregnant does not completely mask the reactivity of the basic carbon material. In the case of the untreated natural graphite grade G, the reactivity was so high that it ignited at 1200°F in air. On the other hand, the untreated lampblack material L did not, in fact, ignite, although the sample temperature rose about 40°F above the furnace temperature. These results are given in Table I in lines 1 and 3, respectively. The meaning of these results is that the natural graphite-based material was of such a reactivity that the heat-release rate greatly exceeded the heat-loss rate. Thus the sample temperature rose to the ignition temperature and from there to the maximum obtainable temperature which, in this case, would be in the bulk-diffusion combustion region, or Zone III. The lampblack-base material was less reactive and showed none of the behavior described above. For a detailed explanation of the significance of this behavior, the reader is referred to an excellent text by Vulis [20].

The same treatment was given each of these base grades and the treated pieces were then tested for OR. As expected, the treated grade G reacted faster than the treated grade L (lines 2 and 4, Table I), even though the former contained almost twice the amount of treatment as the latter.

When industrial carbons are oxidized, it is generally agreed that there is usually a preferential attack on the binder [21]. In the oxidation of phosphate treated carbons, similar results have been noticed. Here again, at the treatment levels used in this work, the phosphate failed to completely mask off the basic reactivity of the materials.

For the purpose of completeness, glassy carbon material was also oxidized (line 9, Table I). This impervious material ran 10.5 hours to 10 percent weight loss. It would seem that from the viewpoint of OR, phosphate-coated glassy carbon would be quite acceptable. In a practical sense, however, application and fabrication problems would make this an unlikely choice.

V. CONCLUSIONS

When evaluating phosphate treatments for oxidation resistance, one should have information not only on the total amount of treatment within the carbon but the distribution of that treatment as well. Such information could help to explain results which otherwise would appear quite contradictory.

The factors which determine the effectiveness of a particular OR treatment, other than percent pickup and distribution, include the glassy properties of the treatment, the thermal stability of the compounds formed at the test temperature (1200°F in this work) and, in some cases, the reactivity of the base grade.

Properties other than OR may disqualify an impregnation from being considered for commercial use. In the case of phosphates, the tendency to exude a sticky solution is usually the most troublesome behavior.

VI. REFERENCES

- [1] Wicke, E., "Fifth Symposium on Combustion," New York: Reinhold, p. 245, 1955.
- [2] Arthur, J.R., Trans. Faraday Soc., 47, 164, 1951.
- [3] Arthur, J.R., J. R. Bowering, J. Chim. Phys., 47, 540, 1950.
- [4] Hadman, G., H. W. Thompson, and C. N. Hinshelwood, Proc. of Royal Soc., (London), A137, 87, 1932.
- [5] Day, R.J., Ph.D. Thesis, The Pennsylvania State University, 1949.
- [6] Hedden, W.L., G. J. Dienes, Advances in Catalysis, 9, 398, 1957.
- [7] Pallmer, P.G., Carbon, New York: Pergamon Press Ltd., 4, p. 145, 1966.
- [8] Schultz, D.A., P.H. Higgs, and J.D. Cannon, authors, "Oxidation-Resistant Coatings for Graphite," WADD TR61-72, Vol. XXXIV, Union Carbide Corp., June, 1964.
- [9] Paxton, R.R. and G.I. Beyer, U.S. Patent 3,342,627, 1967.
- [10] Woodburn, J., and R.F. Lynch, U.S. Patent 2,685,539, 1954.
- [11] Woodburn, J., and R.F. Lynch, U. S. Patent 2,685,540, 1954.
- [12] Woodburn, J., and R. F. Lynch, U.S. Patent 2,685,541, 1954.
- [13] Woodburn, J., and R.F. Lynch, U.S. Patent 2,685,542, 1954.
- [14] Walker, P.L., F. Rusinko, and L.G. Austin, Advances in Catalysis, XI, 134, 1959.
- [15] Khitrin, L.N., "Sixth Symposium (International) on Combustion," New York: Reinhold, 1951.
- [16] Lain, N.R., F. J. Vastola, and P.L. Walker, J. Phys. Chem., 67, p. 2030, 1963.
- [17] Austin, L.G., Ph.D. Thesis, The Pennsylvania State University, 1961.
- [18] Essenhigh, R.H., R. Froberg, J.B. Howard, Ind. Eng. Chem., 57, p. 33, 1965.
- [19] Gregg, S.J., and R.F.S. Tyson, Carbon, New York: Pergamon Press Ltd., 3, p. 39, 1965.
- [20] Vulis, L.A., Thermal Regimes of Combustion, New York: McGraw-Hill, 1961.
- [21] Froberg, R.W., Ph.D. Thesis, The Pennsylvania State University, 1967.

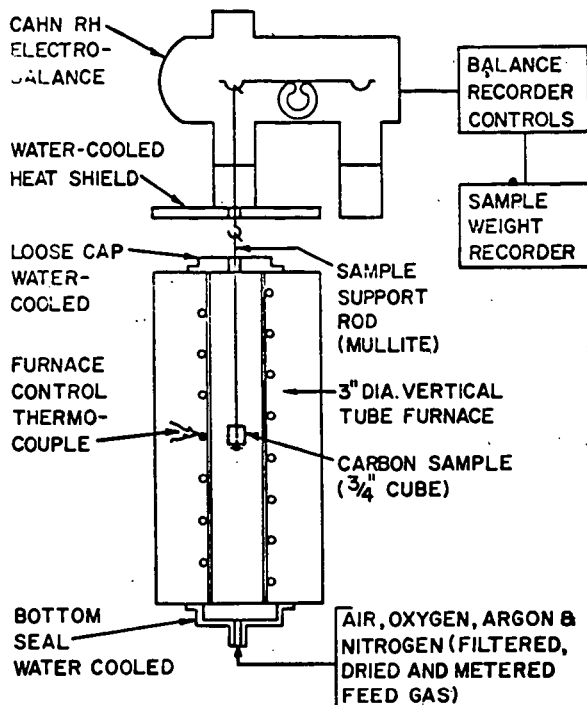


FIG. 1 OXIDATION RESISTANCE TEST SYSTEM

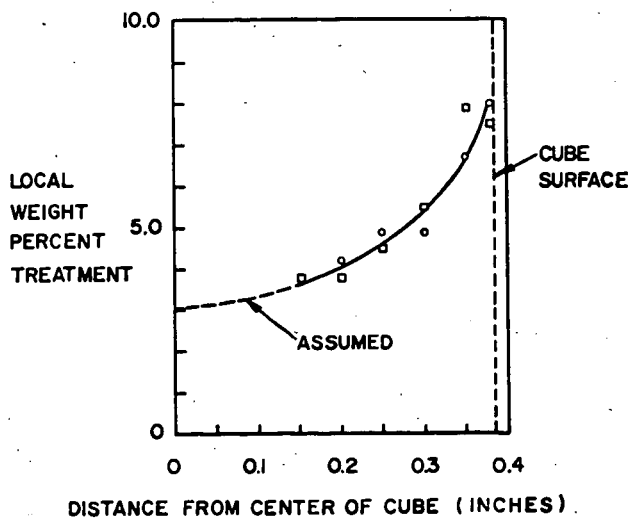


FIG. 2 LOCAL DISTRIBUTION OF PHOSPHATE TREATMENT WITHIN CUBE OF GRADE L (LAMPBLACK BASE)